

TECHNISCHE UNIVERSITÄT MÜNCHEN

TUM School of Life Sciences

**Influence of Fine Particles on the Compression in
Multilayered Filter Cakes**

Martin Paul Hennemann

Vollständiger Abdruck der von der TUM School of Life Sciences der Technischen Universität München zur Erlangung des akademischen Grades eines

Doktors der Ingenieurwissenschaften (Dr.-Ing.)

genehmigten Dissertation.

Vorsitzende:

Prof. Dr. Mirjana Minceva

Prüfer der Dissertation:

1. Prof. Dr.-Ing. Thomas Becker
2. Prof. Dr.-Ing. Jörg E. Drewes

Die Dissertation wurde am 27.10.2021 bei der Technischen Universität München eingereicht und durch die TUM School of Life Sciences am 05.05.2022 angenommen.

Acknowledgments

I would like to express my sincere gratitude to my supervisor Prof. Dr.-Ing. Thomas Becker, who gave me the opportunity to carry out this thesis. He encouraged me to question my results in many challenging discussions, which has greatly improved the outcome of this work as well as my personal development.

I would also like to thank the examination board, Prof. Dr. Mirjana Minceva and Prof. Dr.-Ing. Jörg E. Drewes, for their time and effort in reviewing this thesis.

My sincere thanks go to Dr. Martina Gastl, who was a great group leader and always had an open ear for me. The numerous meetings with her have been encouraging and she has always given me constructive advice.

Special thanks go to Dr. Ehsan Fattahi and Dr.-Ing. Johannes Tippmann for their scientific advice and helpful hints that have improved the result of this work.

Many thanks to the teams of the laboratories and the technicians in the brewery as well as my students, who supported me in preparing this work.

I would like to thank my colleagues at the Chair of Brewing and Beverage Technology, especially from the research group Raw Material Based Brewing and Beverage Technology, where I not only found colleagues, but many good friends.

This thesis would not have been possible without my parents and family, who particularly supported me during my studies. Many thanks.

By far the biggest gratitude goes to my dear Regina. This work was only possible thanks to your great support, scientific knowledge, and helpful advice during this challenging time.

Preface and Peer-Reviewed Publications

The results and publications of this thesis were produced from 2017 to 2021 at the Technical University of Munich, Chair of Brewing and Beverage Technology, Research Group Raw Material Based Brewing and Beverage Technology under the supervision of Prof. Dr.-Ing. Thomas Becker.

The following peer-reviewed publications (shown in chronological order) were generated in the period of this work:

1. Hennemann, M., Gastl, M., and Becker, T. (2019). Inhomogeneity in the lauter tun: a chromatographic view. *Eur Food Res Technol*, 245:521–533.
2. Hennemann, M., Gastl, M., and Becker, T. (2021). Optical method for porosity determination to prove the stamp effect in filter cakes. *J Food Eng*, 293:110405.
3. Hennemann, M., Gastl, M., and Becker, T. (2021). Influence of particle size uniformity on the filter cake resistance of physically and chemically modified fine particles. *Sep Purif Technol*, 272:118966.
4. Hennemann, M., Fattahi, E., Gastl, M., and Becker, T. (2021). Compression mechanism in multilayered filter cakes. *Chem Eng Technol*, 44:1900–1907.
5. Hennemann, M., Gastl, M., and Becker, T. (2021). Influence of temperature on the filter cake resistance in a lauter tun. *Brew Sci*, 74:100–106.

Contents

Acknowledgments	I
Preface and Peer-Reviewed Publications	II
Contents	III
Abbreviations	V
Summary	VIII
Zusammenfassung	X
1 Introduction	1
1.1 Basic Principles of Cake Filtration	2
1.2 Porosity Reduction in Compressible Filter Cakes	3
1.3 Influence of Particle Size on the Filter Cake Resistance	4
1.4 Formation and Characteristics of Multilayered Cakes	9
1.5 The Lautering Process in Beer Production	12
1.6 Hypotheses	15
1.7 Thesis Outline	18
2 Methods	19
3 Results	21
3.1 Summaries of Thesis Publications	21
3.2 Thesis Publications	26
3.2.1 Inhomogeneity in the Lauter Tun: a Chromatographic View	26
3.2.2 Influence of Temperature on the Filter Cake Resistance in a Lauter Tun	39
3.2.3 Optical Method for Porosity Determination to Prove the Stamp Effect in Filter Cakes	46

CONTENTS

3.2.4	Compression Mechanism in Multilayered Filter Cakes	54
3.2.5	Influence of Particle Size Uniformity on the Filter Cake Resistance of Physically and Chemically Modified Fine Particles	62
4	Discussion	73
4.1	Formation and Characteristics of the Multiple Cake Layers	74
4.2	Compression Effects in Multilayered Cakes	77
4.3	Prevention of Compression in Multilayered Cakes	82
5	Conclusions	87
	References	88
A	Appendix	96
A.1	Non-Reviewed Paper	96
A.2	Oral and Poster Presentations	96

Abbreviations

Greek Symbols

α_{bot}	Mass-related specific filter cake resistance of the bottom layer (m kg^{-1})
α_h	Specific filter cake resistance (m^{-2})
α_m	Mass-related specific filter cake resistance (m kg^{-1})
$\alpha_{m,0}$	Mass-related specific filter cake resistance at pressure p_0 (m kg^{-1})
α_{top}	Mass-related specific filter cake resistance of the top layer (m kg^{-1})
β	Filter medium resistance (m^{-1})
γ	Reynolds number-dependent factor (-)
δ	Concentration factor (-)
ϵ	Porosity (-)
ϵ_0	Porosity at pressure p_0 (-)
η	Dynamic viscosity (Pa s)
ρ_f	Fluid density (kg m^{-3})
ρ_p	Particle density (kg m^{-3})
σ_g	Geometric standard deviation (-)
ϕ	Packing density (-)

Roman Symbols

A	Area (m^2)
C	Volume concentration (-)
C_u	Coefficient of uniformity (-)
c_w	Drag coefficient (-)
d	Particle diameter (m)
$D_{3,2}$	Area-weighted mean particle size (Sauter diameter) (m)
$D_{4,3}$	Volume-weighted mean particle size (De Brouckere mean diameter) (m)
D_{50}	Median of particle size distribution (m)
D_i	Midpoint of i -th size class (m)
D_x	Diameter at which x percent of particles are smaller (m)
g	Gravitational acceleration (m s^{-2})
h	Filter cake height (m)
K	Permeability (m^2)
k_{KC}	Kozeny-Carman factor (-)
m	Mass (kg)
n_i	Number of particles in i -th size class (-)
p, q	Powers of D in moments (-)
p_0	Normalization pressure (Pa)
p_L	Hydraulic pressure (Pa)
p_S	Compressive pressure on solids (Pa)
p_{tot}	Total pressure (Pa)
Δp	Total pressure drop (Pa)
Δp_1	Pressure drop across the filter cake (Pa)

Δp_2	Pressure drop of filter medium (Pa)
Re	Reynolds number (-)
S_V	Volume specific surface area (m^{-1})
t_0	Time point before filtration (s)
t_1	Time point after filtration (s)
u, v	Coefficients of compressibility (-)
\dot{V}	Flow rate ($\text{m}^3 \text{s}^{-1}$)
V_{total}	Total volume (m^3)
V_{void}	Void volume (m^3)
w_f	Settling velocity (m s^{-1})

Summary

Suspensions with a wide particle size distribution in combination with sedimentation effects lead to the formation of multilayered filter cakes. This is due to differences in the settling velocity of the particles based on their size and density. A prominent example of a multilayered filter cake is lautering in the brewing process. Larger particles of the suspension settle first and form a compressible bottom layer on which fine particles then form a top layer. This top layer has a high resistance to flow due to the small size of the particles in the layer. In contrast to homogeneously layered filter cakes, the location of the greatest pressure drop is not at the filter medium in multilayered cakes, but on the top layer. The hypothesis is therefore that the fine particles can be viewed as a solid layer with high resistance, which is moved downwards due to the differential pressure during the filtration. This reduces the porosity of the compressible bottom layer, which increases the resistance of the entire filter cake and lowers the flow rate.

The multilayered filter cake was examined in three steps using the example of the lautering process: 1) The formation of the filter cake and the characteristics of the different layers were determined, 2) the compression mechanism during the filtration was examined, and 3) measures to prevent the compression were developed.

A calculation of the settling velocities confirmed the dependence of the formation of the multilayered filter cake on the particle size. In addition to the particle size, the high temperature during filtration in the lauter tun also influences sedimentation. Fine particles are prevented from settling by buoyancy due to thermal convection. In contrast, large particles settle faster at higher temperatures. These opposing effects further promote the formation of the different layers. Different substances are present in different concentrations in the various particles of the suspension, which is why a filter cake with an inhomogeneous chemical composition results that affects the filtration process.

Due to the high resistance of the fine particle layer, it compresses the filter cake from above during the filtration. A new method of cake fixation as well as an optical porosity determination via measuring the surface roughness were introduced to prove the compression. The effect was confirmed by modifying the fine particles and determining

Summary

the resulting effects on the compression. To verify the compression in multilayered filter cakes, a model cake was used, which consisted of an inert, compressible bottom layer. It was confirmed that the high resistance of the top layer creates a differential pressure. The fine particles act as a stiff layer that is pulled down during the filtration and thus compresses the bottom layer. In addition to an artificial top layer, various types of particles were also tested as a fine particle layer. The resistances of the fine particles were compared with the resulting change in the resistance of the bottom layer. The compression by the top layer occurred when its resistance was higher than that of the bottom layer.

A decrease in compression was expected by influencing the fine particle layer. Chemical and structural analysis showed that the fine particles in the lautering process consist to a large extent of protein and starch. In order to specifically influence these components, physical and chemical modifications were applied in a model experiment. The resulting effects on the particle interactions led to changes in the particle size distribution, which influenced the filter cake resistance. The resistance is not only influenced by the mean size of the particles; rather, a high particle uniformity is responsible for a low resistance. To verify the effects of the uniformity on the resistance, a model filter cake consisting of glass beads was used. In addition, the resistance of the fine particle layer could be reduced by high temperatures. The reason for this is the buoyancy effect, which leads to a loosely packed layer. Since modifications to the particles and increased temperatures cannot be used for every filtration process, a technique was developed in which the fine particles were removed before filtration. This prevented the compression of the bottom layer. The resulting shortened process time was verified on a pilot scale.

Zusammenfassung

Suspensionen mit breiter Partikelgrößenverteilung führen in Kombination mit Sedimentationseffekten zur Ausbildung mehrschichtiger Filterkuchen. Grund dafür sind Unterschiede in der Sedimentationsgeschwindigkeit der Partikel basierend auf deren Größe und Dichte. Ein prominentes Beispiel für einen mehrschichtigen Filterkuchen ist der Läutervorgang im Brauprozess. Hier sedimentieren größere Partikel der Suspension zuerst und bilden eine komprimierbare Bodenschicht, auf der anschließend Feinpartikel eine Deckschicht formen. Aufgrund der kleinen Partikelgröße in der Deckschicht weist diese einen hohen Durchflusswiderstand auf. Im Gegensatz zu homogen geschichteten Filterkuchen findet daher bei mehrschichtigen Kuchen der größte Druckverlust nicht am Filtermedium, sondern an der Deckschicht statt. Die Hypothese lautet daher, dass die Feinpartikel als eine feste Schicht mit hohem Widerstand betrachtet werden können, welche aufgrund des Differenzdruckes während der Filtration nach unten bewegt wird. Dadurch verringert sich die Porosität der komprimierbaren Bodenschicht, wodurch der Widerstand des gesamten Filterkuchens erhöht und die Durchflussrate verringert wird.

Der mehrschichtige Filterkuchen wurde anhand des Beispiels des Läuterprozesses in drei Schritten untersucht: 1) Die Ausbildung des Filterkuchens sowie die Eigenschaften der verschiedenen Schichten wurden bestimmt, 2) der Kompressionsmechanismus während der Filtration wurde untersucht und 3) Maßnahmen zur Vermeidung der Komprimierung wurden entwickelt.

Eine Berechnung der Sedimentationsgeschwindigkeit bestätigte die Abhängigkeit der Bildung des mehrschichtigen Filterkuchens von der Partikelgröße. Neben der Partikelgröße beeinflusst auch die hohe Temperatur während der Filtration im Läuterbottich die Sedimentation. Feinpartikel werden durch Auftrieb aufgrund thermischer Konvektion an der Sedimentation gehindert. Große Partikel setzen sich bei höheren Temperaturen hingegen schneller ab. Diese gegensätzlichen Effekte begünstigen die Bildung der verschiedenen Schichten. Da in den verschiedenen Partikeln der Suspension einzelne Stoffgruppen in unterschiedlicher Konzentration vorliegen, ergibt sich ein in der chemischen Zusammensetzung inhomogener Filterkuchen, was sich auf den Filtrationsprozess auswirkt.

Zusammenfassung

Aufgrund des hohen Widerstandes der Feinpartikelschicht komprimiert diese den Filterkuchen während der Filtration von oben. Für den Nachweis der Komprimierung wurde eine neue Methode der Kuchenfixierung sowie eine optische Porositätsmessung mit Hilfe der Oberflächenrauheit eingeführt. Durch Modifikation der Feinpartikel und Ermittlung der Auswirkungen auf die Komprimierung konnte der Effekt bestätigt werden. Zur Verifikation der Kompression in mehrschichtigen Filterkuchen wurde ein Modellkuchen genutzt, welcher aus einer inerten, kompressiblen Bodenschicht besteht. Es wurde bestätigt, dass durch den hohen Widerstand der obersten Schicht ein Differenzdruck entsteht. Die Feinpartikel wirken dabei als feste Schicht, welche während der Filtration nach unten gezogen wird und so die Bodenschicht komprimiert. Als Feinpartikelschicht wurden neben einer künstlichen Kunststoffschicht auch verschiedene Partikelarten getestet. Die Widerstände der Feinpartikel wurden der resultierenden Änderung des Widerstandes der Bodenschicht gegenübergestellt. Die Kompression durch die Feinpartikelschicht trat auf, wenn deren Widerstand höher als der der Bodenschicht war.

Es wurde erwartet, dass eine Verringerung der Kompression durch die Beeinflussung der Feinpartikelschicht möglich ist. Chemische und strukturelle Analysen zeigten, dass die Feinpartikel im Läuterprozess zu einem großen Teil aus Protein und Stärke bestehen. Um diese Bestandteile gezielt zu beeinflussen, wurden physikalische und chemische Modifikationen in einem Modellexperiment angewendet. Die resultierenden Auswirkungen auf die Partikelinteraktionen führten zu Änderungen in der Partikelgrößenverteilung, wodurch der Filterkuchenwiderstand beeinflusst wurde. Nicht nur die mittlere Größe der Partikel beeinflusst den Widerstand, auch eine hohe Partikeluniformität ist für einen geringen Widerstand verantwortlich. Um die Auswirkungen der Uniformität auf den Widerstand zu verifizieren, wurde ein aus Glaskugeln bestehender Modellfilterkuchen genutzt. Außerdem konnte der Widerstand der Feinpartikelschicht durch hohe Temperaturen verringert werden. Grund dafür ist der Auftriebseffekt, welcher zu einer locker gepackten Schicht führt. Da Modifikationen der Partikel sowie erhöhte Temperaturen nicht für jeden Filtrationsprozess angewendet werden können, wurde ein Verfahren entwickelt, bei dem die Feinpartikel vor der Filtration entfernt wurden. Dadurch konnte die Kompression der Bodenschicht vermieden werden. Die daraus resultierende verkürzte Prozesszeit wurde im Pilotmaßstab verifiziert.

1 Introduction

Cake filtration is a process used in many industries to separate solid particles from the liquid phase of a suspension. It is applied, for example, in the paper industry [Mattsson et al., 2012], in the biotechnology industry [Gözke and Posten, 2010, Sievers et al., 2015, Rhea et al., 2017], in the dewatering of sewage sludge [Shi et al., 2020], or in the food and beverage sector [Bayindirli et al., 1989, Salmela and Oja, 2006, Tippmann et al., 2010]. The principle of cake filtration is the deposition of particles on a filter medium on which a filter cake is formed. In most cases, the filter cake is compressible, which means that its porosity and thus the resistance to flow are affected during filtration [Alles and Anlauf, 2003]. Because a high flow rate is important to achieve efficient and economical separation, compression of the cake must be avoided. Thus, cake compaction plays an important role in filtration, especially with multilayered filter cakes. This type of filter cake is a result of a wide particle size distribution of the suspension in combination with particle settling. If a high-resistance fine particle layer settles on top of the coarse particles of the cake, a compaction of the compressible bottom layer is to be expected. Up to now, compression in multilayered cakes has not yet been studied in detail. Therefore, the formation and characteristics of the multilayered filter cake are described in this thesis. The compression mechanism is investigated and measures to prevent the compression are presented.

Basic principles of filtration and compression of filter cakes are described in the following. The importance of fine particles and the influence of their particle size on the filtration process is shown. Then, the basic knowledge about multilayered filter cakes is summarized. An overview of the lautering process, which serves as a prominent example of filtration with a multilayered cake, is given. Finally, the hypotheses and outline of the thesis are presented.

1.1 Basic Principles of Cake Filtration

The principle of filtration is the separation of a suspension into the solid and the liquid phase using a filter medium. It can be divided into two types: depth and surface filtration. In depth filtration, particles are retained within the filter medium, while in surface filtration, the particles are deposited on the filter medium. Surface filtration can be further subdivided into cross-flow, blocking, and cake filtration, the latter being of particular interest for this thesis. In cake filtration, retained particles form a filter cake, which then serves as filter medium for smaller particles [Luckert, 2004].

The flow through a filter cake can be described according to Darcy's law as through a porous medium [Darcy, 1856]. The pressure drop across the porous cake (Δp_1) is proportional to the flow rate (\dot{V}) per area (A), the cake height (h), and the liquids dynamic viscosity (η) according to

$$\Delta p_1 = \frac{\dot{V}}{A} \cdot h \cdot \eta \cdot \alpha_h \quad (1.1)$$

with the specific filter cake resistance (α_h) as the reciprocal value of the permeability (K):

$$K = \frac{1}{\alpha_h}. \quad (1.2)$$

The height of the filter cake is often difficult to determine in filtration experiments. Therefore, it is convenient to describe the cake height as mass of solids (m) per unit area [Ripperger et al., 2012]. The mass-related specific filter cake resistance (α_m) is then used in a different form of Equation 1.1:

$$\Delta p_1 = \frac{\dot{V}}{A} \cdot \frac{m}{A} \cdot \eta \cdot \alpha_m. \quad (1.3)$$

In addition to the pressure drop across the filter cake, there is a pressure drop in the filter medium (Δp_2) that is described by its resistance (β) [Ripperger et al., 2012]:

$$\Delta p_2 = \frac{\dot{V}}{A} \cdot \eta \cdot \beta. \quad (1.4)$$

The combination of Equations 1.1 and 1.4 gives the total pressure drop (Δp) of the filtration process:

$$\Delta p = \Delta p_1 + \Delta p_2 = \frac{\dot{V}}{A} \cdot \eta \cdot (h \cdot \alpha_h + \beta). \quad (1.5)$$

1 Introduction

The resistance of the filter medium is often low compared with the cake and can be neglected in practical processes. More importantly, the resistance of the filter cake gives an indication of the ease with which the liquid flows through the cake. Based on the work of Kozeny [Kozeny, 1927] and Carman [Carman, 1937], the filter cake resistance can be approximated for a cake consisting of monosized spherical particles according to

$$\alpha_h = k_{KC} \cdot \frac{(1 - \epsilon)^2 \cdot 36}{\epsilon^3 \cdot D_{3,2}^2}. \quad (1.6)$$

The resistance depends on the particles Sauter diameter ($D_{3,2}$) and the Kozeny-Carman factor (k_{KC}), which has to be determined experimentally [Luckert, 2004]. The porosity (ϵ) is the ratio of void volume (V_{void}) to total volume (V_{total}) [Stieß, 1995a]:

$$\epsilon = \frac{V_{void}}{V_{total}}. \quad (1.7)$$

In general, Equation 1.6 shows that the filter cake resistance can be influenced mainly by two parameters: cake porosity and particle size. Due to the great influence of these parameters on the resistance and thus on the filtration behavior, cake porosity and particle size effects are described in detail in the following (Sections 1.2 and 1.3, respectively). When sedimentation is involved in filtration, the settling velocities of the particles can be taken into account, e.g., to predict the filter cake resistance [Bockstal et al., 1985] or the influence on the cake formation. An overview of the basic principles of sedimentation is given in Section 1.4.

1.2 Porosity Reduction in Compressible Filter Cakes

Most filter cakes are compressible, which means that their structure compacts during filtration [Tiller et al., 1987, Alles and Anlauf, 2003]. The compaction is based on the flowing liquids drag force that causes a compressive pressure (p_S) on the particles. This compressive stress is transmitted via contact points from particle to particle. A corresponding drop in the hydraulic pressure (p_L) results according to [Tiller et al., 1972]

$$dp_S = -dp_L. \quad (1.8)$$

At a certain height within the cake, the sum of both pressures corresponds to the total pressure (p_{tot}) applied [Luckert, 2004]:

$$p_S + p_L = p_{tot}. \quad (1.9)$$

1 Introduction

The compaction reduces the average porosity and thus increases the filter cake resistance, which can be expressed by empirical equations according to

$$(1 - \epsilon) = (1 - \epsilon_0) \cdot \left(1 + \frac{p_S}{p_0}\right)^u \quad (1.10)$$

and

$$\alpha_m = \alpha_{m,0} \cdot \left(1 + \frac{p_S}{p_0}\right)^v, \quad (1.11)$$

where $\alpha_{m,0}$ describes the mass related filter cake resistance and ϵ_0 the porosity at the normalization pressure (p_0 , empirical parameter) [Tiller et al., 1987, Alles and Anlauf, 2003]. The exponents u and v are coefficients used to express the compressibility of the cake. For incompressible cakes, v is equal to zero and increases to a value of one for a slightly to highly compressible material. As a general rule, v is four times larger than u [Tiller et al., 1987].

Hydraulic and compressive pressure vary not only in the course of filtration but also within the filter cake. In direction to the filter medium, the pressure on the particles rises and reaches a maximum at the filter medium [Tiller and Green, 1973, Tiller et al., 1987]. Consequently, the porosity is at a maximum at the cake surface layer and decreases in the direction of the filter medium. As the pressure difference increases during filtration, the cake porosity next to the filter medium continues to decrease. Consequently, a skin layer with high filter cake resistance develops in the area close to the filter medium [Lu et al., 1998]. The formation of this skin layer is particularly pronounced in highly compressible cakes [Tiller and Green, 1973, Tiller et al., 1987].

In summary, a structurally inhomogeneous cake with regard to porosity and filter cake resistance can be caused by compaction during the filtration with compressible material. However, these concepts of compression described in the literature were developed for the filtration of suspensions with homogeneous particle sizes. For the filtration of suspensions with a wide particle size distribution, differences in the settling velocity of the various particles also influence the structure of the cake. The resulting formation of structurally inhomogeneous multilayered filter cakes is described in Section 1.4.

1.3 Influence of Particle Size on the Filter Cake Resistance

Suspensions are often characterized by analyzing the particle size distribution, which provides information about their physical properties (e.g., resistance to flow). A description of these properties often requires a single number that identifies the relevant

1 Introduction

parameters of the particle size distribution [ISO, 2014]. In the following, different types of descriptors for the particle size and the width of the particle size distribution are described. In order to change the physical properties of the suspension, methods for influencing these descriptors are summarized.

Percentiles are often used to describe the particle size distribution. In general, D_x refers to the diameter at which x percent of the particles in the distribution are smaller. The median (D_{50}) is defined as the size at which half of the particles reside below this point [Stieß, 1995a]. Other common percentiles are the D_{10} and D_{90} , which describe the finest and coarsest parts of the distribution, respectively.

The mode is the particle size that appears most frequently in the distribution. Distributions with two maxima are called bimodal, while multimodal distributions have multiple maxima [Stieß, 1995a].

Another way of describing the particle size distribution are moment (or weighted) mean values. They describe the center of gravity around which the particle size distribution revolves. The general definition of moment mean sizes is

$$D_{p,q} = \left[\frac{\sum_i n_i D_i^p}{\sum_i n_i D_i^q} \right]^{1/(p-q)}, \text{ if } p \neq q \quad (1.12)$$

with D_i as the i -th size classes midpoint and n_i as the number of particles in the i -th size class. The exponents p and q can be any numerical value. For example, the De Brouckere mean diameter ($D_{4,3}$) describes the volume-weighted mean particle size. The previously described (Equation 1.6) Sauter diameter ($D_{3,2}$) is the area-weighted mean size, which is inversely proportional to the volume specific surface area (S_V) [ISO, 2014]:

$$D_{3,2} = \frac{6}{S_V}. \quad (1.13)$$

The Sauter diameter is an important characteristic to describe the particles influence on the filter cake resistance. Equation 1.6 shows that in general a large particle size is required for a low resistance to flow.

Not only the mean size, but also parameters such as the particle shape [Li and Ma, 2011, Bourcier et al., 2016] or the particle size distribution [Kinnarinen et al., 2015, Kinnarinen et al., 2017] can affect the resistance to flow. According to Bourcier et al. [Bourcier et al., 2016], however, the particle shape is only important if it deviates significantly from cubic particles (e.g., for needles). This is supported by Taylor et al. [Taylor et al., 2019] who showed that changes in the particle size distribution are a more relevant parameter than particle shape. In addition, particle shape is rather important

1 Introduction

for large particle sizes. For small sizes ($<10\text{--}20\ \mu\text{m}$), particle aggregation determines the cake porosity [Tiller et al., 1987]. Therefore, it can be concluded that the particle size distribution is one of the most important particle characteristic (in addition to the mean particle size) that influences the porosity and thus the filter cake resistance.

Sohn and Moreland [Sohn and Moreland, 1968] investigated the influence of the particle size distribution on the packing density (ϕ), which is related to porosity according to

$$\phi = 1 - \epsilon. \quad (1.14)$$

They came to the conclusion that the packing density and thus the porosity depends on the size distribution of the system (expressed as dimensionless standard deviation) and is independent of the mean particle size. Hence, this influence of the particle size distribution on the cake porosity affects the resistance according to Equation 1.6 under the assumption of a constant mean particle size. These results are supported by Kinnarinen et al. [Kinnarinen et al., 2015, Kinnarinen et al., 2017] who showed that the width of the size distribution has a strong correlation with the porosity. As a result, a lower cake resistance was found for a narrower particle size distribution even when the mean particle size was reduced.

Differences in the porosity for various particle size distributions can be explained by the cavern effect [Sohn and Moreland, 1968, Hwang et al., 1997, Lu et al., 1998]. The presence of a wide range of different particle sizes (poly-disperse) results in voids between larger particles being occupied by smaller particles (Figure 1.1, a, assuming that no sedimentation effects occur). In contrast, a uniform particle size distribution (mono-disperse) results in larger voids within the cake structure (Figure 1.1, b). Compared with a mono-dispersed size distribution, the cake structure is more compact for a poly-dispersed distribution. The resulting decrease in porosity hinders the liquid flow and increases the resistance [Lu et al., 1998].

The cavern effect shows that not only the mean particle size but also the entire particle size distribution must be taken into account for an evaluation of the filter cake resistance. Therefore, descriptors are required to describe the width of the particle size distribution. Kinnarinen et al. [Kinnarinen et al., 2015, Kinnarinen et al., 2017] used the span

$$\text{span} = \frac{D_{90} - D_{10}}{D_{50}} \quad (1.15)$$

1 Introduction

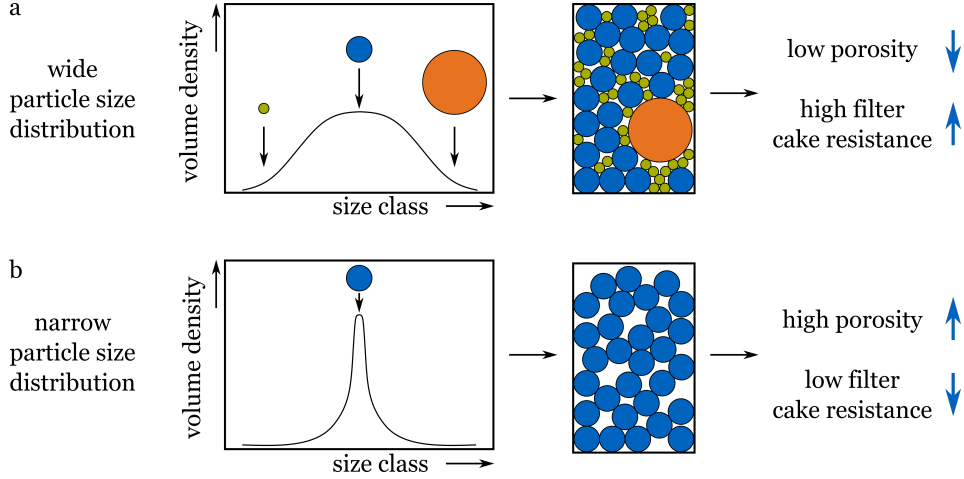


Figure 1.1: Comparison of the particle size distributions of poly- (a) and mono-dispersed (b) suspensions. Corresponding filter cakes are illustrated and the influence on porosity and filter cake resistance are indicated. Figure modified from the literature [Hennemann et al., 2021a].

and the difference between volume- and area-weighted mean size ($D_{4,3} - D_{3,2}$) as descriptors of the width. Another descriptor for a log-normal particle size distribution is the geometric standard deviation (σ_g) [Papastefanou, 2012]

$$\sigma_g = \frac{D_{84.13}}{D_{50}} = \frac{D_{50}}{D_{15.87}}, \quad (1.16)$$

which becomes

$$\sigma_g = \sqrt{\frac{D_{84.13}}{D_{15.87}}} \quad (1.17)$$

for bimodal size distributions. A common descriptor of the particle size distribution that is used, e.g., in soil mechanics and for sand filters, is the coefficient of uniformity (C_u) [Sohn and Moreland, 1968, Holtz and Kovacs, 1981, Taylor et al., 2019]:

$$C_u = \frac{D_{60}}{D_{10}}. \quad (1.18)$$

The particle sizes and thus the width of the size distribution of a suspension can be manipulated in order to affect the physical properties. This can be achieved by altering the agglomeration or de-agglomeration behavior of the particles through chemical or physical influences. One type of physical influence is the particle agglomeration due to increasing temperature, e.g., via denaturation of the particles protein fraction. Bühler et al. [Bühler et al., 1995, Bühler et al., 1996b] showed that the mean particle size of a

1 Introduction

biological suspension can be increased by elevated temperatures. This lowered the filter cake resistance and improved the filtration process. On the other hand, agitation was shown to affect the particle size by mechanical attrition [Tse et al., 2003]. The resulting reduction of the mean particle size decreased the filterability [Bühler et al., 1995].

Chemical influences on the interparticle forces are another way to affect particle sizes. Interparticle forces determine the stability and thus the particle agglomeration behavior in suspensions. These forces predominate for particles smaller than 10–20 μm , where the surface area to volume ratio is high and gravitational forces can be neglected [Tiller et al., 1987]. A modification of the electrostatic forces to influence the stability of the suspension can change the particle size, which then affects the porosity and resistance of the filter cake [Roth, 1991]. This was confirmed, e.g., for inorganic powder [Hieke et al., 2009] or biopolymers [Hofmann and Posten, 2003]. Interparticle forces can be distinguished into repulsive and attractive forces. This effect was first described by Derjaguin, Landau, Verwey, and Overbeek [Derjaguin and Landau, 1941, Verwey and Overbeek, 1948]. The repulsion is based on the electrically charged particle surface and its magnitude is quantified by the zeta potential. The electrical charge depends on the pH value and the ion content of the surrounding liquid. With a high surface charge (high zeta potential), strong repulsive forces prevent the accumulation of particles. If there are no electrical charges at a zeta potential of zero (isoelectric point), there is no repulsion and particles can agglomerate due to opposing forces of attraction. This attraction is based on van der Waals forces and increases when the distance between two particles decreases [Ripperger et al., 2012]. When repulsive forces prevail, the suspension is stable and particles remain dispersed (Figure 1.2, a). In contrast, particles agglomerate in unstable suspensions when attractive forces dominate (Figure 1.2, b) [Roth, 1991]. Unstable suspensions result in high porosity filter cakes that can be easily compacted, while filter cakes made from stable suspensions are usually more compact (Figure 1.2).

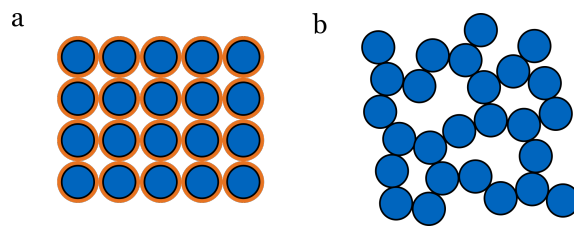


Figure 1.2: Comparison of filter cakes from stable (a) and unstable (b) suspensions. Orange circles indicate repulsive electrostatic forces that prevent particles (blue dots) from agglomeration in stable suspensions.

1 Introduction

Another way to influence the particle size is the addition of flocculants. Due to floc formation, the size of particle agglomerates increases, which improves the filtration process. This is known for the water treatment process [Jiao et al., 2017] and was also shown to be valid for the filtration of biological suspensions [Bandelt Riess et al., 2018].

The particle size distribution not only influences the porosity of the filter cake. It also affects the cake structure due to differences in particle settling of the various size classes, which is described in the following section.

1.4 Formation and Characteristics of Multilayered Cakes

A suspension that consists of particles with uniform size leads to a homogeneously structured filter cake when compression effects are neglected. Often, however, there are different particle sizes present, e.g., as with a bi- or multimodal size distribution. Differences in the size and density of the particles influence their settling velocity and can lead to the formation of multilayered filter cakes. This effect is particularly pronounced when there is a sedimentation rest prior to the filtration [Lu et al., 1998]. In the following, the theoretical aspects of particle sedimentation are summarized. Afterwards, the impact of a wide particle size distribution on the formation of the filter cake is described. The special case of a multilayered cake and its characteristics are presented.

Three forces act on a stationary settling particle: the gravitational force, the buoyancy force, and the frictional force [Draxler and Siebenhofer, 2014]. Equating these forces gives the general relationship between the settling velocity (w_f) of a spherical particle and its diameter (d):

$$w_f = \sqrt{\frac{4}{3} \cdot \frac{d \cdot g \cdot (\rho_p - \rho_f)}{c_w \cdot \rho_f}}. \quad (1.19)$$

The settling velocity also depends on the gravitational acceleration (g) as well as the density difference between the particle (ρ_p) and the fluid (ρ_f). The drag coefficient (c_w) is a function of the Reynolds number (Re) and can be calculated for $0 < Re < 10^5$ according to Martin [Martin, 1980]:

$$c_w = \frac{1}{3} \cdot \left(\sqrt{\frac{72}{Re}} + 1 \right)^2 \quad (1.20)$$

with

1 Introduction

$$Re = \frac{w_f \cdot d \cdot \rho_f}{\eta}. \quad (1.21)$$

For particles with a diameter of up to about 100 μm , there is a laminar flow (Stokes area, $Re < 0.25$) and the settling velocity can be calculated according to

$$w_f = \frac{d^2 \cdot g \cdot (\rho_p - \rho_f)}{18 \cdot \eta}. \quad (1.22)$$

The Reynolds number increases with increasing particle size and is then described by the transition area ($0.25 \leq Re \leq 2 \cdot 10^3$), which has to be determined analytically or numerically. For the Newtonian area ($2 \cdot 10^3 \leq Re \leq 2 \cdot 10^5$), the settling velocity can be approximated based on [Stieß, 1995b]

$$w_f = 1.74 \cdot \sqrt{\frac{(\rho_p - \rho_f)}{\rho_f} \cdot g \cdot d}. \quad (1.23)$$

The sedimentation process also depends on the particle shape. Non-spherical particles have a higher frictional force compared with ideal spheres, which reduces the settling velocity [Draxler and Siebenhofer, 2014]. Correction can be made by multiplying the settling velocity with a shape factor [Wadell, 1935]. Typical shape factors are, e.g., 0.81 for rounded and 0.61 for elongated particles [Draxler and Siebenhofer, 2014].

The concentration of the suspension can also affect the settling. For a dilute suspension, the settling of particles is independent. With an increasing concentration, small particles impede the settling of faster moving larger particles. As a result, the point of zone sedimentation is reached at which all particles have the same relative settling velocity [Tiller et al., 1995]. The influence of the concentration can be corrected according to Richardson and Zaki [Richardson and Zaki, 1954] by multiplying the settling velocity with a concentration factor (δ), which depends on the suspension concentration (C):

$$\delta = (1 - C)^{\gamma(Re)}. \quad (1.24)$$

The Reynolds number-dependent exponent (γ) has a value of 4.65 for $Re < 0.5$ and 2.4 for the Newtonian area [Draxler and Siebenhofer, 2014].

In summary, the sedimentation process depends on various characteristics of the suspension: the difference in density between liquid and particles, the particle shape, the suspension concentration, and the particle size. The dependence of the settling velocity on the Reynolds number, which is a function of the particle size (Equation 1.21), shows that the size has a great influence. This is especially important when a wide range

1 Introduction

of different sizes is present in the suspension, which leads to different settling rates of the individual particles (at a low concentration in the absence of zone sedimentation). Smaller particles settle later than larger particles. In addition, there is a relative motion between the fine and large particles. The higher settling velocity of larger particles generates an upward flow of the liquid, which hinders the finer particles from settling [Lu et al., 1998].

The differences in the particles settling rates play a special role when sedimentation effects are present prior to the filtration because it impacts the structure of the filter cake. This was investigated by Lu et al. [Lu et al., 1998], who examined the differences in particle settling between gravity filtration and sedimentation. In sedimentation, only the upward frictional force and the downward force based on the particle weight affect the process. In gravity filtration, an additional frictional drag due to the flow of liquid increases the downward movement of the particle. This reduces the relative settling velocity between particles of different sizes. As a result, filter cakes are more homogeneous in gravity filtration compared with sedimentation [Lu et al., 1998]. Consequently, sedimentation processes can affect the structural composition of the filter cake if there are different particle sizes in the suspension (Figure 1.3, a). For the ideal case when there is no sedimentation effect, a filter cake with a homogeneous distribution of the particles along its height results (Figure 1.3, b). If there is a sedimentation rest prior to the filtration, a multilayered filter cake can result based on the differences in the settling rates of the individual particles. In a dual-dispersed suspension, a bottom layer consisting of larger particles is formed, on which a fine particle layer is then deposited (Figure 1.3, c).

In general, fine particles can flow through voids in a porous filter cake. Under the assumption that the bottom layer serves as filter medium for the upper layer particles, fine particles are retained at the top during filtration. In this case, no migration of fine particles into the lower layer occurs according to the literature [Engstle et al., 2017, Hennemann et al., 2021b]. The fine particles, which usually have the lowest permeability [Tiller et al., 1987], then accumulate on the top of the filter cake. In contrast to filtration with homogeneously layered filter cakes, the position of the highest resistance to flow is therefore in multilayered filter cakes at the top. A highly compressed skin layer, which leads to a high resistance next to the filter medium in homogeneous filter cakes (Section 1.2), has therefore only a reduced impact in multilayered filter cakes.

The formation of multilayered filter cakes was confirmed in the literature, e.g., for simulations [Lu et al., 1998] as well as suspensions of drilling fluids [Yao et al., 2014] or alumina and limestone [Löwer et al., 2020]. Another prominent example for filtration with a multilayered filter cake is the lautering process in beer production [Engstle et al.,

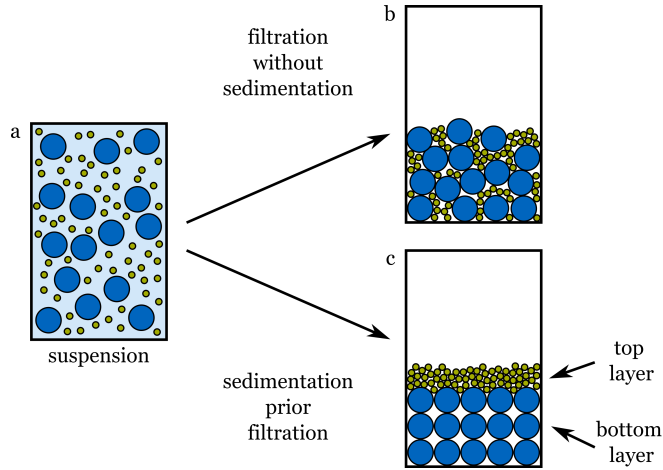


Figure 1.3: Illustration of a homogeneous, dual-dispersed suspension (**a**), which forms a homogeneous filter cake (**b**) without and a multilayered filter cake (**c**) with the influence of particle sedimentation prior to the filtration. Particles are assumed to be incompressible and no zone sedimentation occurs. Figure prepared according to Lu et al. [Lu et al., 1998].

2017]. In addition, not only the structure of filter cakes, but also other types of packed beds are influenced by sedimentation effects. For example, wide particle size distributions can lead to gradients in the packing density of chromatography columns [Carta and Jungbauer, 2020].

The compression mechanism and the influence of the resistance of the fine particles in multilayered filter cakes is currently insufficiently investigated in the literature. Therefore, this work sheds light on the influence of the characteristics of the different filter cake layers and their impact on the filtration process. The lautering process in beer production, which is described in the next section, serves as example in this thesis to investigate the multilayered filter cakes.

1.5 The Lautering Process in Beer Production

Beer production begins with the raw material malt. Malt is processed grain, which is germinated and then dried by kilning in a malting plant [Narziß and Back, 2009]. In the brewery, the first step is grinding of the malt to break up the grains. The malt grist is mixed with water during the mashing process, in which the soluble malt components are transferred into the liquid phase of the mash. Substances of interest from the malt are mainly fermentable sugars but also, e.g., degradation products of proteins, non-starch polysaccharides (β -glucan, arabinoxylan), or fatty acids. The different substances are

1 Introduction

extracted from the solid by means of enzymatic degradation at different temperatures. The degradation of these substances affects the extract yield, the product quality, and the processability in the subsequent production steps [Narziß and Back, 2009]. For example, the degree of modification can influence the filtration rate [Muts and Pesman, 1986, Gastl et al., 2020b]. After mashing, the liquid phase of the suspension that is used for the following production steps, the wort, is separated from the solids in a cake filtration process: the lautering [Narziß and Back, 2009].

Lautering is usually carried out using either the lauter tun or the mash filter [Tippmann et al., 2010, Tippmann and Becker, 2016]. Among these separation devices, the lauter tun is a special type of filtration based on the presence of a multilayered filter cake [Engstle et al., 2017]. Therefore, in this work, filtration with the lauter tun was used as an example for investigating this type of filter cake.

A lauter tun is a filter that consists of a slotted false bottom, which serves as filter medium to hold back the mash particles (Figure 1.4) [Tippmann and Becker, 2016]. The housing of the lauter tun is insulated to maintain the high mash temperatures of up to 78 °C [Narziß and Back, 2009].

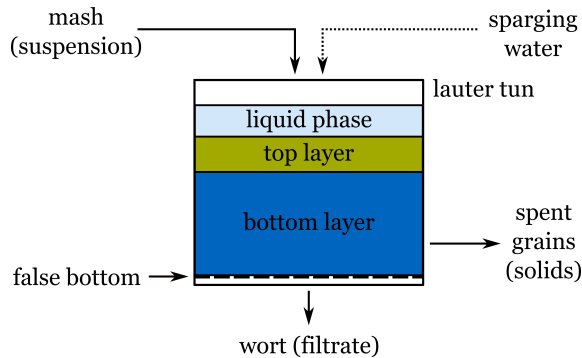


Figure 1.4: Scheme of filtration with the lauter tun. Mash is transferred to the filter and forms a filter cake consisting of a top layer (fine particles) and a bottom layer (coarse particles) on the false bottom (filter medium). After filtration of the first wort, the cake is washed with sparging water. The spent grains are disposed at the end of the process. Figure modified from the literature [Hennemann et al., 2019].

The procedure with the lauter tun consists of different steps [Kunze, 2004, Narziß and Back, 2009]. Overlaying the false bottom with hot water is the first step to heat the lauter tun. This also ensures that no air is entrapped under the false bottom, which would lead to an inhomogeneous extraction process. Mash is then transferred from the mash tun to the lauter tun via inlet valves from below. Immediately after the mash transfer, a multilayered filter cake forms on the false bottom (Figure 1.4) [Tippmann et al., 2010, Engstle et al., 2017]. The formation of the different layers is

1 Introduction

usually supported by a sedimentation rest. At the beginning of filtration, cloudy wort with high turbidity is located under the false bottom and is recirculated back below the liquid level until the filtrate is clear. Then, the filtration of the first wort starts, which is collected in the wort kettle. The cake structure is loosened during filtration using vertically rotating raking knives to reduce the blockage of the filter cake and maintain a high flow rate. When the liquid level reaches the top of the filter cake, hot sparging water is applied to wash the cake. After run-off of this second wort, filtration is finished and the remaining solids, the spent grains, are disposed. The wort is then processed into the final product beer in the following steps [Kunze, 2004, Narziß and Back, 2009]. Although a total processing time of around two hours can be achieved with modern lauter tuns [Tippmann et al., 2010], lautering is usually the time-limiting step in wort production (depending on the mashing process).

The formation of the multilayered cake in the lauter tun is due to the different particle sizes in the mash, which depends on the grinding of the malt grain. Grinding is carried out using a roller mill to preserve the husks of the malt that serve as filter medium [Narziß and Back, 2009]. Consequently, there is a wide particle size distribution (nano- to milli-meter sizes) in the mash [Tippmann et al., 2011], which consists of small fine particles (e.g., starch granules) and larger fragments (e.g., husks) [Narziß and Back, 2009]. Compared with the particle sizes in other filtration areas [Droppo, 2006], the size range in mash is particularly large. A filter cake with different layers parallel to the filter medium results [Bühler, 1996, Engstle et al., 2017, Hennemann et al., 2021c]. Coarse particles settle first and form a compressible bottom layer; fine particles settle later on top of this bottom layer. The fine particles are retained by the bottom layer through the cake filtration mechanism and there is no migration of small particles from the top into the bottom layer during the filtration [Engstle et al., 2017, Hennemann et al., 2021b]. The result is a filter cake with a height of around 30–35 cm [Narziß and Back, 2009].

One has to take into account that there is no clear separation between particles in the upper and lower layers [Bühler, 1996]. Fine particles can also be found in a concentration of around 10–20% in the bottom layer [Engstle et al., 2015]. This is due to zone sedimentation before filtration starts based on the high concentration of mash (up to a solid-liquid ratio of 1:2.5 [Narziß and Back, 2009]). In addition, there are already fine particles present in the bottom layer before sedimentation begins because the mash is pumped into the lauter tun from below. Nevertheless, the largest amount of fine particles is located within the top region of the filter cake [Engstle et al., 2015, Engstle et al., 2017].

1 Introduction

Fine particles of the mash consist in a high concentration of proteins, which negatively affect the flow rate [Barrett et al., 1975, Lewis and Oh, 1985, Muts and Pesman, 1986]. According to Moonen et al. [Moonen et al., 1987], this is due to the high molecular weight gelproteins that form networks via disulfide bridges. The effect is even more pronounced when the gelprotein network is expanded through oxidation [Muts and Pesman, 1986], which is why the input of oxygen has to be avoided during mashing and lautering [Narziß and Back, 2009]. It has been shown that removing the protein layer around the small starch particles increases the permeability of the filter cake [Barrett et al., 1973], which confirms the great influence of proteins on the flow rate. In addition, the high resistance of the fine particles depends on their small size. A larger amount of small particles, e.g., small starch molecules, increases therefore the filtration time [Barrett et al., 1973]. The fine particles can change in size through aggregation of proteins at high temperatures, which leads to an increase in the flow rate [Bühler et al., 1996b, Engstle and Först, 2015]. In contrast, a decrease in the particle size through attrition decreases the flow rate [Bühler et al., 1995]. An influence on the surface forces of the fine particles by changing the pH value also changes the filtration behavior [Engstle and Först, 2015]. However, the reasons for the particle size-related changes in the flow rate are currently only insufficiently investigated.

The differences in the composition between the top and bottom layer influences their filtration characteristics. The permeability of the top layer is significantly lower compared with the bottom layer [Bühler, 1996, Bühler et al., 1996a, Engstle et al., 2015]. In addition, both layers are compressible [Bühler et al., 1996a, Engstle et al., 2014]. In combination with the location of the highest resistance to flow on the top of this multilayered filter cake, the compression of the bottom layer depends on the fine particle layer. This effect was first suggested by Bühler et al. [Bühler, 1996, Bühler et al., 1996a]. So far, however, this has not been confirmed by experiments in the literature, neither for lautering nor for other filtration processes. Additionally, the consequences of the cake compression on the filtration process is unknown. Therefore, one aim of this thesis was the investigation of the cake compression in multilayered filter cakes, which depends on the fine particles at the top.

1.6 Hypotheses

It is hypothesized that filtration of mono-dispersed suspensions differs from those with dual- or poly-dispersed particle sizes. In the case of mono-dispersed suspensions, a homogeneous filter cake forms (Figure 1.5, a, t_0). In this type of cake, the highest

1 Introduction

pressure drop occurs next to the filter medium due to the increasing compressive pressure at this location (Section 1.2). The resulting reduction in the porosity based on this compression increases the filter cake resistance at this skin layer (Figure 1.5, a, t_1). Therefore, the skin effect determines the flow rate in compressible filter cakes from suspensions with homogeneous particle sizes [Tiller and Green, 1973].

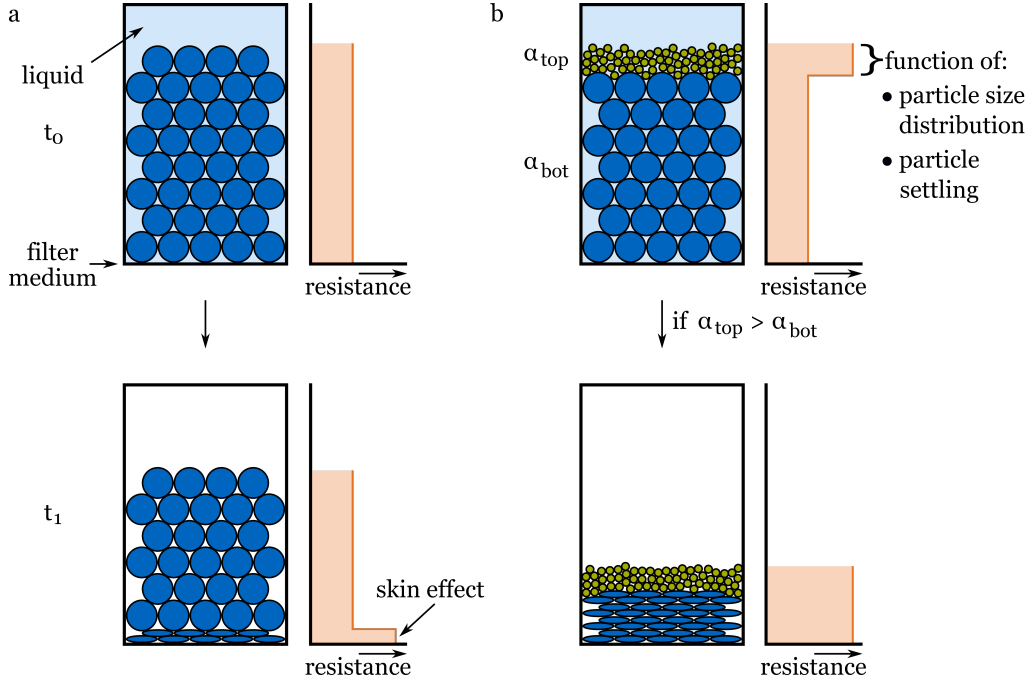


Figure 1.5: Comparison of the filter cake structure of suspensions with mono-dispersed particles that form a homogeneous (a) and dual-dispersed particles that form a multilayered (b) compressible filter cake. Compression in the multilayered filter cake occurs when the resistance in the top layer (α_{top}) is higher compared with the bottom layer (α_{bot}). The states before (t_0) and after (t_1) filtration are shown. The cake compression is illustrated and the filter cake resistance (orange) along the height is indicated. No migration of particles from the top layer into the bottom layer as well as complete particle settling prior to the filtration are assumed. The compression of the particles in the top layer is neglected in this illustration.

In contrast, a dual- or poly-dispersed suspension that is exposed to sedimentation can lead to the formation of a multilayered filter cake because of differences in the settling velocities of the individual particles (Figure 1.5, b, t_0) [Lu et al., 1998]. The hypothesis is that if the filter cake resistance of the top layer is less than or equal to that of the bottom layer, the compression behavior is similar to that of the homogeneous cake. However, if the filter cake resistance of the top layer is greater than that of the bottom layer, the highest pressure difference is located at the top of the cake. During filtration, the

1 Introduction

differential pressure pulls the top layer downwards (similar to a piston in the expression of filter cakes [Shirato et al., 1970]). This compression decreases the porosity of the bottom layer, which increases the resistance of the entire filter cake and adversely affects the flow rate (Figure 1.5, b, t_1). Because the compressive pressure based on the liquids drag force is low at the top of the cake (Section 1.2), the compression of the fine particle layer is neglected. A retention of fine particles by the bottom layer is assumed [Engstle et al., 2017, Hennemann et al., 2021b]. Hence, there is no particle migration into the bottom layer.

The degree of compression of the multilayered filter cake depends on the resistance of the top layer. With a high resistance of the fine particles, the top layer is assumed to act as a stiff layer that compresses the bottom layer. A high resistance results in a higher compression compared with a low resistance. Small sizes of fine particles at the top generally result in a higher resistance compared with larger particles (Equation 1.6). In addition to the mean particles size, the particle size distribution determines the porosity and thus the resistance (Figure 1.1). This particle size effect is known for suspensions of inorganic materials [Kinnarinen et al., 2015, Kinnarinen et al., 2017]. However, it has not yet been confirmed for suspensions made from biological material (e.g., mash). Differences in the filtration behavior of these suspensions were only explained by the influence of the mean particle size [Bühler et al., 1995, Bühler et al., 1996b]. Therefore, an influence on the particle size distribution of the fine particles in the biological suspension under investigation is expected to influence the resistance of the top layer of the multilayered filter cake. This influence can be based on agglomeration or de-agglomeration through physical or chemical modifications of the suspension (Section 1.3).

The resistance of the top layer is further expected to depend on the particle settling behavior. Due to the small particle size, the settling of fine particles is strongly influenced by changes in the viscosity and density of the liquid (Equation 1.19). Both parameters are affected by temperature. Therefore, high temperatures, which are usually applied during lautering, influence the settling velocity and thus the resistance of the fine particle layer. This is expected to affect the compression of the bottom layer.

It is further assumed that a removal of the fine particles at the top of the filter cake prior to the filtration reduces the compression of the bottom layer. Thus, a higher flow rate is expected.

1.7 Thesis Outline

Mash separation using the lauter tun serves as an example in this thesis to investigate the compression in multilayered filter cakes and the role of the fine particle layer on this process. The thesis is structured as follows:

1. Formation and characteristics of the multiple cake layers
 - The formation of the multiple layers of the lauter tun filter cake is revealed in a literature review. The cake formation due to sedimentation effects is investigated by determining differences in the settling velocities of the various particle sizes of the suspension.
 - An impact of temperature on the particle settling and thus cake formation is investigated.
 - Structural and chemical characteristics of the different filter cake layers are described.
2. Compression effects in multilayered cakes
 - The compression of the bottom layer caused by the fine particle layer during filtration is examined. An optical method for porosity measurement is established to determine the cake compression.
 - A model is used to confirm the compression in the multilayered cake and to investigate the underlying mechanism.
 - Different types of fine particles are tested to verify the universal validity of the compression.
3. Prevention of compression in multilayered cakes
 - Structural and chemical characteristics of the fine particles are determined.
 - Physical and chemical modifications to influence the resistance of the fine particle layer are applied. Reasons for the high resistance of the fine particles in terms of particle size effects are evaluated and a model suspension is used for verification.
 - The influence of temperature on the resistance of the fine particle layer is investigated.
 - A filtration technique is developed to avoid the compression in multilayered filter cakes.

2 Methods

The mashing procedures to produce the suspensions for the filtration tests were described in Sections 3.2.2, 3.2.3, and 3.2.5. Grinding of the malt was constant in all experiments to maintain constant conditions in terms of particle sizes, unless otherwise stated.

Filtration tests can be distinguished according to the scale of the filter. A small scale filter was used to determine the filter cake resistance of fine particles according to the Verein deutscher Ingenieure [VDI, 2010] (Sections 3.2.4 and 3.2.5). Flow rate, filter cake height, cake compression, and differential pressure were determined using mid (Sections 3.2.2 and 3.2.3) or large scale filters (Sections 3.2.3 and 3.2.4). Lab scale lautering tests were carried out without washing the cake and the use of raking knives to prevent an influence on the cake structure. A new filtration technique and its upscale on a pilot plant is described in Section 3.2.3.

Fine particles were separated from the mash by wet sieving as described in Sections 3.2.2, 3.2.3, and 3.2.5. Chemical analysis of particles and filtrate were carried out (Table 2.1).

Table 2.1: Chemical analysis of particles and filtrate.

Analysis	Method/principle	Sections
Arabinoxylan	Douglas method [Kiszonas et al., 2012]	3.2.5
Ash	Combustion	3.2.5
β -Glucan	Enzymatic assay	3.2.5
Iodine value	MEBAK [Miedaner, 2002]	3.2.3
Lipids, polyphenols	Soxhlet extraction	3.2.5
Protein	Dumas	3.2.5
Starch	Enzymatic assay	3.2.5
Washable extract	MEBAK [Miedaner, 2002]	3.2.3

Physical and chemical modifications of mash and fine particles as well as the use of different malt types are described in Sections 3.2.3 and 3.2.5. Unless stated otherwise, the same malt batch was used in all trials to maintain constant parameters of the suspension

2 Methods

(e.g., density and viscosity). Structural and physical analysis of the suspension, the filtrate, and the particles were performed (Table 2.2).

Table 2.2: Structural and physical analysis of suspension, filtrate, and particles.

Analysis	Method/principle/device	Sections
Fluid density	Pycnometric, density meter	3.2.2, 3.2.3, 3.2.5
Particle structure	Confocal laser scanning microscopy,	3.2.5
	Fourier transform infrared spectroscopy	3.2.5
Particle density	Pycnometric	3.2.2
Particle size distribution	Dynamic image analysis	3.2.2
	Laser diffraction	3.2.2, 3.2.4, 3.2.5
Settling velocity	Stokes' Law, sedimentation test	3.2.2
Turbidity	Turbidimeter	3.2.3
Viscosity	Rheometer	3.2.2, 3.2.5

Fixation and sampling of filter cakes are described in Sections 3.2.3 and 3.2.4. An optical method for the determination of the filter cake porosity via the surface roughness was developed (Section 3.2.3). Model filter cakes used for the verification experiments are described in Sections 3.2.4 and 3.2.5. Characteristics of the filter cakes were determined (Table 2.3).

Table 2.3: Determination of filter cake characteristics.

Analysis	Method/principle	Sections
Compression mechanism	Compression test	3.2.4
Filter cake resistance	Darcy's law	3.2.4, 3.2.5
	Carman-Kozeny	3.2.2, 3.2.4, 3.2.5
Porosity	Gravimetric, volumetric	3.2.2, 3.2.3, 3.2.4, 3.2.5

Statistical analysis were performed to determine significant differences between means using analysis of variance and t-tests. Standard deviations were calculated. Each analysis and experiments were done in triplicates ($n = 3$) and particle size measurements are the average of 30 measurement points ($n = 30$), unless stated otherwise.

3 Results

3.1 Summaries of Thesis Publications

Part I: Inhomogeneity in the Lauter Tun: a Chromatographic View (pages 26–38)

This literature review gives an overview about the formation of the multiple filter cake layers in the lauter tun. Factors that determine the layering, e.g., sedimentation effects or the wide particle size distribution of the mash, are summarized. As a result of the multiple layers, a structurally inhomogeneous filter cake forms. Small fine particles are present in a higher concentration at the top of the cake; coarse particles form the bottom layer. Due to the differences in the chemical composition of the different types of particles, the multiple layers of the filter cake differ also in their chemical composition. The distribution of the different components (e.g., proteins, lipids) within the filter cake is summarized. The degrees of extraction of these substances during filtration were shown using a novel chromatographic view. For example, the filtration-critical protein fraction is only slightly soluble while the greatest amount of starch is extracted from the cake.

Contribution

The doctoral candidate carried out the conception of the study, the literature research, the analysis as well as interpretation of the data, and drafted and revised the manuscript.

Part II: Influence of Temperature on the Filter Cake Resistance in a Lauter Tun (pages 39–45)

Filtration in the lauter tun is usually carried out at high temperatures to reduce the process time. This affects the filtration process in two ways: First, there is an increase in the flow rate due to a decrease in viscosity; secondly, the settling behavior of the particles is influenced, which was assumed to influence the filter cake structure. Especially fine particles at the top of the cake are expected to be influenced by temperature in a high degree. The aim of the study was to investigate this temperature-dependent influence on the structure of the multilayered cake, which then affects the filter cake resistance during filtration. The formation of the different cake layers was investigated by calculating the settling velocities of different particle sizes within the wide size distribution of the mash. Temperatures in a range of 40–78 °C were tested, which revealed an increase in the settling velocity at higher temperatures based on a reduction in viscosity and density of the liquid. While this was confirmed for coarse particles using a sedimentation test, the settling of fine particles was hindered at high temperatures. Because the settling of fine and coarse particles is affected by temperature in different ways, the formation of the multiple cake layers is favored with increasing temperature. A measurement of particle sizes in the supernatant of the cake showed that fine particles remain in suspension due to buoyancy by thermal convection that counteracts settling at increasing temperature. This was confirmed by a high correlation between the buoyancy indicator of the fine particles and temperature. In addition, a high correlation of the buoyancy indicator with the filter cake resistance and flow rate was found, which explains the higher flow rate at high temperatures in addition to a reduction in viscosity.

Contribution

The doctoral candidate designed the study, carried out the literature research, experiments, data analysis and interpretation, statistical analysis, and drafted and revised the manuscript.

Part III: Optical Method for Porosity Determination to Prove the Stamp Effect in Filter Cakes (pages 46–53)

The horizontal layers of the multilayered filter cake in the lauter tun have different characteristics. While the fine layer on top has a high resistance to flow, the bottom layer is highly compressible. It was assumed that the fine particles at the top act as a stiff layer that compresses the bottom layer during filtration (stamp-effect hypothesis), which reduces the porosity of the cake and thus decreases the flow rate. The porosity of the bottom layers was determined as an indicator of the compression. A method was established to preserve the cake structure by freezing. This enabled sampling at different time points during filtration and from different horizontal cake layers. The porosity of the cake samples was then determined via an optical method, which is based on a measurement of the layers surface roughness. Modifications of the fine layer (e.g., oxidation, different raw materials) proved that the compression of the bottom layer during filtration is caused by the top layer. The compression resulted in a reduced flow rate. Because the cake compression has to be avoided during filtration, a filtration technique was developed based on the new findings. Fine particles at the top were removed by suction prior to the filtration, which reduced the cake compression and increased the flow rate.

Contribution

The doctoral candidate designed the study, carried out the literature research, experiments, data analysis and interpretation, statistical analysis, and drafted and revised the manuscript.

Part IV: Compression Mechanism in Multilayered Filter Cakes (pages 54–61)

The high resistance of the top layer of the multilayered filter cake results in a compression of the bottom layer. This was previously shown for the example of the filter cake in the lauter tun. The aim of this study was to verify the universal validity of the compression effect and to investigate the compression mechanism using a model filter cake. The model cake was composed of a compressible glass fiber bottom layer and an artificial top layer. Characteristics of the cake (cake height, porosity, filter cake resistance) and the filtration process (differential pressure) were compared between multilayered and homogeneously layered filter cakes. A volumetric method of porosity measurement was established to investigate the compression. The multilayered filter cake was compressed in a higher degree compared with the homogeneous cake. Compression starts from the top and is then transferred to the lower layers. Different types of top layer particles that differ in their resistance were tested. This showed that if the resistance at the top layer is higher compared with the bottom layer, a compression of the bottom layer resulted. The compression is based on a differential pressure, which pulls the fine particle layer down.

Contribution

The doctoral candidate designed the study, carried out the literature research, experiments, data analysis and interpretation, statistical analysis, and drafted and revised the manuscript.

Part V: Influence of Particle Size Uniformity on the Filter Cake Resistance of Physically and Chemically Modified Fine Particles (pages 62–72)

Fine particles at the top of the multilayered filter cake have a high resistance to flow compared with coarse particles of the bottom layer. According to Carman-Kozeny, the cake porosity and the mean particle size determine the resistance of this top layer. However, the porosity depends on the particle size distribution of the fines. This means that not only the mean particle size but also the entire size distribution must be taken into account when evaluating the resistance. This impact of particle size characteristics on the filter cake resistance was investigated using the example of the fine particles in lautering. Fine particles were separated from the coarse particles of the mash and the chemical composition and structural features of these particles were determined. This enabled the introduction of physical (heating and agitation) and chemical (prevention of oxidation, polyphenol addition, pH adjustment, and ion concentration alteration) modifications. An influence of these modifications on the interparticle interactions resulted in an alteration of the particle size distribution and thus affected the filter cake resistance. It was shown that not only the mean particle size but also the uniformity of the size distribution determines the resistance. A narrow particle size distribution resulted in a lower filter cake resistance compared with a wide distribution. The effect was verified using a glass beads model system.

Contribution

The doctoral candidate designed the study, carried out the literature research, experiments, data analysis and interpretation, statistical analysis, and drafted and revised the manuscript.

3.2 Thesis Publications

3.2.1 Inhomogeneity in the Lauter Tun: a Chromatographic View

European Food Research and Technology (2019) 245:521–533
<https://doi.org/10.1007/s00217-018-03226-4>

REVIEW ARTICLE



Inhomogeneity in the lauter tun: a chromatographic view

Martin Hennemann¹ · Martina Gastl¹ · Thomas Becker¹

Received: 22 October 2018 / Revised: 21 December 2018 / Accepted: 22 December 2018 / Published online: 21 January 2019
 © Springer-Verlag GmbH Germany, part of Springer Nature 2019

Abstract

The purpose of lautering in beer brewing is to separate the wort, which contains soluble malt components from the solids, the brewer's spent grains. Lautering is a critical point in wort production and its primary objective is the efficient recovery of extract. Lautering is a special type of cake filtration; the particle sedimentation behavior of the mash results in an inhomogeneous filter cake whose structure has an impact on its chemical composition. Components of interest within the filter cake are polysaccharides, such as starch byproducts, β -glucan, and arabinoxylan, as well as proteins, lipids, polyphenols, and metal ions. The distribution of these components within the inhomogeneous filter cake is presented in this review. Lautering is a combination of separation and extraction. During extraction, the solubility of each filter cake component is different. Therefore, in this paper, lautering is considered from a new angle—a chromatographic viewpoint. The initial concentration of the components in malt is compared to their degree of retention in the filter cake and extraction into the wort. Differences in the analyses of brewer's spent grains due to different sampling points within the filter cake are addressed in this review. This new information is important for the use of spent grains in biotechnological processes and enables a more accurate comparison of components from different brewer's spent grain analyses.

Keywords Brewer's spent grains · Cake filtration · Chromatography · Extraction · Inhomogeneity · Lautering

Introduction

Filtration is a processing stage used in many branches of the food industry. One example is the recovery of juice from fruit [1–3]. In beer production, filtration plays an important role in clarifying the product from yeast and haze [4]. The second important step in the brewing process is lautering, a type of cake filtration [4, 5]. It is a separation of the liquid phase of the mash, the wort, from the insoluble solids that form the filter cake, the brewer's spent grains (BSG) (Fig. 1). The wort is the product of interest for beer production, whereas the BSG is used mainly as animal feed. However, there is a growing interest to use the BSG for various biotechnological processes [6–11].

Lautering takes place after mashing, which is primarily the enzymatic hydrolysis of the starch polymers in malt. In wort production, lautering is the rate-limiting step and a

complex process [12, 13]. Many factors can influence the lautering performance, such as raw material quality [14], particle-size distribution of mash particles [15], the presence of barley-associated bacteria [16], or high-molecular-weight polysaccharides and their degradation during mashing [17–22]. Therefore, one aim of the current research is to predict the lautering performance based on raw material quality [23–26].

For mash separation, the two main devices used in breweries are the lauter tun and the mash filter [27]. Since approximately 75% of beer in the world is produced using the lauter tun [12, 28], this review focuses on this mash separation device. The false bottom of the lauter tun serves as a supporting screen that retains the filter cake forming solids (Fig. 1). Once formed, this filter cake composed of larger particles serves as a filtering medium for fine particles.

The malt grist used for the lauter tun is rather inhomogeneous, resulting in a wide particle-size distribution of the mash particles [29]. The husks of the malt serve as a filter medium and must be preserved during milling. The result is an inhomogeneous particle sedimentation behavior in the lauter tun that is followed by the formation of a multi-layered cake structure

✉ Martina Gastl
martina.gastl@tum.de

¹ Technische Universität München, Chair of Brewing and Beverage Technology, Weihenstephaner Steig 20, 85354 Freising, Germany

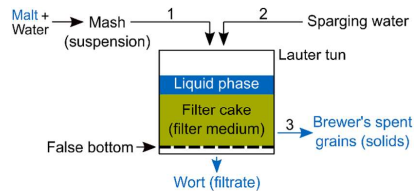


Fig. 1 Scheme of the lautering process. Mash, a suspension of water and malt grist, is transferred to the lautering tun (1). The false bottom serves as supporting screen and retains the filter cake. After formation of the filter cake, run-off of first and second wort (filtrate) occurs. Thereby, filter cake components are extracted by hot sparging water (2). After lautering, brewer's spent grains (solids) are disposed (3)

[5, 15, 30]. One focus of this review is the complex process of the filter cake formation in the lautering tun.

The inhomogeneous structure of the filter cake not only has an impact on its structural features, but also on the distribution of the different malt components within the filter cake. Components like polysaccharides (starch byproducts, β -glucan, and arabinoxylan), proteins, lipids, polyphenols, or metal ions are of interest. The distribution of these components within the inhomogeneous filter cake is provided in this review.

Lautering is a special type of cake filtration: it involves the extraction of the remaining value-giving components from the filter cake. This extraction step is called sparging, which is the rinsing of the filter cake using hot water. Based on the solubility of the components, the extraction from the filter cake into the wort differs. Therefore, this review considers the lautering tun from a new angle—chromatography. The amount of each malt component retained in the filter cake or extracted into the wort during lautering is presented and discussed.

In summary, this review gives an overview of the inhomogeneity occurring in the lautering tun. On one hand, the structural and chemical inhomogeneity of the filter cake is described; on the other hand, the inhomogeneous extraction of the different malt components into wort and their retention in the filter cake during lautering is presented from a chromatographic viewpoint.

In addition, differences in the analyses of BSG due to different sampling points within the filter cake are presented in this review. This new information is important to understand the extraction process in the lautering tun as well as for the use of the BSG in biotechnological processes.

Sampling points of the BSG and the filter cake during lautering

In this review, analyses of the filter cake and the BSG are distinguished. Thereby, the term filter cake analysis refers to the study of the intact cake, which is done, i.e., to investigate

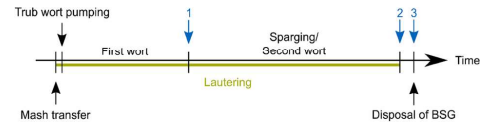


Fig. 2 Process steps and sampling points (1–3) of the filter cake during lautering

the structure of the cake or to reveal differences in the chemical composition of its horizontal layers. BSG analysis refers to the study of the chemical components without considering the differences in the structure of the filter cake.

To compare the different analyses of the filter cake and the BSG in the lautering tun found in the literature, it is important to understand the moment at which the process is investigated (Fig. 2). For example, particle sedimentation is considered in a filter cake that is analyzed after run-off of the first wort before the application of sparging water (sampling point 1). The distribution of the chemical components within the filter cake was mostly analyzed at the end of the lautering process after run-off of the second wort during sparging (sampling point 2). To analyze the chemical composition of the BSG, samples are often taken after the disposal (sampling point 3), at which point the sample of the whole filter cake is rather homogenized.

Therefore, the sampling point can have a great impact on the results of the filter cake and BSG analysis. In this review, the point of sampling (Fig. 2) is considered, and the differences in the structure and chemical composition of the filter cake and the BSG based on the sampling are revealed.

Filter cake formation and fluidic aspects

Based on the wide particle-size distribution in the mash, the irregular sedimentation behavior of the mash particles determines the formation of the inhomogeneous filter cake structure in the lautering tun. This has been extensively investigated in the last years [15, 29–32]. Small-scale lautering systems were used to preserve the structure of the filter cake for analysis. No raking knives were used, and no sparging water was applied to the filter cake after run-off of the first wort (Fig. 2, sampling point 1).

In general, the sedimentation of particles in the lautering tun is dependent on two factors. On the one hand, the velocity of the particles increases as they approach the false bottom of the lautering tun due to the gravitational force. On the other hand, the friction between the particles surface and the fluid opposes this movement. As the particle velocity increases, the magnitude of the frictional drag increases even more rapidly compared to the effect of gravitational force. Consequently, the drag and gravitational forces become equal.

Only obstruction or additional opposing forces influence the particle settlement [33].

The sedimentation velocity (w_f) is a function of the drag coefficient (c_w), which depends on the Reynolds number (Re) [34]. According to Stoke's Law, it can be described as:

$$w_f = \sqrt{\frac{4}{3} \frac{\rho_s - \rho_f}{\rho_f} g \cdot d \frac{1}{c_w(\text{Re})}} \quad (1)$$

This velocity depends on the gravitational acceleration (g) and the difference in the particle (ρ_s) and fluid (ρ_f) densities. The difference in density between the different mash particles has a great effect on the sedimentation velocity, since husks and larger husk fragments have a greater density compared with fine particles and smaller husk fragments [35]. In addition, the dependence on the particle diameter (d) describes the sedimentation of large particles, like husks, settling more rapidly than small, fine particles.

For laminar flow and considering the viscosity (η), the sedimentation velocity can be written as:

$$w_f = \frac{\rho_s - \rho_f}{18 \cdot \eta} g \cdot d^2 \quad (2)$$

The large influence of the particle diameter is evident in Eq. (2). In addition to large diameter, low-particle sphericity reduces the sedimentation velocity [33].

However, these equations can only be applied on homogeneous particles (size, shape, and density) in low concentration [34]. Since mash exhibits a wide particle-size distribution [29] and the characteristics differ among the particles, this concept serves only as a starting approximation.

Alongside malt milling, the final mashing temperature and the suspension concentration influence the particle sedimentation behavior [33].

Due to the wide particle-size distribution of mash [29] and the density difference of the particles [35], the solids form an inhomogeneous, multi-layered cake structure [5, 15, 30] (Fig. 3). The formation of the layers can be explained by a cluster sedimentation where all particles except those larger than 1 mm have a similar velocity of sedimentation (swarm velocity). The larger particles settle faster as compared to the fine particles, leading to a classifying sedimentation [30], which is rather unusual for cake filtration processes.

Mainly husks and coarse particles form the bottom fraction (Fig. 3c), whereas fine particles form the upper fraction (Fig. 3b). These fine particles (< 800 μm) form a jelly-like layer on the top of the filter cake, which has a negative effect on the filtration performance [14, 15, 30, 36–38]. The presence of this layer distinguishes lautering from other forms of cake filtration. Fine particles predominantly consist of proteins. This protein fraction can adsorb lipids, but also

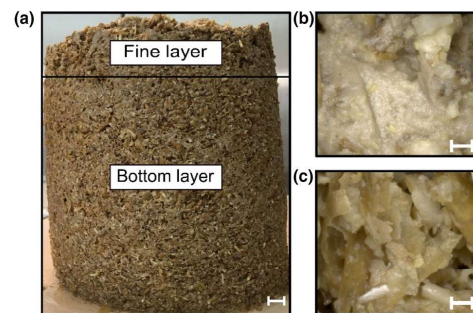


Fig. 3 Filter cake from a pilot scale lautering obtained after lautering. **a** Side view of the filter cake showing the horizontal fine layer and the bottom layer. Light microscope images taken at 20 \times magnification from the top of the different horizontal layers after segmentation: **(b)** jelly-like fine layer consisting mainly of proteins in complex with small starch granules and lipids; **(c)** bottom layer showing mainly husks and husk fragments. The scale bars represent 1 cm in **(a)** and 1 mm in **(b)** and **(c)**

small starch granules, arabinoxylan, and β -glucan are bound in the fine particles [14, 39]. Since these fine particles differ chemically from the husks and coarse particles, the chemical composition of the horizontal layers of the filter cake varies.

Extraction and retention of malt components during lautering

One task of lautering is the separation of the malt components into the value-giving wort and the remaining solids, the BSG. However, the degradation of malt components during mashing and the subsequent extraction during lautering are rather different for each component. For example, starch byproducts from the malt are degraded almost entirely in the mashing process. In contrast, insoluble components such as lignin or cellulose remain in the BSG and play no role in the subsequent steps of beer production. Components that are rather soluble include β -glucan, arabinoxylan, proteins, polyphenols, lipids, and metal ions; they contribute to the composition of the wort and influence the final product.

The following sections provide an overview of the solubility of the different malt ingredients during lautering. In Table 1, the concentration of the components in the malt (average of minimum and maximum value found in literature, unless stated otherwise), their degree of extraction into the wort, and their remaining concentration in the BSG are given.

Most of the analyses found in the literature were performed on BSG provided by commercial breweries that were sampled at the end of the lautering process when the BSG

was disposed (Fig. 2, sampling point 3) unless stated otherwise for both phases: the wort and BSG. Only wort made from barley malt is considered, and the following concentrations in the malt and BSG refer to dry matter.

The concentrations of the components in the malt, wort, and BSG represent levels found in the literature. For some components, numerous sources are available, whereas the other components are investigated only by one or a few authors and, therefore, represent values that have not necessarily been reproduced.

Polysaccharides

Starch byproducts and extract

In the whole review, the term “extract” refers to the entire amount of degraded starch byproducts from the malt forming the extract in the wort regardless of the byproduct fermentability; these include fructose, glucose, saccharose, maltose, maltotriose, and other dextrins and limit dextrins [40]. In addition to degraded starch byproducts, small starch granules can be found in the BSG [41]. These starch granules are involved in the formation of the fine layer [36, 39], as previously explained.

Depending on the cultivar and malting procedure, the amount of starch in barley is between 51 [42] and 64% [42, 43]. In malt, the starch content lies between 61 and 65% [44] and it is the major polysaccharide.

Malt milling, the mash procedure, the type of beer, and the efficiency of the lautering system have an influence on the amount of the resulting extract content in wort, which is about 80% [35, 45]. The extract contains 63–68% fermentable sugars [40]. According to Barrett et al. [36], less than 1% of the total extract content of malt remains in the BSG. This corresponds to starch content found in the dry matter of

the BSG between 1.0 [46] and 2.2% [36]. It is also in agreement with the brewer’s goal to reduce the remaining total extract in the BSG to a maximum value of 0.5–1.2% [35].

β -Glucan

According to Betts et al. [44], the β -glucan content in malt is between 1.3 and 2.7%. Han [47] investigated β -glucan in different malts and found lower values (between 0.5 and 0.6%). However, for high β -glucan barley, levels up to about 7% were found in malt [48] (high value not considered in the summary in Table 1).

A comparison of different β -glucan analysis methods in wort is only possible to a limited extent [49, 50]. Although a high correlation in the analysis of the fluorometric and the enzymatic method was found for high-molecular-weight β -glucan [51], low-molecular-weight β -glucan is only partially detected using the fluorometric analysis [52]. Therefore, the following overview of β -glucan content in wort refers to the values determined by the enzymatic method only. Lee and Bamforth [53] showed that wort β -glucan ranges between 19 and 73 mg L⁻¹ for well-modified malts. As stated by O’Rourke [54], the specification for β -glucan in wort made of lager malt is less than 250 mg L⁻¹. However, wort β -glucan can reach levels up to about 700 mg L⁻¹ for poorly modified malts [53]. Higher β -glucan concentrations are also possible depending on the type of malt and its progress in cytolysis. In modern malts, β -glucan is mainly degraded during malting and, in a minor degree, during mashing [53, 55, 56]. Therefore, the malt modification as well as the milling and mashing procedures have an impact on the concentration of β -glucan in wort.

As summarized by Jin et al. [21], approximately 70% of the β -glucan is extracted, while 30% remains in the BSG. In the BSG, the β -glucan content was found to be between

Table 1 Overview of the concentration of malt components from the literature

Malt component	Concentration in malt [%]	Extracted into wort [%]	Remaining in BSG [%]	Source
Starch byproducts	63.0 ^a	99	1	[36, 44]
β -Glucan	1.6 ^a	70	30	[21, 44, 47]
Arabinoxylan	7.0 ^b	16 ^a	84 ^a	[46, 59, 61, 62]
Proteins	10.4 ^a	35	65	[46, 67]
Polyphenols	1.4 ^a	26	74	[67, 74, 75]
Lipids	3.1	16	84	[79]
Total ash ^c	2.4 (0.6)	40 ^d	60 ^d	[85, 86, 90]

Malt component extraction into the wort and the concentration remaining in BSG are shown. All values for malt and the BSG show dry weight. Not shown: cellulose and lignin

^aAverage between minimum and maximum found in literature

^bMaximum value

^cThereof metal ions calculated from potassium, magnesium, calcium, and sodium in parentheses

^dCalculated from the average of zinc, magnesium, and calcium

0.3% [46] and up to about 1.0% [11, 57]. Vičtor et al. [57] showed that the β -glucan content in the fraction on the top of the BSG in an intact filter cake (Fig. 2, sampling point 2) has a lower value (0.61–0.67%) as compared to that in the bottom fraction (0.89–1.38%) depending on the type of malt.

Arabinoxylan

Similar to β -glucan, a comparison of different arabinoxylan analysis methods is only possible to a limited extend, as summarized by Kiszonas et al. [58]. However, this is only stated briefly, since a discussion of different arabinoxylan analysis methods used for the following summary is not subject of this review.

In barley malt, the total arabinoxylan content is about 7% [46, 59], although lower values between 3 and 4% were also found [47] (low values not considered in the summary in Table 1). Krahl et al. [60] investigated the arabinoxylan level during the brewing process and provided an example of how the arabinoxylan concentration varies during wort production. At the end of the mashing procedure, the water-extractable arabinoxylan content is 2.40 g L⁻¹. This level was also found in the first wort (2.44 g L⁻¹). However, the amount reduces during lautering from the first (2.25 g L⁻¹) and second (0.53 g L⁻¹) sparging to the last run (0.22 g L⁻¹). In the kettle-full wort, a level of 1.53 g L⁻¹ was found [60]. This level is in agreement with the values reported by Vičtor et al. [57], who found an arabinoxylan content in wort between 1.5 and 1.7 g L⁻¹. Approximately 12–20% of arabinoxylan from malt can be found in wort [61, 62]. Consequently, more than 80% of the arabinoxylan remains in the BSG. The arabinoxylan concentration in the BSG was found to be between 20.7 and 26.9% [46, 63]. This high range of arabinoxylan concentration in the BSG might be due to the sampling location, since a lower arabinoxylan content of 5% only was found by Barrett et al. [39] in the fine particles at the top of the filter cake (Fig. 2, sampling point 2). Similar to β -glucan, an unequal distribution of arabinoxylan in the filter cake was found by Vičtor et al. [57] (Fig. 2, sampling point 2) who showed a higher level of non-starch polymers in the bottom fraction (38–47%) as compared to that in the top fraction (24–37%). Moreover, the arabinoxylan level in the wort depends not only on the arabinoxylan content in the malt but also on the mashing variables [64].

Proteins

As previously stated, proteins play an important role in the formation of the fine layer at the top of the filter cake and are responsible for impeding the filtration during lautering. In general, the total protein concentration in malt is about 10 [46, 65] to 11% [66]. Protein levels between 8.2 and 12.6% [67] or even higher levels were also reported, but barley

showing extreme protein values are normally not considered for malting. Parameters like temperature, pH, or reducing and oxidizing agents influence the proteolytic activity and, thereby, the solubility of proteins during mashing [55, 68, 69]. Jones and Budde [70] showed that at a mash pH of 6.0 on average 32% of wort proteins are soluble in barley. This solubility raises in malt to 46%. As found by Gorinstein et al. [71], after mashing, the wort has a protein concentration of about 9–11 g L⁻¹. Thirty-five percent of malt proteins can be found in wort and, consequently, 65% of the protein content of malt remains in the BSG [46].

According to Osborne [72], proteins in cereals can be divided based on their solubility into four classes: albumins, globulins, prolamins, and glutelins. As shown by Celus et al. [46], malt and BSG contain different levels of these Osborne protein fractions, which are expressed as extraction yield. For example, the yield of hordeins from malt (about 2.5%) is much lower than that found in the BSG (about 11.5%). In contrast, the albumin concentration in malt is high but represents only a minor concentration in the BSG. Glutelins have a small yield in malt but are present in the BSG in a larger concentration (exact numbers for albumins and glutelins are not available).

The protein content found in the BSG varies between 15 [73] and 35% [63] depending on the analyzed sample. Lynch et al. [8] showed a high variation in the protein content from 19 to 30%. Where the sample is taken from the BSG may explain the variation. Analysis of the protein content at different positions of the BSG (Fig. 2, sampling point 2) revealed a higher protein content in the top fraction (24%) as compared to that in the middle (16%) and bottom fractions (16%) [57]. This correlates to the finding from Barrett et al. [39] (Fig. 2, sampling point 2), who reported that the fine layer at the top of the filter cake has a high protein concentration (42%). These proteins in the top layer of the filter cake are responsible for the limitation of the filtration rate in the lauter tun due to gel-protein formation [14, 36, 39].

Polyphenols

The reported total polyphenol levels in malt (expressed as gallic acid equivalent) vary. Fărcaș et al. [74] found approximately 0.15% polyphenols (fresh weight) in pilsner malt, whereas Ye et al. [67] found about 2.7%. Fumi et al. [75] identified the total concentration of phenolic compounds in the mash before the lauter tun to be about 572 mg L⁻¹.

After lautering, the polyphenol concentration in the wort was about 147 mg L⁻¹ [75]. This means that the soluble polyphenol content is reduced by 74% during lautering. Consequently, 26% only of the polyphenols are transferred into the wort. A reason for this low amount of extracted polyphenols can be the formation of polyphenol–protein complexes during mashing and lautering at higher temperatures [76].

This is in agreement with the observations made by McMurrough and Delcour [77] who measured lower amounts of polyphenols in wort during lautering when the temperature is held at 70 °C.

The concentration of the total phenolic compounds that remain in the BSG is up to about 1.7%, as shown by Stefanello et al. [78].

Lipids

Anness and Reed [79] showed that the total lipid content of malt is 3.1%. Of the malt lipids, 1.4% only can be found in kettle-full wort [79], which is in agreement with Rettberg [80] who found that 1% only of the lipids from the malt are eluted during lautering. An amount of 84.3% of lipids remain in the BSG, and the remaining 14.3% are degraded during mashing [79]. Anness and Reed [79] suggested that the degradation products are also passed into the wort, though they are not detectable. A lipid concentration in the wort of about 64 mg L⁻¹ was measured by Anness and Reed [79] before boiling, which is in agreement with the average long-chain fatty acid content of about 43 mg L⁻¹ [35, 81] in kettle-full wort.

It should be noted that the lipid concentration in wort can be influenced by the type of lautering, since intense raking or the recirculation of unfiltered first wort can significantly influence the lipid content [82]. In addition, lipid levels are dependent on mashing conditions. Evans et al. [83] showed that the total wort fatty acid concentration increased at mash-in temperatures larger 65 °C.

The lipid concentration in the BSG lies between 7 [63] and 10% [84]. Within the filter cake, a decrease of fatty acids in deeper layers was observed [15].

Metal ions

Malt is the largest contributor of metal ions during beer production. Its total ash concentration is between about 1.9 and 2.8% depending on the type of malt [85]. Thereby, all ash constituents present in the malt are considered, including, i.e., silica and iron. As summarized by Montanari et al. [86], phosphates and potassium are further primary constituents that contribute to the total ash content in malt. Since potassium, magnesium, calcium, and sodium are the main minerals in the barley grain [87], the average metal ion content of malt (about 0.6%) (Table 1) was calculated using only these metals based on the summary of Montanari et al. [86]. However, based on their importance for beer production [88], the following section focuses only on a detailed description of zinc, magnesium, and calcium.

The malt contributes to 79.8% of the zinc, 86.6% of the magnesium, and 96.2% of the calcium input in wort production [89]. The extraction from malt is not the same for

every metal ion. Magnesium extraction from malt into wort is 47–80%, and calcium extraction is 27–56%. However, 5–23% only of the zinc is recovered [90]. The remaining amount of these metal ions is not dissolved into the wort but instead remain in the BSG. This means that the solution process is more responsible for the metal ion concentration in wort than the total amount of metal ions in the malt.

For a consideration of metal ions during wort production, attention has to be paid on their retention by sequestering agents. These metal binders can be, i.e., peptides or polyphenols as well as phytic acid [35, 90]. As suggested by Jacobsen and Lie [90], mashing parameters can have an influence on the metal ion extraction, i.e., by increasing the solubility of sequestering agents or phytase activity.

Considering the extraction rates of zinc, magnesium, and calcium from malt into wort as shown by Jacobsen and Lie [90], this review determined that an average of 40% of the metal ions were extracted into the wort. However, this value represents only an approximation. It was applied on the total amount of ash.

Zinc

Several authors found a zinc content in malt between 18 [89] and 25 mg kg⁻¹ [91, 92], though higher values between 35 and 65 mg kg⁻¹ were also reported by Jacobsen and Lie [90]. In the first wort, the zinc content lies between 0.15 and 0.27 mg L⁻¹, and it decreases further during lautering to a concentration in the kettle-full wort between 0.07 and 0.16 mg L⁻¹ [93]. About 3% of the amount of zinc from the malt can be found in the wort [92, 94]. However, higher extraction levels (5–23%) were found by Jacobsen and Lie [90]. They suggested that the concentration of zinc in the wort depends on the level of amino acids [90]. The amount of zinc in the BSG varies between 19 [91] and 97 mg kg⁻¹ [95] and is approximately equal to the zinc content in the malt [96].

Magnesium

When compared to zinc, magnesium is present in larger concentrations in the malt; the magnesium concentration was found to be between about 1.1 [89] and 1.4 g kg⁻¹ [91] in barley malt, although levels of about 0.7 g kg⁻¹ [90] or up to about 2.4 g kg⁻¹ [97] were also reported for some types of malt. The first wort can have a magnesium content of 109 mg L⁻¹ that reduces slightly to about 107 mg L⁻¹ for an 8% hopped wort as shown, for example, by Poreda et al. [91]. These high values show the high extractability of 47–80% for magnesium [90], thus, leading to around 0.6 [91] to 1.0 g kg⁻¹ [95] of magnesium remaining in the BSG.

Calcium

The calcium content in malt was found to be between about 0.5 [90] and 0.8 g kg⁻¹ [89]. However, calcium levels of up to 4.5 g kg⁻¹ were also reported [97]. For an 8% wort, Jacobsen and Lie [90] showed the calcium level is between about 15 and 35 mg L⁻¹, and it is presumed to depend on the amount of polyphenols. The amount of calcium extracted from the malt was found to be between 27 and 56% [90], thus, resulting in a calcium concentration of about 0.7 g kg⁻¹ in the BSG [95].

Conclusion

Malt ingredients do not extract into the wort at equal rates. At the end of lautering (Fig. 2, sampling point 3), there is an inhomogeneous distribution of these components between the wort and the BSG (Fig. 4). Some components are extracted in a large amount into wort, while the other components are not extracted at all and remain in the BSG.

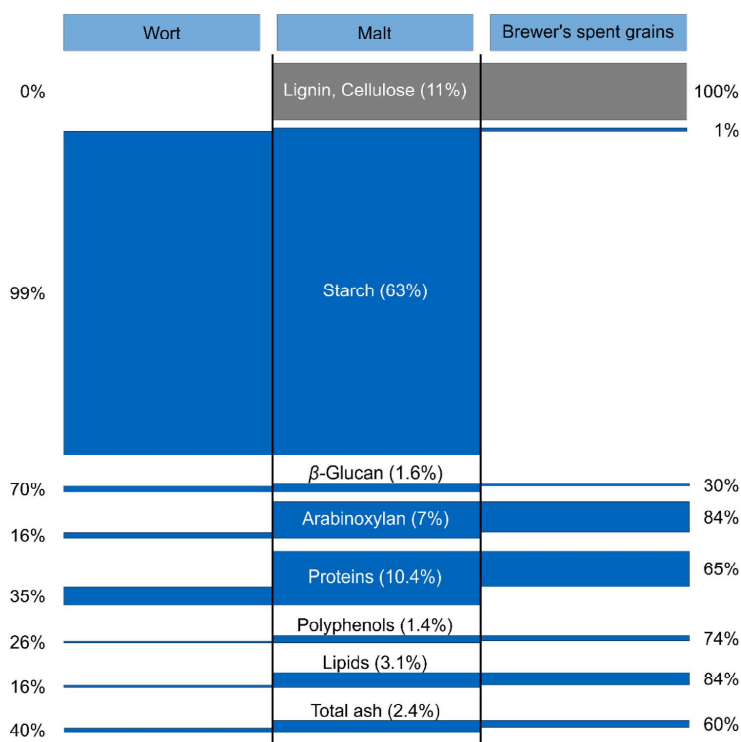
Starch represents the most abundant component in the malt. Nearly its entire content (99%) is degraded, and the

byproducts are extracted into the wort; a small amount only of its byproducts (1%) are found in the BSG at the end of the lautering process.

Although the negative effects of high-molecular-weight β -glucan on the filtration rates of wort and beer are well known [20, 98, 99], there was only little attention in the past on the influence of arabinoxylan on filtration. However, there is growing evidence that arabinoxylan can be related to wort and beer filtration problems [19, 22, 100]. Therefore, this review shows a comparison of the total amount of β -glucan and arabinoxylan in malt. The extraction rates into wort of these polysaccharides during lautering are revealed. Arabinoxylan is present in the malt at a larger concentration (7%) than β -glucan (1.6%). However, there is a much greater amount of β -glucan (70%) solubilized into the wort than arabinoxylan (16%), which ultimately results in an approximately equal concentration of β -glucan and arabinoxylan in the wort. A larger amount of arabinoxylan remains in the BSG compared to β -glucan.

The second largest group of malt soluble components are proteins. Only 35% of the proteins are extracted into the wort, resulting in 65% remaining in the BSG.

Fig. 4 Overview of the distribution of malt components into the wort and BSG based on dry weight at the end of lautering (values and references based on Table 1). The lignin and cellulose fraction contains all the remaining components that are not discussed



According to Jones and Budde [70], the amount of soluble proteins in malt is even up to 46%. The Osborne protein fractions show different concentrations for the malt and BSG.

Similarly to proteins, only a minor amount of polyphenols (26%) and lipids (16%) are extracted into the wort. Most of these components remain in the BSG.

The solubility of metal ions depends on the metal ion type. On average, 40% of the sum of zinc, magnesium, and calcium are dissolved in the wort, whereas 60% remain in the BSG.

Cellulose and lignin are insoluble components and remain completely in the BSG.

The top part of the filter cake has the highest protein concentration (Fig. 5). As summarized, this high protein concentration at the top is responsible for the formation of the jelly-like fine layer, which impedes wort flow during lautering.

Similar to proteins, the concentration of lipids is higher in the top part compared to the bottom (Fig. 5). Contrary, higher concentrations of β -glucan and arabinoxylan were found in the lower parts of the filter cake.

The inhomogeneous chemical composition of the filter cake can be explained by its formation at the beginning of lautering. Fine particles with low-particle diameter, mostly consisting of proteins, settle on the top of the filter cake later during the sedimentation process. Therefore, the top of the filter cake has a high concentration of fine particles. Husks and cell wall residues, which are composed of non-starch polysaccharides in a higher concentration, settle earlier and form the bottom of the filter cake, thus explaining why arabinoxylan and β -glucan content is high in the lower parts of the filter cake. However, the exact distribution of the remaining chemical components, i.e., metal ions, is currently unknown.

In summary, components of the filter cake are inhomogeneously distributed along its height. In addition, these components are extracted from the malt and retained in the filter cake in different manners.

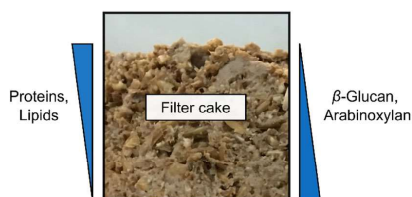


Fig. 5 Qualitative representation of the high proteins and lipids concentration in the top part and high β -glucan and arabinoxylan concentration in the lower part of the filter cake from a lautering tun (side view)

Chromatographic view on lautering

The extraction and retention behavior of the components present in the filter cake resembles a chromatography process. Therefore, lautering is considered from a chromatographic viewpoint.

The principle of chromatography is the separation of components of a mobile phase based on their selective adsorption to a stationary phase. In normal-phase chromatography, a packed column serves as the stationary phase. During elution from this column, components of the mobile phase cause a different retention behavior, resulting in a separation based on their chromatographic properties.

This chromatographic principle is applied to lautering. The filter cake is considered to act like the packed column, while the wort and sparging water serve as the mobile phases. Like in column chromatography, components of the mobile phase are selectively adsorbed to the filter cake and retained based on their chemical properties.

However, the concept of chromatography can be applied to the lautering tun only to a certain point. In contrast to column chromatography, there is an additional extraction of components from the filter cake into the wort. This distinguishes lautering from column chromatography, during which there is no extraction of components from the stationary bed into the mobile phase. Furthermore, the filter cake structure in the lautering tun is inhomogeneously compared to a packed column.

Considering lautering from a chromatographic viewpoint, starch byproducts show the largest extraction rate from the filter cake. This can be explained by the high water solubility of sugars and oligosaccharides that lead to a high extraction efficiency during sparging.

The extraction rate for β -glucan is the next largest; it is dissolved in the wort in a much higher concentration as compared to its remaining content in the BSG. However, the β -glucan concentration in wort is highly dependent on its enzymatic degradation during malting and, therefore, is not only dependent on lautering.

Proteins dissolve in the wort only in a minor concentration compared to their remaining in the BSG. Since the largest amount remains in the BSG, it can be concluded that the protein solubility during lautering is low. Similar to β -glucan, the solubility of proteins in the wort depends mainly on the enzymatic degradation during malting.

The extraction rate for arabinoxylan from the filter cake is very low. However, there is growing evidence that arabinoxylan is important for lautering performance. Therefore, more insights into the extraction process of arabinoxylan during wort production are necessary.

Similar to arabinoxylan, polyphenols and lipids exhibit the lowest extraction rates in the wort, which can be explained by a poor elution from the filter cake.

Metal ions are rather insoluble in sparging water and are retained by the filter cake in a high content.

Compared to the different types of chromatographic columns, i.e., ion exchange or gel filtration, it is difficult to find common features to the complex filter cake in the lauter tun. However, hydrophobic lipids and proteins are mostly present at the top of the filter cake in the fine layer and are eluted only in a minor concentration. This means that these components have a high affinity to hydrophobic column material. On the contrary, hydrophilic sugars are almost entirely eluted from the filter cake. Therefore, it is suggested that the filter cake in the lauter tun is similar to the stationary material of a hydrophobic chromatography column.

The chromatographic view implies that, in addition to fluidics, there is another important factor in the extraction of the components from the filter cake that may be based on the different properties of the components. Therefore, factors like water solubility (starch byproducts) or interactions between the components (i.e., proteins and polyphenols in complex with metal ions) play a role in the elution from the filter cake.

For the chromatic view on lautering, one must consider that this is only a theoretical concept. Currently, there is no complete overview about the extraction process of all malt components available in the literature.

Discussion

Lautering is a complex procedure that can be influenced by many factors. Therefore, the distribution of the components represent only an average of the levels found in the literature. To verify the values presented in Fig. 4, the theoretical concentration of the components in the BSG at the end of the lautering process are calculated (Table 2). The calculation is based on references as summarized in Table 1. Thereby, the retention rate of each component of BSG was multiplied by its concentration in malt. Subsequently, the percentage share based on the total BSG was calculated.

This calculation is confirmed by component concentrations found in the BSG, as summarized by Steiner et al. [11], or found by Mussatto et al. [73] and Kanauchi et al. [84]. The comparison shows that the literature values for hemicelluloses and proteins are in good agreement with the calculated concentrations except for Mussatto et al. [73]. Calculated concentrations for lipids, ash, and the sum of cellulose and lignin are in good agreement with the literature values.

The concentrations of the components in malt, wort, and BSG found in the literature can deviate between different analyses, which may be attributed to the barley breed,

Table 2 Calculations verifying the concentrations of the BSG components presented in the literature as compared to results from Steiner et al. [11], Mussatto et al. [73], and Kanauchi et al. [84]

	Calculated concentration in BSG [%]	Concentration in BSG from literature [%]		
		Steiner et al. [11]	Mussatto et al. [73]	Kanauchi et al. [84] ^d
Starch byproducts	2.1	24 ^a	n. d	n. d
β -Glucan	1.6		28.4 ^c	23 ^c
Arabinoxylan	19.6			
Proteins	22.6	21	15.3	25
Polyphenols	3.5	n. d	n. d	n. d
Lipids	8.7	10	n. d	11
Total ash ^b	4.7 (1.2)	5	4.6	3
Cellulose, lignin	37.1	40	44.6	39

All values are shown in % dry weight. The lignin and cellulose fraction contains all remaining components that are not discussed

n. d. not determined

^aSum of non-cellulosic polysaccharides

^bThereof metal ions calculated from potassium, magnesium, calcium, and sodium in parentheses

^cSum of hemicellulose

^dAll values converted to dry weight

the cultivation, malting conditions, and the type of malt. Depending on the type of beer, the mashing procedure, the brewhouse equipment, and the lauter tun manufacturer, differences in the wort and BSG composition can be found. In addition, the efficiency of the extraction of the soluble components from the filter cake during lautering must be considered. Another important factor is the wort turbidity, which can influence the concentration of, i.e., lipids or metal ions in the wort. Therefore, a comparison of the malt, wort, and BSG samples from different analyses is only possible to a limited extent.

The sampling point also influences the results of an analysis. As shown in Fig. 2, there are different points for sampling during lautering that must be considered to accurately compare BSG and wort analyses.

In the case of the BSG, another factor is important for the analysis—the sampling location within the filter cake. The filter cake in the lauter tun is inhomogeneous along its height, such that the positions in the filter cake at which the samples are taken can have a great influence on the analytical results. For example, since the top layer of the filter cake has a greater concentration of proteins when compared with the bottom fraction, sampling from the top may result in a higher protein concentration than of a sample taken from a homogenized BSG that was tested after its disposal.

Among the surveyed literature, a few authors provided information about the sampling point or the position at which the BSG was sampled within the filter cake, whereas, for most references, this information is missing or unclear. This overlooked variable might explain the high deviation in the reported concentrations of components such as arabinoxylan or proteins.

The inhomogeneous composition of the filter cake has not only an influence on the distribution of its components. Proteins in combination with lipids, starch granules, arabinoxylan, and β -glucan form a jelly-like layer on top of the filter cake. This layer is responsible for impeding wort flow during lautering.

Summary

The new chromatographic view on the separation of components in the lauter tun sheds new light on lautering. It reveals the amount of malt components that are either extracted into wort or remain in the BSG during lautering. This insight supports a better understanding of the extraction process in the lauter tun.

The inhomogeneity occurring in the lauter tun is summarized. The structural features and resulting inhomogeneous chemical composition of the formed filter cake are presented, thus, promoting awareness of the importance of the filter cake structure in the lauter tun.

Finally, this review draws attention to the sampling in BSG analysis. Differences in analyses due to different sampling points during lautering and within the filter cake are addressed. Appreciation of this issue enables a more informed comparison of reported components concentrations from different BSG analyses, which is important for the use of the BSG in biotechnological processes.

Acknowledgements This IGF Project of the FEI was supported via AiF (19359N) within the programme for promoting the Industrial Collective Research (IGF) of the German Ministry of Economic Affairs and Energy (BMWi), based on a resolution of the German Parliament.

Compliance with ethical standards

Conflict of interest The authors declare that they have no conflict of interest.

Compliance with ethics requirements This article does not contain any studies with human or animal subjects.

References

- Echavarría AP, Torras C, Pagán J, Ibarz A (2011) Fruit juice processing and membrane technology application. *Food Eng Rev* 3(3–4):136–158. <https://doi.org/10.1007/s12393-011-9042-8>
- Girard B, Fukumoto LR (2000) Membrane processing of fruit juices and beverages: a review. *Crit Revs Biotechnol* 20(2):109–175. <https://doi.org/10.1080/07388550008984168>
- Urošević T, Povrenović D, Vukosavljević P, Urošević I, Stevanović S (2017) Recent developments in microfiltration and ultrafiltration of fruit juices. *Food Bioprod Process* 106:147–161. <https://doi.org/10.1016/j.fbp.2017.09.009>
- Tippmann J, Becker T (2016) Das Zusammenspiel von Verfahrenstechnik und Technologie in der Brauerei. *Chem Ing Tech* 88(12):1857–1868. <https://doi.org/10.1002/cite.201600058>
- Tippmann J, Scheuren H, Voigt J, Sommer K (2010) Procedural investigations of the lautering process. *Chem Eng Technol* 33(8):1297–1302. <https://doi.org/10.1002/ceat.201000109>
- Aliyu S, Bala M (2011) Brewer's spent grain: a review of its potentials and applications. *Afr J Biotechnol* 10(3):324–331. <https://doi.org/10.5897/AJBx10.006>
- Guido LF, Moreira MM (2017) Techniques for extraction of brewer's spent grain polyphenols: a review. *Food Bioprocess Technol* 10(7):1192–1209. <https://doi.org/10.1007/s11947-017-1913-4>
- Lynch KM, Steffen EJ, Arendt EK (2016) Brewers' spent grain: a review with an emphasis on food and health. *J Inst Brew* 122(4):553–568. <https://doi.org/10.1002/jib.363>
- Mussatto SI (2014) Brewer's spent grain: a valuable feedstock for industrial applications. *J Sci Food Agric* 94(7):1264–1275. <https://doi.org/10.1002/jsfa.6486>
- Mussatto SI, Dragone G, Roberto IC (2006) Brewers' spent grain: generation, characteristics and potential applications. *J Cereal Sci* 43(1):1–14. <https://doi.org/10.1016/j.jcs.2005.06.001>
- Steiner J, Procopio S, Becker T (2015) Brewer's spent grain: source of value-added polysaccharides for the food industry in reference to the health claims. *Eur Food Res Technol* 241(3):303–315. <https://doi.org/10.1007/s00217-015-2461-7>
- Becher T (2016) Die Läuterarbeit in Brauereien: Status quo und künftige Entwicklungsziele. *Chem Ing Tech* 88(12):1904–1910. <https://doi.org/10.1002/cite.201600023>
- Greffin W, Krauß G (1978) Schrotten und Läutern. II. Arbeit mit konventioneller Trockenschrotmühle und Läuterbottich—eine Literaturübersicht. *Monatsschrift für Brauwissenschaft* 31(6):192–212
- Muts G CJ, Pesman L (1986) The influence of raw materials and brewing process on lautertun filtration. In: EBC monograph XI, symposium on wort production. Maffliers
- Engstle J, Briesen H, Först P (2017) Mash separation in the lauter tun—a particle size dependent separation process. *Brew Sci* 70:26–30
- Laitila A, Manninen J, Priha O, Smart K, Tsitko I, James S (2018) Characterisation of barley-associated bacteria and their impact on wort separation performance. *J Inst Brew* 124(4):314–324. <https://doi.org/10.1002/jib.509>
- Wu D, Cai G, Li X, Li B, Lu J (2018) Cloning and expression of ferulic acid esterase gene and its effect on wort filterability. *Biotechnol Lett*. <https://doi.org/10.1007/s10529-018-2511-x>
- Wu D, Zhou T, Li X, Cai G, Lu J (2016) POD promoted oxidative gelation of water-extractable arabinoxylan through ferulic acid dimers. Evidence for its negative effect on malt filterability. *Food Chem* 197(Pt A):422–426. <https://doi.org/10.1016/j.foodchem.2015.10.130>
- Malliet S, De Cooman L, Aerts G (2010) Application of thermostable xylanases at mashing and during germination. *Brew Sci* 63:133–141
- Jin Y-L, Speers R, Paulson T, Stewart AJ R (2004) Effects of β -glucans and environmental factors on the viscosities of wort and beer. *J Inst Brew* 110(2):104–116. <https://doi.org/10.1002/j.2050-0416.2004.tb00189.x>

21. Jin Y-L, Speers RA, Paulson AT, Stewart RJ (2004) Barley β -glucans and their degradation during malting and brewing. *MBAA Tech Q* 41(3):231–240
22. Li X, Gao F, Cai G, Jin Z, Lu J, Dong J, Yin H, Yu J, Yang M (2015) Purification and characterisation of arabinoxylan arabinofuranohydrolase I responsible for the filterability of barley malt. *Food Chem* 174:286–290. <https://doi.org/10.1016/j.foodchem.2014.11.024>
23. Xu J, Kang J, Wang D, Qin Q, Liu G, Lin Z, Pavlovic M, Dostalek P (2016) Mathematical model for assessing wort filtration performance based on granularity analysis. *J Am Soc Brew Chem* 74(3):191–199. <https://doi.org/10.1094/ASBCJ-2016-3706-01>
24. Krause D, Holtz C, Gastl M, Hussein M, Becker T (2015) NIR and PLS discriminant analysis for predicting the processability of malt during lautering. *Eur Food Res Technol* 240(4):831–846. <https://doi.org/10.1007/s00217-014-2389-3>
25. Holtz C, Krause D, Hussein M, Gastl M, Becker T (2014) Lautering performance prediction from malt by combining whole near-infrared spectral information with lautering process evaluation as reference values. *J Am Soc Brew Chem* 72(3):214–219. <https://doi.org/10.1094/ASBCJ-2014-0717-01>
26. Sarx HG (2002) Influence of malt quality on the lauter process. *Brauwelt Int* 6:378–380
27. Andrews J (2004) A review of progress in mash separation technology. *MBAA TQ* 41(1):45–49
28. Bamforth CW (2006) *Brewing: new technologies*. Woodhead publishing series in food science, technology and nutrition, 1st edn. Woodhead Publishing Limited, Cambridge
29. Tippmann J, Voigt J, Sommer K (2011) Measuring particle size distribution of mash with laser diffraction to evaluate the process success. *Brew Sci* 64:13–21
30. Engstle J, Reichhardt N, Först P (2015) Filter cake resistance of horizontal filter layers of lautering filter cakes. *MBAA Tech Q* 52(2):29–35. <https://doi.org/10.1094/tq-52-2-0405-01>
31. Bühler TM, McKechnie MT, Wakeman RJ (1996) A model describing the lautering process. *Monatsschrift für Brauwiss* 77:8:226–233
32. Mathmann K, Kuhn M, Briesen H (2014) Application of micro-computed tomography in food and beverage technology using the examples of textured vegetable protein and filtration steps in the brewing process. In: *Proceedings of conference on industrial computed tomography (iCT2014)*, Wels, Österreich
33. Harris JO (1968) Filtration in brewing—a review. *J Inst Brew* 74(6):500–510. <https://doi.org/10.1002/j.2050-0416.1968.tb03165.x>
34. Schwill-Miedaner A (2011) *Verfahrenstechnik im Brauprozess*. Fachverlag Hans Carl GmbH, Nürnberg
35. Narziß L, Back W (2009) *Die Bierbrauerei: Band 2: Die Technologie der Würzereibereitung*, vol 8. Wiley-VCH, Weinheim. <https://doi.org/10.1002/9783527628636>
36. Barrett J, Clapperton JF, Divers DM, Rennie H (1973) Factors affecting wort separation. *J Inst Brew* 79(5):407–413. <https://doi.org/10.1002/j.2050-0416.1973.tb03558.x>
37. Moonen JHE, Graveland A (1987) The molecular structure of gelprotein from barley, its behaviour in wort-filtration and analysis. *J Inst Brew* 93:125–130
38. Lewis MJ, Oh SS (1985) Influence of precipitation of malt proteins in lautering. *MBAA Tech Q* 22(3):108–111
39. Barrett J, Bathgate GN, Clapperton JF (1975) The composition of fine particles which affect mash filtration. *J Inst Brew* 81(1):31–36. <https://doi.org/10.1002/j.2050-0416.1975.tb03658.x>
40. Kunze W (2004) *Technology brewing and malting*. VLB, Berlin
41. Bathgate GN, Clapperton JF, Palmer GH (1973) The significance of small starch granules. In: *Paper presented at the proceedings of the European brewery convention congress*, Salzburg
42. Kong D, Choo TM, Narasimhalu P, Jui P, Ferguson T, Therrien MC, Ho KM, May KW (1995) Variation in starch, protein, and fibre of Canadian barley cultivars. *Can J Plant Sci* 75(4):865–870. <https://doi.org/10.4141/cjps95-143>
43. Holtekjølen AK, Uhlen AK, Bråthen E, Sahlström S, Knutsen SH (2006) Contents of starch and non-starch polysaccharides in barley varieties of different origin. *Food Chem* 94(3):348–358. <https://doi.org/10.1016/j.foodchem.2004.11.022>
44. Betts NS, Wilkinson LG, Khor SF, Shirley NJ, Lok F, Skadhauge B, Burton RA, Fincher GB, Collins HM (2017) Morphology, carbohydrate distribution, gene expression, and enzymatic activities related to cell wall hydrolysis in four barley varieties during simulated malting. *Front Plant Sci* 8:1872. <https://doi.org/10.3389/fpls.2017.01872>
45. Faltermaier A, Negele J, Becker T, Gastl M, Arendt E (2015) Evaluation of mashing attributes and protein profile using different grist composition of barley and wheat malt. *Brew Sci* 68:67–77
46. Celus I, Brijs K, Delcour JA (2006) The effects of malting and mashing on barley protein extractability. *J Cereal Sci* 44(2):203–211. <https://doi.org/10.1016/j.jcs.2006.06.003>
47. Han J-Y (2000) Structural characteristics of arabinoxylan in barley, malt, and beer. *Food Chem* 70(2):131–138. [https://doi.org/10.1016/S0308-8146\(00\)00075-3](https://doi.org/10.1016/S0308-8146(00)00075-3)
48. Vis RB, Lorenz K (1998) Malting and brewing with a high β -glucan barley. *LWT Food Sci Technol* 31(1):20–26. <https://doi.org/10.1006/food.1997.0285>
49. Kupetz M, Procopio S, Sacher B, Becker T (2015) Critical review of the methods of β -glucan analysis and its significance in the beer filtration process. *Eur Food Res Technol* 241(6):725–736. <https://doi.org/10.1007/s00217-015-2498-7>
50. Anderson IW (1990) The effect of β -glucan molecular weight on the sensitivity of dye binding assay procedures for β -glucan estimation. *J Inst Brew* 96(5):323–326. <https://doi.org/10.1002/j.2050-0416.1990.tb01038.x>
51. Munck L, Jørgensen KG, Ruud-Hansen J, Hansen KT (1989) The EBC methods for determination of high molecular weight β -glucan in barley, malt, wort and beer. *J Inst Brew* 95(2):79–82. <https://doi.org/10.1002/j.2050-0416.1989.tb04612.x>
52. Manzanares P, Navarro A, Sendra JM, Carbonell JV (1991) Selective determination of β -glucan of differing molecular size, using the calcofluor-fluorimetric flow-injection-analysis (FIA) method. *J Inst Brew* 97(2):101–104. <https://doi.org/10.1002/j.2050-0416.1991.tb01057.x>
53. Lee Y-T, Bamforth CW (2009) Variations in solubility of barley β -glucan during malting and impact on levels of β -glucan in wort and beer. *J Am Soc Brew Chem* 67(2):67–71. <https://doi.org/10.1094/ASBCJ-2009-0226-01>
54. O'Rourke T (2002) Malt specification & brewing performance. *BREWERY Int* 2(10):27–30
55. Kühbeck F, Dickel T, Krottenthaler M, Back W, Mitzscherling M, Delgado A, Becker T (2005) Effects of mashing parameters on mash β -glucan, FAN and soluble extract levels. *J Inst Brew* 111(3):316–327. <https://doi.org/10.1002/j.2050-0416.2005.tb00690.x>
56. Evans DE, Goldsmith M, Damberg R, Nischwitz R (2011) A comprehensive reevaluation of small-scale congress mash protocol parameters for determining extract and fermentability. *J Am Soc Brew Chem* 69(1):13–27
57. Viëtor RJ, Voragen AGJ, Angelino SAGF (1993) Composition of non-starch polysaccharides in wort and spent grain from brewing trials with malt from a good malting quality barley and a feed barley. *J Inst Brew* 99(3):243–248. <https://doi.org/10.1002/j.2050-0416.1993.tb01167.x>
58. Kiszonas AM, Courtin CM, Morris CF (2012) A critical assessment of the quantification of wheat grain arabinoxylans using a

- phloroglucinol colorimetric assay. *Cereal Chem* 89(3):143–150. <https://doi.org/10.1094/cchem-02-12-0016-r>
59. Debyser W, Derdelinckx G, Delcour JA (1997) Arabinoxylan and arabinoxylan hydrolysing activities in barley malts and worts derived from them. *J Cereal Sci* 26(1):67–74. <https://doi.org/10.1006/jcrs.1996.0107>
 60. Krahl M, Müller S, Zarnkow M, Back W, Becker T (2009) Arabinoxylan and fructan in the malting and brewing process. *Qual Assur Saf Crop Foods* 1(4):246–255. <https://doi.org/10.1111/j.1757-837X.2009.00035.x>
 61. Preece JA (1940) Pentosans and related products in malting and brewing. *J Inst Brew* 46:38–48. <https://doi.org/10.1002/j.2050-0416.1940.tb06007.x>
 62. Egí A, Speers RA, Schwarz PB (2004) Arabinoxylans and their behavior during malting and brewing. *MBAA Tech Q* 41(3):248–267
 63. Vieira E, Rocha MAM, Coelho E, Pinho O, Saraiva JA, Ferreira IMPLVO, Coimbra MA (2014) Valuation of brewer's spent grain using a fully recyclable integrated process for extraction of proteins and arabinoxylans. *Ind Crops Prod* 52:136–143. <https://doi.org/10.1016/j.indcrop.2013.10.012>
 64. Li Y, Lu J, Gu G (2005) Control of arabinoxylan solubilization and hydrolysis in mashing. *Food Chem* 90(1–2):101–108. <https://doi.org/10.1016/j.foodchem.2004.03.031>
 65. Wu X, Du J, Zhang K, Ju Y, Jin Y (2015) Changes in protein molecular weight during cloudy wheat beer brewing. *J Inst Brew* 121(1):137–144. <https://doi.org/10.1002/jib.198>
 66. Yamashita H, Kühbeck F, Hohrein A, Herrmann M, Back W, Krottenthaler M (2006) Fractionated boiling technology: wort boiling of different lauter fractions. *Brew Sci* 59:130–147
 67. Ye L, Huang Y, Li M, Li C, Zhang G (2016) The chemical components in malt associated with haze formation in beer. *J Inst Brew* 122(3):524–529. <https://doi.org/10.1002/jib.353>
 68. Jones BL, Budde AD (2003) Effect of reducing and oxidizing agents and pH on malt endoproteolytic activities and brewing mashes. *J Agric Food Chem* 51:7504–7512. <https://doi.org/10.1021/jf030206u>
 69. Jones BL, Marinac L (2002) The effect of mashing on malt endoproteolytic activities. *J Agric Food Chem* 50(4):858–864. <https://doi.org/10.1021/jf0109672>
 70. Jones BL, Budde AD (2005) How various malt endoprotease classes affect wort soluble protein levels. *J Cereal Sci* 41:95–106. <https://doi.org/10.1016/j.jcs.2004.09.007>
 71. Gorinstein S, Zemsar M, Vargas-Alboreo F, Ochoa JL, Paredes-Lopez O, Scheler C, Salnikow J, Martin-Belloso O, Trakhtenberg S (1999) Proteins and amino acids in beers, their contents and relationships with other analytical data. *Food Chem* 67(1):71–78. [https://doi.org/10.1016/S0308-8146\(99\)00071-0](https://doi.org/10.1016/S0308-8146(99)00071-0)
 72. Osborne TB (1924) *The vegetable proteins*. Longmans, Green and Co., London
 73. Mussatto SI, Roberto IC (2005) Acid hydrolysis and fermentation of brewer's spent grain to produce xylitol. *J Sci Food Agric* 85(14):2453–2460. <https://doi.org/10.1002/jsfa.2276>
 74. Fărcaș AC, Socaci SA, Dulf FV, Tofană M, Mudura E, Diaconeasa Z (2015) Volatile profile, fatty acids composition and total phenolics content of brewers' spent grain by-product with potential use in the development of new functional foods. *J Cereal Sci* 64:34–42. <https://doi.org/10.1016/j.jcs.2015.04.003>
 75. Fumi MD, Galli R, Lambri M, Donadini G, De Faveri DM (2011) Effect of full-scale brewing process on polyphenols in Italian all-malt and maize adjunct lager beers. *J Food Compos Anal* 24(4–5):568–573. <https://doi.org/10.1016/j.jfca.2010.12.006>
 76. Lewis MJ, Serbia JW (1984) Aggregation of protein and precipitation by polyphenol in mashing. *J Am Soc Brew Chem* 42(1):40–43. <https://doi.org/10.1094/ASBCJ-42-0040>
 77. McMurrough I, Delcour JA (1994) Wort polyphenols. *Ferment* 7:175–182
 78. Stefanello FS, dos Santos CO, Bochi VC, Fruet APB, Soquetta MB, Dorr AC, Nornberg JL (2018) Analysis of polyphenols in brewer's spent grain and its comparison with corn silage and cereal brans commonly used for animal nutrition. *Food Chem* 239:385–401. <https://doi.org/10.1016/j.foodchem.2017.06.130>
 79. Anness BJ, Reed RJR (1985) Lipids in the brewery—a material balance. *J Inst Brew* 91:82–87. <https://doi.org/10.1002/j.2050-0416.1985.tb04310.x>
 80. Rettberg N (2018) Lipids in beer. Paper presented at the 51. Technologisches Seminar, Weihenstephan, February
 81. Holtz C, Gastl M, Becker T (2015) Turbidity potentials of single long-chain fatty acids and gelatinised starch in synthetic lautering wort. *Int J Food Sci Technol* 50(4):906–912. <https://doi.org/10.1111/ijfs.12732>
 82. Wackerbauer K, Bender G, Poloczek K (1983) Die Beeinflussung der freien Fettsäuren durch die technologischen Parameter bei der Sudhausarbeit. *Monatsschrift für Brauwissenschaft* 1:18–25
 83. Evans DE, Goldsmith M, Redd KS, Nischwitz R, Lentini A (2012) Impact of mashing conditions on extract, its fermentability, and the levels of wort free amino nitrogen (FAN), β -glucan, and lipids. *J Am Soc Brew Chem* 70(1):39–49. <https://doi.org/10.1094/ASBCJ-2012-0103-01>
 84. Kanauchi O, Keiichi M, Yoshio A (2001) Development of a functional germinated barley foodstuff from brewer's spent grain for the treatment of ulcerative colitis. *J Am Soc Brew Chem* 59(2):59–62
 85. Comrie AAD (1936) Ash, silica and iron in malts. *J Inst Brew* 42(4):350–351. <https://doi.org/10.1002/j.2050-0416.1936.tb05669.x>
 86. Montanari L, Mayer H, Marconi O, Fantozzi P (2009) Minerals in beer. In: Preedy VR (ed) *Beer in health and disease prevention*. Academic Press, San Diego, pp 359–365
 87. Šterna V, Zute S, Jakobsone I (2015) Grain composition and functional ingredients of barley varieties created in Latvia. *Proc Latv Acad Sci Sect B* 69(4):158–162. <https://doi.org/10.1515/prolas-2015-0023>
 88. Gibson BR (2011) 125th anniversary review: improvement of higher gravity brewery fermentation via wort enrichment and supplementation. *J Inst Brew* 117(3):268–284. <https://doi.org/10.1002/j.2050-0416.2011.tb00472.x>
 89. Wietstock PC, Kunz T (2015) Uptake and release of Ca, Cu, Fe, Mg, and Zn during beer production. *J Am Soc Brew Chem* 73(2):179–184. <https://doi.org/10.1094/ASBCJ-2015-0402-01>
 90. Jacobsen T, Lie S (1977) Chelators and metal buffering in brewing. *J Inst Brew* 83(4):208–212. <https://doi.org/10.1002/j.2050-0416.1977.tb03796.x>
 91. Poreda A, Bijak M, Zdaniewicz M, Jakubowski M, Makarewicz M (2015) Effect of wheat malt on the concentration of metal ions in wort and brewhouse by-products. *J Inst Brew* 121(2):224–230. <https://doi.org/10.1002/jib.226>
 92. Vecseri-Hegybes B, Fodor P, Hoschke A (2005) The role of zinc in beer production I: wort production. *Acta Aliment* 34(4):373–380. <https://doi.org/10.1556/AAlim.34.2005.4.5>
 93. Daveloose M (1987) An investigation of zinc concentrations in brewhouse worts. *MBAA Tech Q* 24(3):109–112
 94. Narziß L, Barth D, Yamagishi S, Heyse K-U (1980) Über den Einfluss des Maischverfahrens auf die Lösung von Stickstoffsubstanzen und Zink in Maische und Würze. *Brauwissenschaft* 33(9):230–237
 95. Bożym M, Florczyk I, Zdanowska P, Wojdalski J, Klimkiewicz M (2015) An analysis of metal concentrations in food wastes for biogas production. *Renew Energy* 77:467–472. <https://doi.org/10.1016/j.renene.2014.11.010>

3 Results

96. Ault RG, Whitehouse AGR (1952) Determination of zinc in beer and brewing materials. *J Inst Brew* 58(2):136–139. <https://doi.org/10.1002/j.2050-0416.1952.tb02667.x>
97. Svetlana N, Özcan MM (2016) Mineral contents of malted barley grains used as the raw material of beer consumed as traditional spirits. *Indian J Traditional Knowl* 15(3):500–502
98. Sadosky P, Schwarz PB (2002) Effect of arabinoxylans, β -glucans, and dextrans on the viscosity and membrane filterability of a beer model solution. *J Am Soc Brew Chem* 60(4):153–162
99. Stewart DC, Hawthorne D, Evans DE (1998) Cold sterile filtration: a small scale filtration test and investigation of membrane plugging. *J Inst Brew* 104:321–326
100. Sun J, Lu J, Xie G (2018) Secretome analysis of *trichoderma reesei* CICC41495 for degradation of arabinoxylan in malted barley. *J Inst Brew* 124(4):352–358. <https://doi.org/10.1002/jib.505>

Publisher's Note Springer Nature remains neutral with regard to jurisdictional claims in published maps and institutional affiliations.

3.2.2 Influence of Temperature on the Filter Cake Resistance in a Lauter Tun

M. Hennemann, M. Gastl and T. Becker

Influence of temperature on the filter cake resistance in a lauter tun

High temperatures are maintained in a lauter tun to reduce the filtration time. The temperature affects the flow rate through the changing viscosity. In addition, the sedimentation behaviour of the particles also depends on the temperature. Changes in the settling velocity are assumed to affect the filter cake resistance and thus the flow rate. The influence of temperature (range: 40–78 °C) on cake formation was investigated. Calculations of the settling velocity revealed a higher settling rate at higher temperatures due to a reduction in the density and viscosity of the liquid. The effect was confirmed for larger particles by performing a sedimentation test, but smaller particles were hindered from settling at higher temperatures. Fine particles remained in suspension because of thermal convection, providing buoyancy to counteract the gravitational sedimentation. The hindered particle settling explained the lower filter cake resistance at high temperatures and thus the higher flow rate.

Descriptors: filter cake resistance, lautering, sedimentation, temperature, viscosity

1 Introduction

Mash separation is one of the most important solid-liquid separation processes in beer production and a time-critical step in the brewhouse [19]. A lauter tun is often used to separate the mash into its solid (spent grains) and liquid (wort) phase. To ensure a short and efficient processing time in the lauter tun, a high flow rate must be achieved. The filtered volume (V) per unit time (t) depends on the filter area (A), differential pressure (Δp), and cake height (h) according to

$$\frac{v}{t} = \frac{A \cdot \Delta p}{h \cdot \eta \cdot \alpha_p} \quad (\text{Eq. 1})$$

A high flow rate requires a low viscosity (η) of the wort and a low filter cake resistance (α_p). These characteristics strongly depend on the quality of the raw materials (e.g., cytolytic modification) [8, 9, 11, 13, 14]. A low viscosity can also be achieved through high temperatures despite the malt quality; hence, lautering is usually conducted at temperatures of up to 78 °C [1, 4, 11, 18]. However, the filtration time does not always correlate with the wort viscosity as summarized by *Greffin and Krauß* [11]. In addition, *Barrett et al.* [2] showed that the viscosity has only a minor influence on the flow rate compared with the physical blocking of the cake. Therefore, it can be concluded that the reduced viscosity is not the only reason

for the higher flow rate at high temperatures. This is supported by *Bühler et al.* [3, 5] who showed that changes in the filterability at different temperatures are not caused by the viscosity; instead, a reduction in the filter cake resistance at higher temperatures is responsible. The influence of temperature on the filter cake resistance is investigated in this work. In contrast to earlier studies [3, 5, 13], this paper does not aim to analyse the temperature-dependent structural changes of the particles that alter the resistance; these particle agglomeration effects were kept constant. It is investigated in this paper how the temperature affects the resistance based on differences in the sedimentation behaviour of the particles.

The settling velocity (w_f) of particles depends on the viscosity and density (ρ_l) of the liquid, and the gravitational field strength (g), particle density (ρ_s) and size (d), according to

$$w_f = \frac{\rho_s - \rho_l}{18 \cdot \eta} \cdot g \cdot d^2 \quad (\text{Eq. 2})$$

Both the viscosity and density are temperature dependent. The dependence of the settling velocity on the particle size and density, in combination with the sedimentation rest [15] and the broad size distribution of particles in the mash [20], results in the formation of a multilayered filter cake. Fine particles (< 500 µm) settle later than larger particles (> 500 µm, e.g., husks) to form a top layer on the compressible bottom layer [7, 12]. This top layer has a high filter cake resistance compared with the bottom layer [2, 13, 14]. The cake layer formation can be divided into three steps (Fig. 1). First, the mash is transferred to the lauter tun (t_1). The particles immediately begin to settle on the filter medium (false bottom) with larger and denser particles sinking faster than smaller ones [15]. After the sedimentation rest (t_2), most of the smaller and less dense particles previously present in the lower regions have been displaced by the coarser particles that form the bottom layer. Some small particles do not settle at all unless the liquid level is decreased during filtration and their buoyancy ceases to exist (t_3). The

<https://doi.org/10.23763/BrSc21-11hennemann>

Authors

Martin Hennemann, Martina Gastl, Thomas Becker, Chair of Brewing and Beverage Technology, Technical University Munich, Freising, Germany; corresponding author: martina.gastl@tum.de

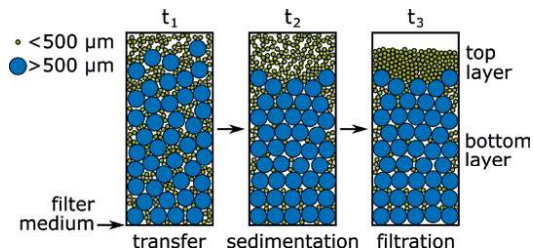


Fig. 1 Schematic illustration of the distribution of small ($< 500 \mu\text{m}$) and large ($> 500 \mu\text{m}$) particles in the filter cake after the mash transfer (t_1), sedimentation rest (t_2), and filtration process (t_3). Compressibility of the bottom layer is neglected in the scheme

concentration of fine particles in the vicinity of the filter medium is reduced by trub wort pumping at the beginning of the filtration step. Most of the fine particles settled on top of the bottom layer by the end of the filtration, resulting in the characteristic layering of the lauter tun filter cake [7, 12]. The migration of the top layer particles into the bottom layer can be neglected during the filtration when there is no raking [7].

The sedimentation behaviour of the fine particles is expected to be influenced by temperature to a higher degree than the larger particles because of the low size and density. It is therefore assumed that the temperature specifically influences the formation, and thus the resistance, of the filtration-critical top layer. Consequently, the temperature dependence of the top layer has a major effect on the flow rate, in addition to a minor effect of the viscosity.

Herein, the influence of temperature (range: 40–78 °C) on the flow rate in the lauter tun is investigated using a lab-scale filtration device. In addition to the practical filtration temperature of 78 °C, lower temperatures are examined to understand temperature-dependent differences in the filtration process.

2 Materials and Methods

2.1 Mashing procedure and filtration test

Malt was ground in a DLFU disk mill (Bühler AG, Uzwil, Switzerland) with a grinding gap of 0.65 mm. Grist (500 g) and distilled water at 62 °C were mixed in a ratio of 1 : 3.5 and stirred on a heating plate at 65 °C for 1 h. The temperature was then increased to 78 °C (maximum temperature to avoid denaturation of enzymes) for each experiment to ensure constant conditions with regard to particle agglomeration [5, 13]. Afterwards, the mash was adjusted to a final mass of 2350 g (solid-liquid ratio: 1 : 4.7) and cooled to the required temperatures for the further tests using a water bath.

Lab-scale lauter tun (diameter: 10 cm, liquid level: ~29 cm) equipped with a false bottom and heating jacket was used for the filtration tests at different temperatures (40, 50, 60, 68, 71, 73, 75, 76, 77, and 78 °C). In addition to the practical lautering temperature of 78 °C, lower temperatures were tested to investigate the influence

of temperature on the filtration process and particle settling. No temperatures higher than 78 °C were applied to avoid particle agglomeration as described in the literature [5, 13]. 100 mL of water was added to the false bottom to exclude trapped air. After a 5 min sedimentation rest, an iPump1Q peristaltic pump (Baoding Signal Fluid Technology Co., Ltd., Baoding, China) was used to recirculate the trub wort at a flow rate of 28 g/min for 5 min. The flow rate was then increased to 118 g/min and the filtrate mass was recorded over time using a scale until at least 1200 g of the filtrate had been filtered. This enabled the detection of a decrease in the flow rate due to a blocking of the cake. Only first wort was filtered without washing the cake and no raking knives were used to preserve the structure of the cake. The cake height was measured using a folding rule.

2.2 Determination of particle and wort characteristics

The characteristics of the mash particles (particle size distribution, density) and wort (density, viscosity) were determined at different temperatures for use in subsequent calculations. The particle size distribution of the entire mash (Fig. 2) was determined using

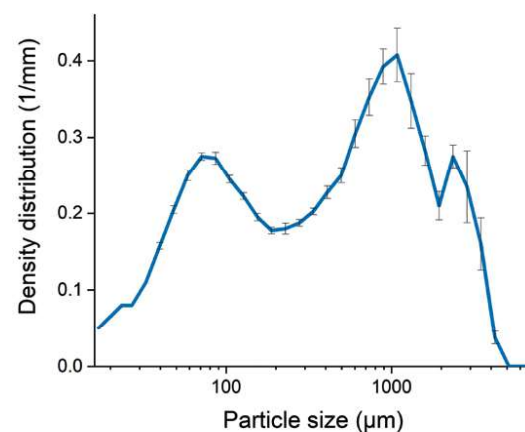


Fig. 2 Particle size distribution of the mash ($n=4$, logarithmic scale)

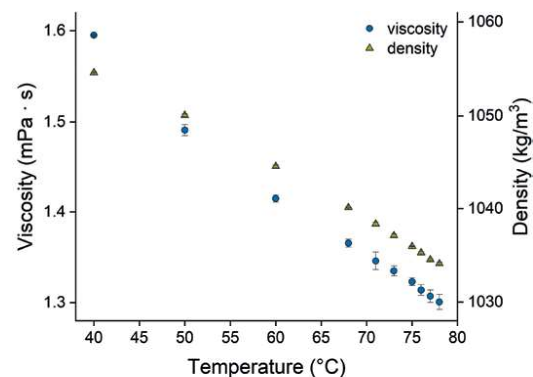


Fig. 3 Viscosity and density of wort at different temperatures ($n=3$)

a QICPIC particle size analyser (Sympatec GmbH, Clausthal-Zellerfeld, Germany).

Fine particles were isolated from the mash by wet sieving (mesh size: 500 μm) using distilled water in a similar way to that in the literature [13]. The particle size distribution of the fine particles was determined using a Mastersizer 3000 (Malvern Panalytical GmbH, Kassel, Germany), which gives a higher resolution at small sizes compared with the QICPIC. The density of the wort (Fig. 3) and filter cake particles was determined using a pycnometer at different temperatures. Different particle densities were found for the top layer ($1432 \pm 6 \text{ kg/m}^3$) and bottom layer particles ($1517 \pm 19 \text{ kg/m}^3$). The wort viscosity at different temperatures (Fig. 3) was determined using an AR-G2 rheometer (TA Instruments Ltd., New Castle, USA) at the constant shear rate of 192 s^{-1} corresponding to the shear rate in the filtrate pipe in the filtration test.

2.3 Calculation of settling velocity

The settling velocity was determined as an example for particle sizes within the mash (125, 250, 500, 1000, 2000, and 4000 μm) at different temperatures. A general form of equation 2 was used to consider differences in the Reynolds numbers (Re) for different particle sizes:

$$w_f = Re \cdot \frac{\eta}{d \cdot \rho_f} \quad (\text{Eq. 3})$$

The calculation considered the density of the particles, which was assumed to be independent of temperature, and the density and viscosity of the liquid at different temperatures were considered. Different shape factors for fine (rounded: 0.81) and bottom layer particles (elongated: 0.61) were assumed [6]. The settling velocity was corrected by multiplying with a concentration factor (β) [17]:

$$\beta = (1 - C)^{\alpha(Re)}, \quad (\text{Eq. 4})$$

which includes the volumetric concentration (C) of the mash and an exponential factor (α) with dependence on the Reynolds number.

2.4 Sedimentation test

Two different sedimentation tests were conducted to verify the calculated settling velocities of the mash particles at different temperatures. Firstly, the entire mash was used to analyse the sediment height of the fine and bottom layers over time (large-scale test). Secondly, the sedimentation behaviour of a suspension consisting only of isolated fine particles (without the influence of coarse particles) was investigated (small-scale test). The mash was transferred to a graduated cylinder (700 mL, height: $\sim 25 \text{ cm}$) with a similar liquid height to that during the filtration for the large-scale test. The cylinder was kept at the required temperatures using a transparent water bath that allowed the measurement of the heights of the layers. The height was measured after 5 and 10 min of sedimentation rest to determine the temperature-dependent differences in the settling of smaller and larger particles. The fine particles did not settle at all due to particle movement at higher temperatures. Therefore, the maximum height of the particles in the suspension was considered as the sediment height (as illustrated in Fig. 1, t_2).

A modified small-scale test was used to analyse the sedimentation behaviour of only the fine particles that remained in suspension in the large-scale test. Isolated fine particles (5.7 g) were suspended in 200 mL of wort to give a particle concentration corresponding to that of the supernatant in the filtration tests. The suspension was transferred to a graduated cylinder (height: $\sim 11 \text{ cm}$). The particles in the supernatant and in the sediment were removed from defined heights (3.7 and 0.5 cm, respectively) after 10-min sedimentation rest using the peristaltic pump. The volume-weighted mean size of these particles ($D[4,3]$) was measured to serve as an indicator of the buoyancy. A reference measurement using distilled water instead of wort was performed at 40 and 78 $^{\circ}\text{C}$ for the supernatant.

2.5 Calculation of filter cake resistance

The filter cake resistance after particle sedimentation (t_2) was estimated for the fine and bottom layers from

$$\alpha_h = 180 \cdot \frac{(1 - \varepsilon)^2}{d^2 \cdot \varepsilon^2} \quad (\text{Eq. 5})$$

The median values of the size distributions of fine particles ($60 \pm 5 \mu\text{m}$) and the entire mash ($1665 \pm 125 \mu\text{m}$) were used as the particle sizes for the fine and bottom layers, respectively. The porosity (ε) was determined from

$$\varepsilon = \frac{V_{total} - V_{particle}}{V_{total}} \quad (\text{Eq. 6})$$

using the total sediment volume (V_{total}) determined by the height measurement in the large-scale sedimentation test. The volume of the particles ($V_{particle}$) was determined by dividing the gravimetrically determined mass of each layer by its corresponding particle density.

2.6 Statistics

Each experiment was performed three times ($n = 3$) unless stated otherwise. Means and standard deviations were calculated, and a statistical evaluation was conducted using OriginPro 2019b (OriginLab Corporation, Northampton, USA). Significant differences between the means were determined using a t-test.

3. Results and Discussion

A filtration test was used to investigate the influence of temperature on the flow rate. A characteristic turning point in the flow rate was observed for each temperature (examples in Fig. 4a) after around 10 min. This drop in the flow rate is based on the high resistance of the fine particle layer causing blocking and thus a compression of the bottom layer of the cake as described in the literature [14].

The average flow rate before and after the turning point was calculated to evaluate the temperature dependence (Fig. 4b). Before the turning point, the flow rate increases only slightly with increasing temperature. After the turning point, the flow rate increases more for temperatures $> 60 \text{ }^{\circ}\text{C}$. Therefore, the flow rate after blocking is influenced by the temperature to a higher degree than before blocking. It can be concluded that the top layer has a greater temperature dependence than the bottom layer as the

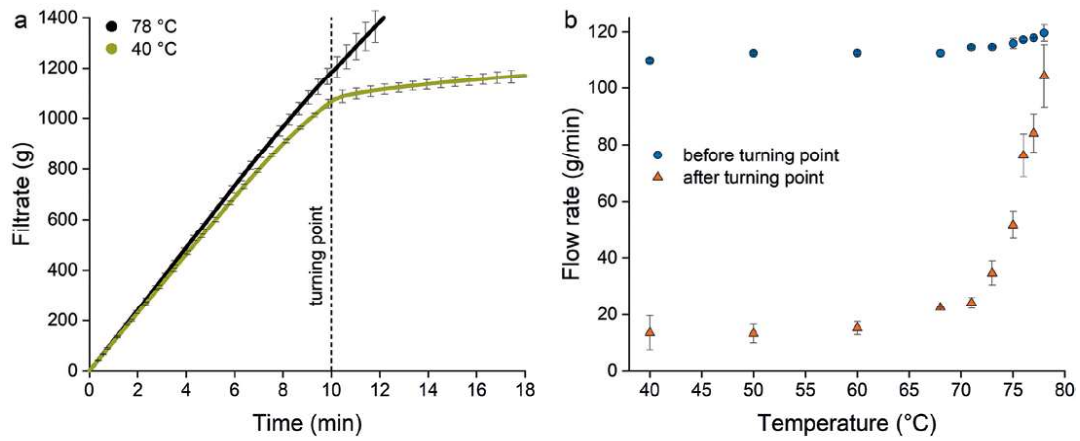


Fig. 4 (a) Filtrate mass per time at 40 and 78 °C. Vertical line indicates the turning point after the filter cake blocking at around 10 min. (b) Average flow rate before and after the turning point at different temperatures (n = 3)

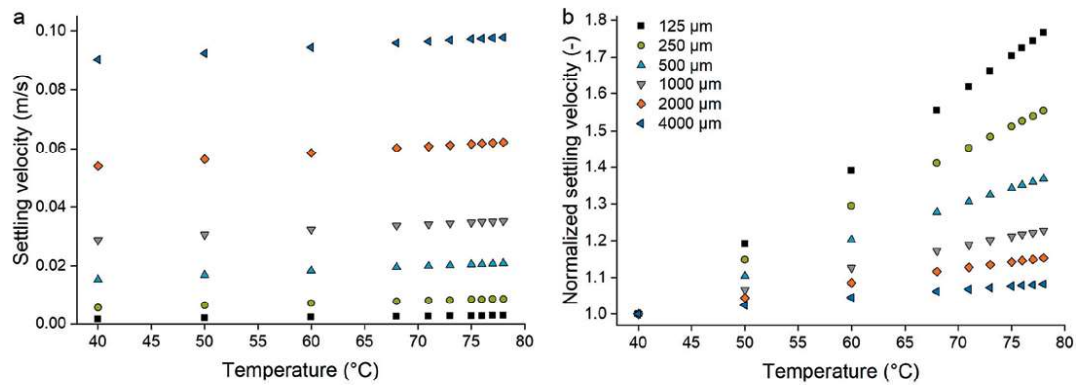


Fig. 5 (a) Calculated settling velocity for various particle sizes at different temperatures and (b) the data normalized to the value at 40 °C

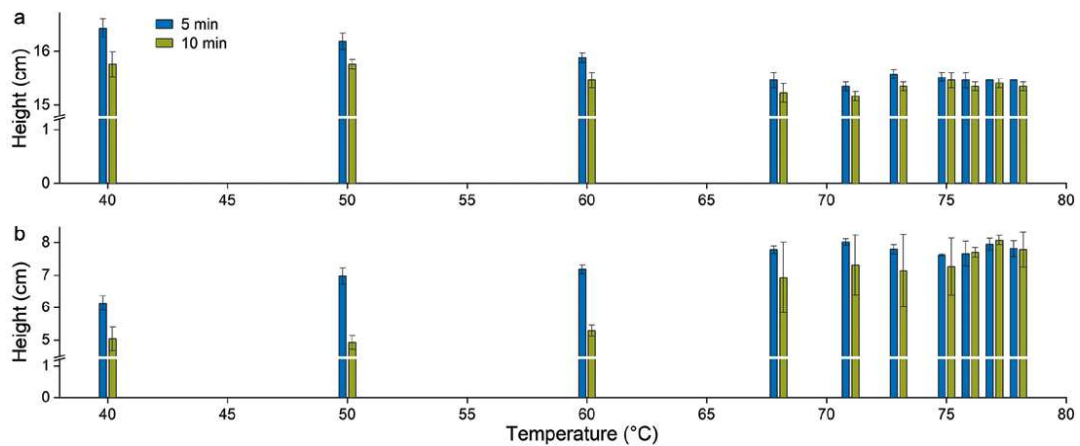


Fig. 6 Sediment height after 5 and 10 min at different temperatures (n = 3) of (a) the bottom layer and (b) the fine particle layer (break in y-axis)

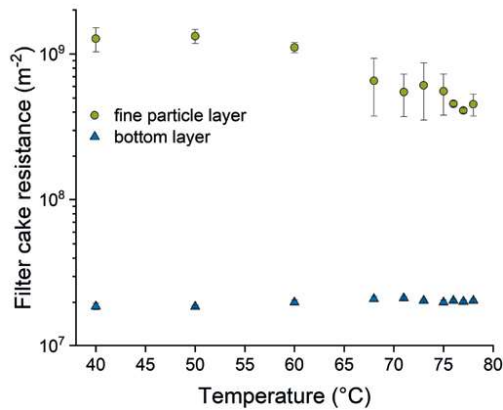


Fig. 7 Filter cake resistance of the fine particle and bottom layers after sedimentation (10 min) at different temperatures (logarithmic scale, $n = 3$)

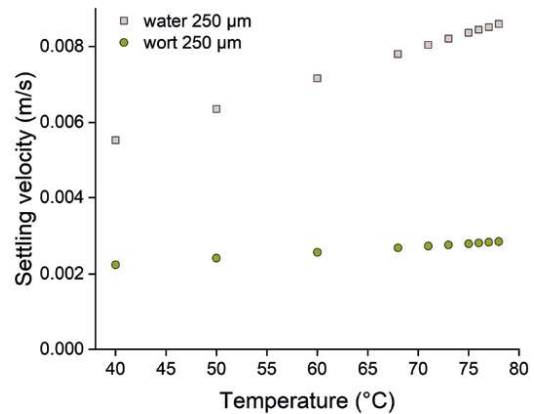


Fig. 9 Calculated settling velocities of particles with a size of 250 µm in water and wort at different temperatures

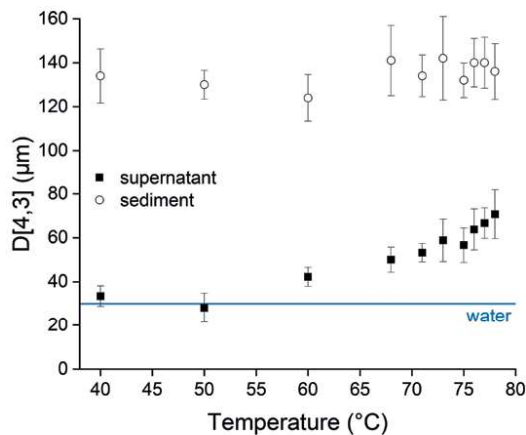


Fig. 8 Mean particle size (D[4,3]) of the supernatant (buoyancy indicator) and sediment in the fine particle sedimentation test after 10 min at different temperatures ($n = 30$). Horizontal line indicates the mean particle size in the supernatant when using water instead of wort

blocking is caused by the high resistance of the fine particle layer [14]. In addition, a higher correlation between viscosity and flow rate before blocking ($R = -0.85$, $p < 0.01$) than after blocking ($R = -0.69$, $p < 0.05$) was found. Therefore, the viscosity has a minor impact after the blocking.

An influence of temperature on the sedimentation behaviour of the different mash particles was expected according to equation 2 as the density is reduced at higher temperatures as well as the viscosity (Fig. 3). Therefore, the settling velocity for different particle sizes at different temperatures was calculated (Fig. 5a).

The larger the particle size, the higher the calculated settling velocity. In addition, the settling velocity increases with higher temperatures. When normalizing the settling velocity to 40 °C (Fig. 5b), it can

be seen that the temperature dependence is stronger for smaller particle sizes. Therefore, it was expected that the sedimentation behaviour of the particles, and thus the structure of the top and bottom layers, differs with temperature. This was investigated by measuring the sediment height of the different layers at different temperatures and after different settling times (Fig. 6).

There is no difference in the height after 10 min over the range between 40 and 78 °C for the bottom layer (Fig. 6a), which means that sedimentation of the bottom layer is finished after 10 min at the latest regardless of the temperature. A significant difference in the sediment height between 5 and 10 min was observed at low temperatures but was reduced as the temperature increased. This confirms the higher settling velocity at higher temperatures as the final sediment height is reached faster at higher temperatures.

The sedimentation test of the fine particle layer showed a different behaviour (Fig. 6b). There is again a significant difference between the 5- and 10-min sedimentation time at 40 °C but not at 78 °C. However, the height of the fine particles in suspension (see Fig. 1, t_2) between 40 and 78 °C still differs after 10 min. Instead of a lower height, as would have been expected due to the higher settling rate of fine particles (Fig. 5), a greater height was found at higher temperature. This means that some of the fine particles do not settle at all at temperatures > 60 °C and remain in suspension. This trend agrees with the flow rate after blocking (Fig. 4b) which increases above this temperature and is a hint that the flow rate depends also on the settling behaviour of the fines.

The porosity of the top layer is increased due to the lower particle packing density when the fine particles do not sediment at higher temperatures. Consequently, the calculated filter cake resistance (at t_2) of the fine particle layer is reduced by 64 % at 78 °C compared with that at 40 °C (Fig. 7). A high correlation ($R = -0.74$, $p < 0.05$) of the resistance of the fine layer with the flow rate after blocking was found, which confirms the dependence of the flow rate on the fine particles.

The resistance of the top layer is about 22 times higher than that of the bottom layer at 78 °C, which is in agreement with the literature [3, 13]. There is no significant difference in the resistance of the bottom layer between 40 and 78 °C meaning that the formation of this layer is not affected by temperature. However, the resistance of the bottom layer can increase during filtration based on compression [14] which was not considered in the calculation.

The decrease in the resistance of the fine layer at higher temperatures results in a lower degree of cake compression. This was verified by measuring the cake height as indicator for the compression. The cake height was 10.8 cm (± 0.2) at 78 °C and 7.97 cm (± 0.05) at 40 °C (compared with the initial cake height of 15.2 ± 0.2 cm prior to the filtration).

The lower resistance of the fine particle layer at increasing temperature could be explained by thermal convection leading to a buoyancy effect that counteracts the particle sedimentation and results in lower particle packing. The mean particle size of the supernatant (buoyancy indicator) was measured to quantify the particles in suspension that did not settle (Fig. 8). The mean particle size of the supernatant increases with increasing temperature meaning that larger particles are held in suspension at higher concentrations. In contrast, there is no significant difference in the particle size of the sediment between 40 and 78 °C, which has a higher particle size in general. This shows that the smaller particles in the top layer are especially affected by buoyancy.

There is a high correlation of the buoyancy indicator with temperature ($R = 0.93$, $p < 0.001$). In addition, a high correlation of the buoyancy indicator with the filter cake resistance ($R = -0.95$, $p < 0.001$) and flow rate ($R = 0.87$, $p < 0.01$) after blocking were found. Therefore, the hindered sedimentation of the fine particles at high temperature is responsible for the lower resistance in this layer, causing the increase in the flow rate.

A control experiment showed that the buoyancy effect at higher temperatures is only present when using wort. The effect was not observed when the particles were suspended in water (Fig. 8, horizontal line) where the mean particle size at 40 °C ($31 \pm 3 \mu\text{m}$) and 78 °C ($30 \pm 12 \mu\text{m}$) did not differ significantly from the value with wort at 40 °C. Therefore, the buoyancy effect that counteracts sedimentation at high temperatures is only present when suspending the particles in wort. This is due to the higher viscosity and density of wort resulting in a lower settling velocity compared with water (Fig. 9, example calculation using a particle size of 250 μm). In this case, the more pronounced buoyancy counteracts the particle sedimentation in wort even when the settling velocity increases at higher temperature. The higher settling rate due to the lower viscosity and density is more pronounced than the buoyancy when suspending the particles in water. Thus, the particles settle in water even at higher temperatures.

The dependence of the buoyancy effect on the viscosity and density of the liquid shows that it can be affected by the characteristics of the wort and malt. For example, a higher wort gravity results in a higher density and viscosity, which favours the buoyancy at high temperature. An increase in viscosity due to poor cytolitic modification could also increase the buoyancy effect. In these cases,

however, the flow rate is also influenced by the negative effect of the high viscosity and therefore gives no advantage for the filtration process.

It is proposed that the buoyancy effect is dependent on thermal convection, based on a temperature difference in the lauter tun (Fig. 10). The temperature of the suspension is constant on the sides due to the insulation of the wall (T_1). However, the temperature can decrease in the upper centre (T_2) where there is no insulation, which means the density increases at this location.

The resulting difference in the density can result in a circulating motion of the suspension, similar as described in the literature [10]. As a result, there is an upward flow of particles on the sides and a downward flow in the centre. This movement of the liquid prevents particles from settling, which was observed visually during the experiments. Due to the size of the particles, Brownian motion can be excluded as an explanation of the particle movement [16]. In contrast, if the temperature is generally lower and therefore assumed to be equal at both locations ($T_1 = T_2$), then it is expected that there is no density difference and thus no particle movement and buoyancy. Consequently, the particles can settle at lower temperatures.

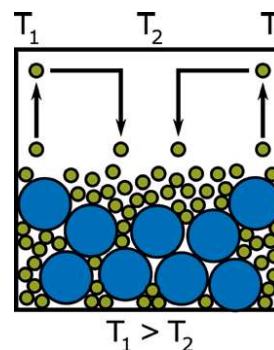


Fig. 10 Illustration of particle movement because of thermal convection with a high temperature difference between lauter tun wall (T_1) and centre (T_2)

4. Conclusions

A high temperature is usually maintained in the lauter tun to increase the flow rate. However, the temperature-dependent viscosity is not the main factor that determines flow rate. It was shown that the filter cake resistance of the fine layer decreases at higher temperatures in addition to the less important viscosity reduction. A buoyancy effect based on thermal convection at high temperatures is responsible for the lower resistance as the particles are hindered from settling, resulting in a lower particle packing of the fine layer. Consequently, blocking of the filter cake is reduced resulting in a higher flow rate.

The results show that high temperatures are essential in lautering to maintain a low resistance of the critical fine particle layer. During the filtration process, however, the temperature cannot be kept constant by heating the lauter tun. Proper temperature insulation of the filter is therefore essential. In addition, temperature losses during the mash transfer should be avoided, e.g. by pumping in the mash from below.

The sedimentation of the fine particles should be avoided for as long as possible during lautering to maintain a low filter cake resistance. This requires a high buoyancy effect. Therefore, the liquid level should not be allowed to decrease to the level of the top of

the filter cake during the filtration of the first wort to maintain the buoyancy at the beginning of the second wort.

The buoyancy effect at high temperatures can reduce the resistance of the fine particle layer. Nevertheless, fine particles hinder the filtration process even at high temperatures. In order to avoid the negative effect of fine particles at all, an alternative lautering technique was recently presented in the literature [14], in which the resistance of the top layer was reduced by removing the fine particles prior to the filtration.

The differences in the particle settling of fine and coarse particles at high temperatures affect the structure of the cake. On the one hand, fine particles are hindered from settling and are therefore present at the top in a higher concentration. On the other hand, the settling velocity of coarse particles is increased. This favours the formation of the multilayered filter cake.

Funding

This IGF Project of the FEI was supported via AiF (19359N) within the programme for promoting the Industrial Collective Research (IGF) of the German Ministry of Economic Affairs and Energy (BMWi) based on a resolution of the German Parliament.

Acknowledgment

We are grateful to the Chair of Process Systems Engineering (Technical University Munich) for the skilful help with the particle size measurement (QICPIC).

5. References

- Asselmeyer, F.; Höhn, K.; Issing, E.: Die Temperaturabhängigkeit von Viskosität und Dichte bei Bieren, Ausschlag- und Vorderwürzen, *Brauwissenschaft* **26** (1973), no. 4, pp. 93-101.
- Barrett, J.; Clapperton, J. F.; Divers, D. M.; Rennie, H.: Factors affecting wort separation, *J Inst Brew* **79** (1973), no. 5, pp. 407-413.
- Bühler, T. M.: Effects of physical parameters in mashing on lautering performance, 1996.
- Bühler, T. M.; McKechnie, M. T.; Wakeman, R. J.: A model describing the lautering process, *Monatsschrift für Brauwissenschaft* **7/8** (1996), pp. 226-233.
- Bühler, T. M.; McKechnie, M. T.; Wakeman, R. J.: Temperature induced particle aggregation in mashing and its effect on filtration performance, *Food Bioprod Process* **74** (1996), no. 4, pp. 207-211.
- Draxler, J.; Siebenhofer, M.: *Verfahrenstechnik in Beispielen*, Auflage: Springer Vieweg, 2014.
- Engstle, J.; Briesen, H.; Först, P.: Mash separation in the lauter tun – a particle size dependent separation process, *BrewingScience* **70** (2017), pp. 26-30.
- Evans, D. E.: The Impact of Malt Blending on Lautering Efficiency, Extract Yield, and Wort Fermentability, *JASBC* **70** (2012), no. 1, pp. 50-54.
- Gastl, M.; Kupetz, M.; Becker, T.: Determination of Cytolytic Malt Modification – Part II: Impact on Wort Separation, *J Am Soc Brew Chem* (2020), pp. 1-9.
- Gotoh, K.; Yamada, S.; Nishimura, T.: Influence of thermal convection on particle behavior in solid-liquid suspensions, *Adv Powder Technology* **15** (2004), no. 5, pp. 499-514.
- Greffin, W.; Krauß, G.: Schrotten und Läutern. II. Arbeit mit konventioneller Trockenschrotmühle und Läuterbottich – eine Literaturübersicht, *Monatsschrift für Brauwissenschaft* **31** (1978), no. 6, pp. 192-212.
- Hennemann, M.; Gastl, M.; Becker, T.: Inhomogeneity in the lauter tun: a chromatographic view, *Eur Food Res Technol* **245** (2019), pp. 521-533.
- Hennemann, M.; Gastl, M.; Becker, T.: Influence of particle size uniformity on the filter cake resistance of physically and chemically modified fine particles, *Sep Purif Technol* **272** (2021), pp. 118966.
- Hennemann, M.; Gastl, M.; Becker, T.: Optical method for porosity determination to prove the stamp effect in filter cakes, *J Food Eng* **293** (2021), pp. 110405.
- Lu, W.-M.; Tung, K.-L.; Pan, C.-H.; Hwang, K.-J.: The Effect of Particle Sedimentation on Gravity Filtration, *Sep Sci Technol* **33** (1998), no. 12, pp. 1723-1746.
- Newburgh, R.; Peidle, J.; Rueckner, W.: Einstein, Perrin, and the reality of atoms: 1905 revisited, *Am J Phys* **74** (2006), no. 6, pp. 478-481.
- Richardson, J. F.; Zaki, W. N.: The sedimentation of a suspension of uniform spheres under conditions of viscous flow, *Chem Eng Sci* **3** (1954), no. 2, pp. 65-73.
- Schaus, O. O.: Elevated temperature lautering, *MBAA Tech Q* **9** (1972), no. 4, pp. 192-194.
- Tippmann, J.; Scheuren, H.; Voigt, J.; Sommer, K.: Procedural investigations of the lautering process, *Chem Eng Technol* **33** (2010), no. 8, pp. 1297-1302.
- Tippmann, J.; Voigt, J.; Sommer, K.: Measuring particle size distribution of mash with laser diffraction to evaluate the process success, *BrewingScience* **64** (2011), pp. 13-21.

Received 6 July, 2021, accepted 21 July, 2021

3.2.3 Optical Method for Porosity Determination to Prove the Stamp Effect in Filter Cakes

Journal of Food Engineering 293 (2021) 110405



Contents lists available at ScienceDirect

Journal of Food Engineering

journal homepage: <http://www.elsevier.com/locate/jfoodeng>



Optical method for porosity determination to prove the stamp effect in filter cakes

Martin Hennemann, Martina Gastl^{*}, Thomas Becker

Technical University Munich, Chair of Brewing and Beverage Technology, Weihenstephaner Steig 20, 85354, Freising, Germany

ARTICLE INFO

Keywords:

Cake filtration
Fine particle
Lauter tun
Porosity
Skin effect
Surface roughness

ABSTRACT

During lautering, a filtration process in beer production, an inhomogeneous filter cake composed of different horizontal layers is formed. Fine particles settle slower than coarse particles and form a layer on top of the cake. Due to its low permeability, the fine layer acts as a stamp on the compressible bottom layer, thus resulting in cake compression and reduced flow rate (stamp effect). A method to prove the stamp effect and investigate its impact on the filtration was developed. The structure of the cake was preserved by freezing, which enabled sampling from different layers at different filtration times. An optical porosity determination (surface roughness) was established to study the compression. A predominant impact of the stamp effect compared with a less pronounced skin effect was shown. To avoid the stamp effect during filtration, a filtration technique was developed, which includes the removal of fines from the filter cake.

1. Introduction

Cake filtration is a type of solid–liquid separation process that is applied in numerous industrial sectors. It is performed after extracting valuable substances from the raw material when the liquid of interest is separated from the insoluble particles of the suspension. Among the processes of cake filtration, the lautur tun (LT) operation in beer production is extraordinary. The batch-wise process is a unique type of filtration based on the suspension to be filtered. The suspension (mash) is produced in the preceding mash tun (MT) operation by mixing the milled raw material (malt grist) with water. During the malt milling process, the husks must be preserved to maintain a porous filter cake structure in the LT. As a result, the suspension has a wide particle size distribution (Tippmann et al., 2011). The differences in the diameter (d) and density (ρ_s) of the particles lead to an irregular sedimentation behaviour when transferring the suspension from the MT into the LT, which affects the sedimentation velocity (w_f) according to

$$w_f = \frac{\rho_s - \rho_f}{18 \cdot \eta} \cdot g \cdot d^2. \quad (1)$$

The sedimentation velocity depends on the fluid density (ρ_f), gravitational field strength (g) and viscosity (η). Accordingly, coarse particles settle earlier and form a bottom layer, whereas fine particles ($<500 \mu\text{m}$) sediment later on top of the bottom layer (Engstle et al., 2017). This

results in the formation of an inhomogeneous, multi-layered filter cake structure. The resulting horizontal layers differ not only in their chemical composition but also in their filtration characteristics (Hennemann et al., 2019).

Especially the fine layer determines the flow rate based on its low permeability, which results in the formation of a blocking layer on the top of the cake (Barrett et al., 1973; Bühler et al., 1996; Engstle et al., 2015). The predominant impact of the fine layer on the flow rate compared with the bottom layer distinguishes the LT operation from other filtration types. It is suggested that a skin layer next to the filter medium that regulates the filtration—as observed in other types of cake filtration (Alles and Anlauf, 2003; La Heij et al., 1996; Tiller and Green, 1973)—plays only a minor role in the LT.

In addition to its low permeability, the fine layer affects the cake filtration in another way. Based on its location on top of the cake, the drag force transmitted to the fine layer during filtration compresses the underlying compressible bottom layer similar to a stamp (stamp effect). This compression reduces the porosity of the bottom layer and results in a decrease in the flow rate. Although compression by the fines was previously suggested (Bühler et al., 1996), the stamp effect is currently not proven. Therefore, this paper aimed to investigate the stamp effect-dependent decrease in the cake porosity and the resulting flow rate reduction.

The two filtration characteristics to describe the stamp effect—flow rate (Q) and porosity—are correlated according to

^{*} Corresponding author.

E-mail address: martina.gastl@tum.de (M. Gastl).

<https://doi.org/10.1016/j.jfoodeng.2020.110405>

Received 12 August 2020; Received in revised form 19 October 2020; Accepted 7 November 2020

Available online 16 November 2020

0260-8774/© 2020 The Authors.

Published by Elsevier Ltd.

This is an open access article under the CC BY-NC-ND license

<http://creativecommons.org/licenses/by-nc-nd/4.0/>.

Abbreviations

LT	Lauter tun
MT	Mash tun
SF	Standard filtration

$$Q = \frac{k \cdot A \cdot \Delta p}{h \cdot \eta}, \quad (2)$$

which includes the cross-sectional area (A), pressure difference (Δp) and cake height (h). The permeability (k) is related to the porosity (ϵ) according to

$$k = \frac{d^2}{180} \frac{\epsilon^3}{(1-\epsilon)^2}. \quad (3)$$

This relation indicates that a high permeability and, thus, a high flow rate depend on a high cake porosity. The porosity is defined by the relation between the cavity volume (V_{cav}) and the total volume (V_{tot}) according to

$$\epsilon = \frac{V_{cav}}{V_{tot}}. \quad (4)$$

For the determination of porosity in porous media, various methods are available in the literature (Bühler et al., 1996; La Heij et al., 1996; Martin et al., 2013; Mathmann et al., 2014). Although these methods can be employed to determine the filter cake porosity, there are disadvantages for an investigation of the stamp effect. For example, gravimetric porosity measurements are time-consuming and, therefore, are often only used as a reference for the calibration of another method (La Heij et al., 1996; Martin et al., 2013; Sakai and Nakamura, 2005). Another method for porosity determination based on the cake height was already applied for lautering (Bühler et al., 1996; Engstle et al., 2015), but only an average porosity of the inhomogeneous filter cake could be determined. Furthermore, the method enables porosity determination only of the peripheral filter cake area without insights into the centre of the cake. Micro-computed tomography was also employed to study the filter cake in the LT (Mathmann et al., 2014). An advantage of tomography is that insights into the centre structure of the cake and the different layers are possible. Because the sample was measured at the end of the filtration process from a dry filter cake, no insights into the cake compression during filtration were obtained.

The summary of the literature revealed that the available methods do not satisfy the requirements for investigating the stamp effect. Furthermore, the stamp effect is a unique and rather unusual mechanism among the filtration processes. Moreover, it has been neglected in the literature because it occurs exclusively during lautering in the brewing process. Therefore, the main aim of the paper was to prove the stamp effect using a new developed method for porosity determination.

The first step was the detection of the stamp effect in lab-scale filtration experiments. Using a small-scale filter, the blocking of the cake was triggered to examine the effects on flow rate and pressure drop in the filtrate pipe. The cake height measurement revealed the compression during filtration. Because the small-scale filter allowed no detailed insights into the cake compression, measurement of the porosity of the individual layers was required. Therefore, a second larger lab filter was developed to obtain filter cakes with practical dimensions (30–40 cm). The cake could be frozen to enable fixation of its structure at different filtration times. Sampling from different horizontal layers enabled the consideration of the structural inhomogeneity. A new optical method was developed to rapidly assess the porosity. The method is based on the measurement of the layer surface roughness—the arithmetical mean height of a surface profile—that correlates with the internal cake porosity. This correlation has already been validated, e. g.,

for the measurement of asteroid surface analogues (Sakai and Nakamura, 2005) or rocks (Rebollo et al., 1996). After the optical method was calibrated with a reference porosity measurement, it was employed to study the change in the porosity during the compression.

To prove the stamp effect, the filtration experiments were modified. Using different types of malt, the influence of the raw materials on the effect was investigated. The raw materials were selected based on their variations in the filtration behaviour. In another modification, an oxidised form of the fines was used, which decreased their permeability. The resulting accentuation of the stamp effect was investigated. The fines were removed prior to the filtration in another modification to show their requirement for the cake compression. These modifications enabled the stamp effect to be proven and revealed its predominant impact compared with a less pronounced skin effect.

Because several factors (e. g. raw material) are provided in the process, the stamp effect cannot be avoided in the conventional LT operation. Therefore, a new filtration technique was established to avoid the stamp effect by the removal of the fines. After a successful implementation in the lab scale, the technique was verified in an upscale, and the effects on the process time, yield and product quality were examined.

2. Materials and methods

2.1. Lab-scale filtration

As the first step to detect the stamp effect-dependent cake blocking, lab-scale filtration experiments were conducted using a small-scale filter (LT-1, height: 29 cm, Fig. 1a). Contrary to the practical process, the filter was used to deliberately cause the cake blocking by applying a consistent high flow rate (117 g/min) using an iPump1Q peristaltic pump (Baoding Signal Fluid Technology Co., Ltd., Baoding, China). This allowed the determination of the filtrate mass per time using a scale. The pressure in the filtrate pipe was recorded using a DRTR-AL-10 V/20 mA relative pressure transmitter (B + B Thermo-Technik GmbH, Donaueschingen, Germany) to detect the pressure drop after the cake blocking. Cake compression was examined by measuring the height (average of one central and four peripheral measurements) from the top using a folding rule.

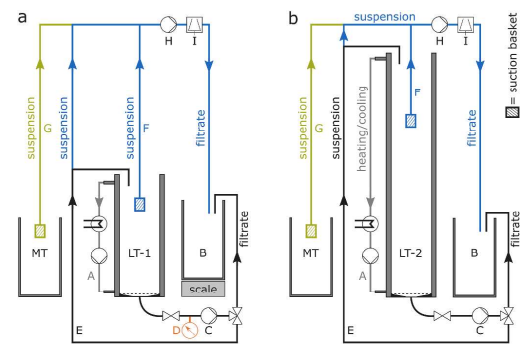


Fig. 1. Lab-scale filters: a) Lauter tun filter 1 (LT-1) with heating circuit (A), filtrate collector (B) placed on a scale, filtrate pipe with peristaltic pump (C), pressure sensor (D) and recirculation pipe for cloudy filtrate (E). b) Lauter tun filter 2 (LT-2) with an additional cooling circuit. Suspension is produced in a laboratory mash tun (MT). Suctions from LT-1/LT-2 (F, blue, LT-trial) and combined suction from MT and LT-1/LT-2 (G, green/blue, MT/LT-trial) using a suction basket connected to a peristaltic pump (H) and centrifuge (I). (For interpretation of the references to colour in this figure legend, the reader is referred to the Web version of this article.)

3 Results

After the stamp effect detection, a second larger-scale filter (LT-2, height: 58 cm, Fig. 1b) was constructed to obtain filter cakes with practical dimensions. The cakes were used for the subsequent porosity determination to enable detailed insights into the compression. Compared with filtration in LT-1, a lower and practical filtration flow rate (43 g/min) was applied. This allowed the evaluation of the compression at different filtration states. Filtration was stopped after 56 min as a standardized process before the cake went dry, unless stated otherwise.

Both filters were heated to a practical filtration temperature of 78 °C. The filter medium (diameter: 10 cm) was overlaid with 100 mL of water to exclude the entrapped air. Contrary to the practical lautering process, no sparging water was used for cake washing, and no raking was performed to preserve the cake structure.

The setups without modifications as described in this section are referred to as standard filtration (SF) in the following.

The suspension was produced in a laboratory MT (Dinkelberg Analytics, Gablingen, Germany). Raw material (malt) was milled to grist using a DLFU disc mill (Bühler AG, Uzwil, Switzerland) at a grinding gap of 0.65 mm. Grist (LT-1: 500 g, LT-2: 1035 g) and distilled water of 60 °C were mixed at a ratio of 1:3.5. For extraction and enzymatic conversion, the suspension was heated under stirring to 62 °C (30-min rest) and 72 °C (30-min rest). After heating to a practical filtration temperature of 78 °C, the suspension was transferred to the filter.

Pre-trials revealed that oxidation exhibited a negative influence on the flow rate. Therefore, reducing agent (0.6 g/L potassium metabisulfite, Merck KGaA, Darmstadt, Germany) was added to the suspension. However, for the experiments in LT-1, no reducing agent was added to emphasise the cake blocking by the negative effects of oxygen.

After transfer to the filter, a 10-min rest allowed sedimentation of the particles. Afterwards, cloudy filtrate was recirculated back on the top of the filter in a standardised procedure until filtrate was clear (LT-1: 28 g/min for 5 min, LT-2: 21 g/min for 7.5 min).

2.2. Filter cake fixation and optical porosity determination

To obtain detailed insights into the cake compression, a new method for porosity determination was established and applied on the samples produced using LT-2. To fix the cake structure at the end of the experiment, the filter was pre-cooled to room temperature, followed by freezing overnight in a fridge.

It is known that slow freezing can affect the ultrastructure of biological particles based on the formation of ice crystals. However, no crystals were observed on a macroscopic scale during the experiments. Therefore, the obtained porosity values can be used for a comparison within the experiments in this paper.

The frozen cake was removed from the filter and cut into five horizontal layers (fine layer and four bottom layers 1–4) of equal height using a mitre-box saw. From each layer, two sample slices were cut out. The peripheral area was removed to avoid wall effects. After unfreezing at room temperature for 24 h, the porosity of the cake slices was determined by measuring their surface roughness. To correlate the values of the surface roughness with porosity, the optical method was first calibrated using a gravimetric method as reference.

The first step of the calibration was to determine a reference porosity using one of the two sample slices. The volume of the cavities in the filter cake corresponded to the amount of liquid occupying the voids. Therefore, V_{cav} could be determined by measuring the weight loss (m) when the liquid drains from the cavities by unfreezing of the slice. The slice was placed on a filter paper in a funnel to remove the liquid phase. To avoid the liquid from evaporating within the particles, the filter cake was not dried at high temperatures. Thereby, only the macro pores between the particles but not the internal particle porosity was considered as filter cake porosity. A conversion of m into V_{cav} was performed by considering ρ_f , which was determined using a DMA 4500 density metre (Anton Paar GmbH, Graz, Austria). Accordingly, Equation (4) was

modified to

$$\varepsilon = \frac{m}{V_{tot} \cdot \rho_f} \quad (5)$$

V_{tot} was determined by measuring the side length of a frozen cake slice using a slide gauge.

Parallel to the determination of the reference porosity, the surface roughness of the second slice of the layer was measured. It was placed on a porous medium during unfreezing, which allowed a slow absorption of the liquid to avoid disruption of the cake structure. The surface roughness was analysed by scanning the sample using a VHX-950F digital microscope (Keyence Deutschland GmbH, Neu-Isenburg, Germany) at a magnification of $50\times$. Gaussian filters (low-pass: 800 μm , high-pass: 2.5 mm) were applied for smoothing and removal of undulations using the microscopes software (VHX-H4M). The data was merged with MATLAB R2018b (The MathWorks, Inc., Natick, USA). Six measurements were recorded from each slice to obtain an average value of the surface roughness.

The small particle size of the fines did not allow the determination of their surface roughness, thus limiting the application of the method to the magnification of the microscope. However, the fine layer is a variable and will be modified or removed in the subsequent experiments. Therefore, the fine layer was excluded from the calibration, and the stamp effect was investigated indirectly via a change in the compression of the four bottom layers.

To obtain porosity values in a wide range for the calibration, filter cakes from the lowest (Fig. 2, point A) to the highest (Fig. 2, point D) compression were produced by varying the volume of the filtrate. A high surface roughness corresponds to a high porosity, and a linear correlation between surface roughness and porosity was observed ($R^2 = 0.97$; $p < 0.001$). The correlation enables the determination of the porosity via a measurement of the surface roughness. This is consistent with similar calibration methods found in the literature (Sakai and Nakamura, 2005; Rebollo et al., 1996) where the measurement was validated using conventional methods.

After the successful calibration, both slices per layer could be used to measure the surface roughness in the following experiments to obtain an average of 12 measurements.

2.3. Modification of filtration tests

To prove the stamp effect, the suspensions were modified to either emphasise or lower the fine-particle-dependent cake compression.

Three different types of malt were used to investigate the dependence of the compression on the raw material. The malts differed in their cytolytic degree of modification and the barley variety in order to obtain different filtration behaviors. As determined in the pre-trials, the malts varied in their flow rate (#1: medium, #2: high, #3: low). Malt 1 with an intermediate flow rate was used for all trials as standard, unless stated otherwise.

An emphasised stamp effect was examined via an oxidation of the suspension where no reducing agent was added compared with the SF-trial. Contrarily, a lower stamp effect was tested by removing the fines by performing wet sieving of the suspension over a sieve (mesh size: 500 μm). The volume of the removed particles was replaced by a filtrate from a previous test, and no modification of the larger particles ($>500 \mu\text{m}$) occurred.

2.4. Development of filtration technique

After the stamp effect has been proven, a new filtration technique was established to avoid the formation of the blocking layer by the removal of the fine particles.

The technique was based on a standardised suction of the fines prior to filtration from the top of the filter cake. It was applied to both lab-scale filters to study the impact on flow rate and cake porosity

3 Results

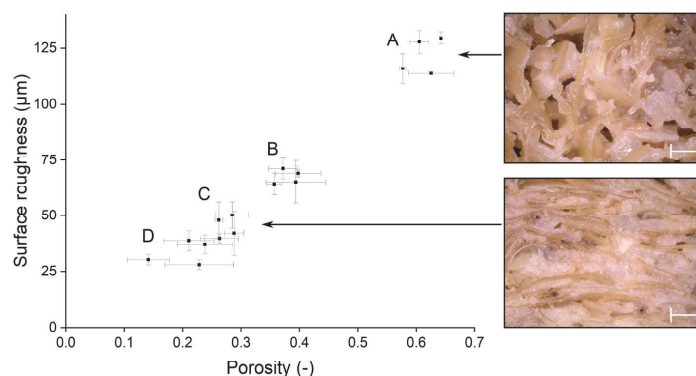


Fig. 2. Surface roughness as a function of the gravimetric reference porosity (left, $R^2 = 0.97$, $n = 3$). Four states of compression are presented from minimum (A) to maximum compression (D). Only the bottom layers are presented. Representative microscopic images of cake layers (right) show the state of compression before the start of filtration (A) and after the standard filtration test (C). Scale bar represents 1 mm.

compared with the SF-trial without suction. In the first setup (LT-trial, Fig. 1, blue), ~30% of the suspension was removed from the top of the filter after the sedimentation rest using a suction basket (mesh size: 500 µm) connected to the previously described peristaltic pump. The suction basket was placed above the cake to avoid the uptake of coarser particles.

The second setup involved the suction not only from the filter but already from the preceding step in the MT. In this combined suction from MT and LT (MT/LT-trial, Fig. 1, green/blue), ~24% of the suspension was first removed from the MT before transferring to the filter and then additionally ~30% from the LT. For the suction from the MT, a sedimentation rest of 5 min without stirring allowed the coarser particles to settle. The amount of the removed suspension from the MT was replaced by an equal amount of water (78 °C). Filtration was conducted for both setups until the same amount of filtrate was collected as for the SF-trial. Cloudy filtrate was not recirculated back to the filter for the suction trials but was added to the fine-particle suspension instead. Clear filtrate was retained from the suspension by centrifugation (Fig. 1, I) at 4000 rpm for 5 min in a Heraeus Multifuge 4 KR (Thermo Fisher Scientific Inc., Waltham, USA).

2.5. Pilot scale

The new filtration technique was verified on a pilot-scale plant. The effect of the fine-particle removal by suction on the process time, extract yield and filtrate quality was investigated.

The suspension was produced according to the lab scale. Raw material (8.3 kg) was milled on a two-roller mill (Künzel Maschinenbau GmbH, Mainleus, Germany) at a milling gap of 0.8 mm. A 5-min sedimentation rest after transfer to the LT was followed by 5 min of cloudy filtrate recirculation. After collecting the first wort (15 kg), two equal batches of water (sparging) were applied to wash the filter cake until 63 kg of total filtrate was obtained. The filter cake permeability was maintained by standardised raking, as conducted in the practical LT operation. Filtration was performed at constant parameters (flow rate, cloudy filtrate recirculation and sparging), unless stated otherwise. For suction trials, the fine-particle suspension was removed using a suction basket (mesh size: 500 µm) attached to a JP-06 pump (ESSKA.de GmbH, Hamburg, Germany). For the MT/LT-trial, ~43% of the first sparging water was used in the MT prior to the transfer to the LT to replace the volume of the removed fine-particle suspension.

The extract yield and the washable extract (dry matter) in the fines and filter cake were determined according to MEBAK

(Mitteleuropäische Brautechnische Analysenkommission) (Miedaner, 2002). The extract was measured using the previously described density metre. The filtrate characteristics (turbidity and photometric iodine value) were determined based on their importance for the subsequent production steps in brewing (e.g. fermentation) and their impact on the product quality (e.g. shelf life). Turbidity was measured using a LabScat turbidimeter (Sigris-Photometer AG, Ennetbürgen, Switzerland) after cooling the filtrate to room temperature. The photometric iodine value was determined according to MEBAK.

2.6. Statistics

Each filtration test in the lab and pilot scale was conducted in triplicates. The means and standard deviations were calculated. Statistical evaluation was conducted using OriginPro 2019b (OriginLab Corporation, Northampton, USA). Analysis of variance and *t*-test ($p < 0.05$) were employed to determine significant differences between means.

3. Results and discussion

3.1. Proof of the stamp effect and its impact on the cake compression

To identify the stamp effect during filtration, LT-1 was used to trigger cake compression. A sudden decline in the flow rate at 9.1 min (Fig. 3a, point C) was observed, where it decreased from 116.5 g/min (± 0.6) to 22.0 g/min (± 0.3).

However, this point of decrease is delayed compared with the pressure drop in the filtrate pipe: first, the pressure starts to drop at 6.5 min (Point B), and then, the flow rate decreases at point C. Cake height measurement sheds light on the process (Fig. 3b). Between points A and B, only a small decrease in height by 1.0 cm (compaction rate: 0.15 cm/min) and no change in the flow rate were observed. At point B, high amount of fine particles are deposited on the top of the cake. Consequently, the permeability on the top decreases and the blocking starts. From point B, the filter cake shrinks by 2.4 cm at a high compaction rate of 0.92 cm/min until point C is reached. This indicates the compression of the bottom layer by the stamp effect. No change in the flow rate is observed because the remaining liquid in the bottom layer flows out of the cake without resistance during the compression. This ends at point C, where the rate of pressure drop decreases and a significant decrease in the flow rate occurs. After point C, the low permeability of the top layer impairs the liquid flow, and the filtration rate is determined by the flow resistance of the fine layer. Up to point D, there is only a small

3 Results

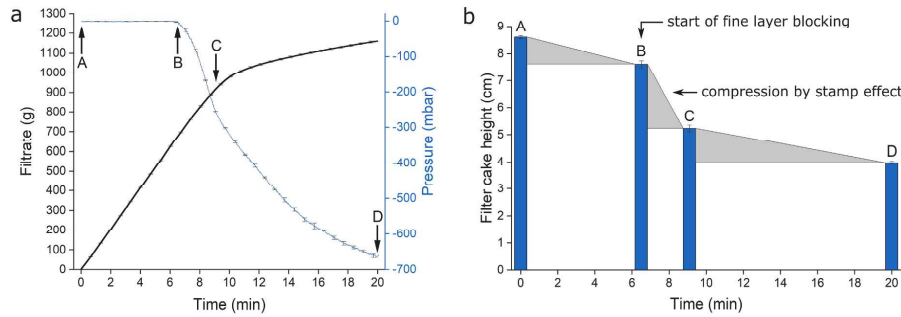


Fig. 3. a) Comparison of filtrate mass per time (black) and pressure drop (blue) in the filtrate pipe; b) filter cake height ($n = 3$). Indicated are the start of filtration (A), start of pressure drop (B), turning point of flow rate (C) and end of filtration (D). (For interpretation of the references to colour in this figure legend, the reader is referred to the Web version of this article.)

compression of 1.2 cm (compaction rate: 0.11 cm/min) until the maximal compression is reached at the end of filtration.

The cake compression and flow rate reduction observed using LT-1 indicate the influence of the stamp effect on filtration. However, the cake height provides no detailed insights into the change of the porosity during filtration. Therefore, the new method for cake fixation and porosity determination was applied to evaluate the individual cake layers obtained using LT-2.

After the sedimentation rest, the average porosity of the bottom layers 1–4 is 0.623 (± 0.002) at the start of filtration (Fig. 4, start filtration). This is in agreement with the porosity value of 0.68 for filter cakes in the LT indicated in the literature (Bühler et al., 1996). During filtration, the average porosity reduces to 0.312 (± 0.005) for the SF-trial (Fig. 4, SF). The change in the filter cake porosity can be observed visually (Fig. 2). While cavities in the cake are visible at the start of filtration, the structure is more compressed and cavities are reduced after the SF-trial.

The highest layer (1) for the SF-trial indicates a significant lower porosity compared with layers 2 and 3, which is in contrast to the respective layers at the start of filtration. This is based on the fines that are deposited on top of layer 1 during filtration and indicates the compression based on the stamp effect.

The significant lower porosity of layer 4 compared with layer 3 in the SF-trial is based on the skin effect that occurs next to the filter medium. However, the porosity reduction of layer 4 during filtration is rather low compared with layer 1. This distinguishes the LT operation from other

types of cake filtration, in which the porosity decreases based on the skin effect from top to bottom. It indicates that the stamp effect is predominant in lautering compared with the skin effect.

Using various types of malt, the impact of the stamp effect on the filtration of suspensions produced from different raw materials was checked. In addition to malt #1 as in the SF-trial, the flow rates of malts #2 and #3 were evaluated in the filtration tests using LT-1 (Fig. 5).

Similar to the SF-trial, the two other malts exhibit a characteristic reduction in the flow rate after the occurrence of blocking. Compared with the SF-trial ($22.6 \text{ g/min} \pm 0.3$), malt #2 ($36 \text{ g/min} \pm 1$) shows a higher and malt #3 ($19 \text{ g/min} \pm 1$) a lower flow rate. Because the permeability of the fine layer determines the rate of flow, the differences indicate the intensity of the stamp effect for the respective malt types. The higher porosity for malt #2 (0.43 ± 0.01) (Fig. 4, malt #2) and the lower value for malt #3 (0.26 ± 0.01) (Fig. 4, malt #3) compared with the SF-trial match the difference in the flow rate and, thus, the impact of the stamp effect. In addition, no significant difference was observed between the porosity in all layers for malt #2. This indicates that the stamp effect is less pronounced for this malt, which is in agreement with the higher flow rate and higher average porosity. Malt #3 shows a significant lower porosity for layer 1 compared with layer 2, similar to that observed in the SF-trial. Because there is no significant difference among layers 2–4, the skin effect was not detected at all for this malt. This is a further hint on the predominant impact of the stamp effect, particularly when low flow rates are detected.

The use of different malts revealed that the stamp effect depends on

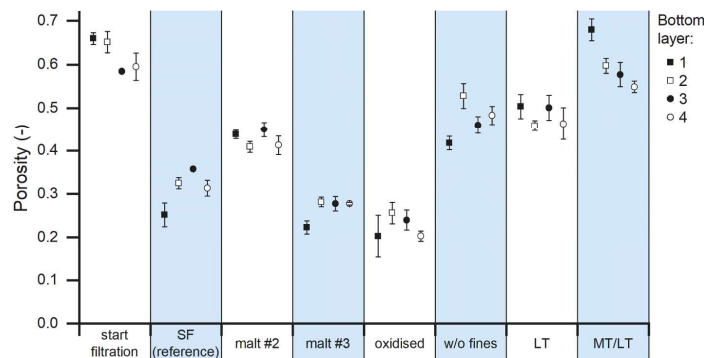


Fig. 4. Porosity of the filter cake layers from 1 (uppermost bottom layer next to the fine layer) to 4 (lowest bottom layer next to the filter medium) for different experiments ($n = 3$, SF = standard filtration test as reference, LT = suction from lauter tun, MT/LT = combined suction from mash and lauter tun).

3 Results

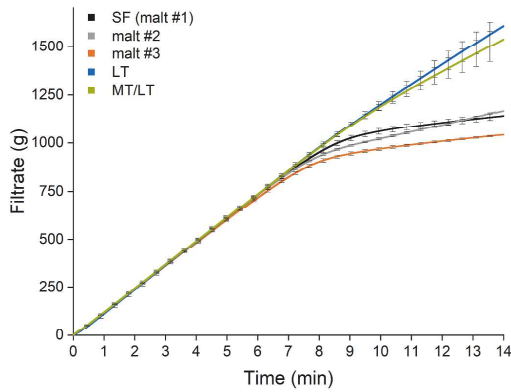


Fig. 5. Filtrate mass per time for standard filtration (SF) test as reference, different malt types (malt #2 and #3) and filtration techniques that include suction from lauter tun (LT) or combined suction from mash and lauter tun (MT/LT) (n = 3).

the raw material. Furthermore, it verifies the method of porosity measurement, which is in agreement with the flow rate when considering filter cakes that are differently produced.

To prove the stamp effect, the fine particles were modified, and the influence on the cake porosity was evaluated. Compared with the SF-trial, an oxidised form of the fine particles results in a lower average porosity of 0.23 (± 0.03) (Fig. 4, oxidised). This can be explained by the negative effect of oxidation that decreases the permeability of the fine layer, which results in a more pronounced stamp effect. Conversely, the removal of the fines results in a higher average porosity of 0.47 (± 0.01) (Fig. 4, w/o fines). The low porosity of layer 1 in this test indicates that fine particles were not completely removed and a low stamp effect is still present.

Considering the modifications of the SF-trial, it can be concluded that the fine layer has the largest impact on the cake compression and serves as proof of the stamp effect. The skin effect is less pronounced compared with the stamp effect.

The difference between stamp and skin effect is summarized in a scheme (Fig. 6) that was created on the basis of the present filtration experiments. In the case of the skin effect, the lowest porosity can be observed near the filter medium. In contrast to this, the porosity at the

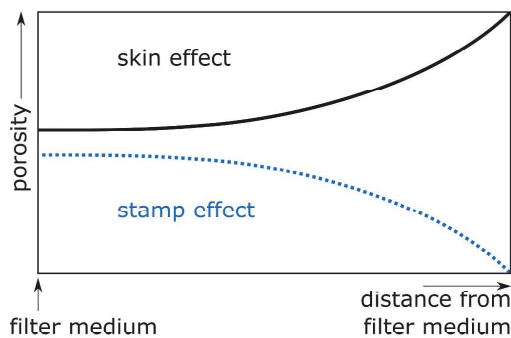


Fig. 6. Representation of the differences in the porosity of the filter cake for the stamp (dotted line) and skin (solid line) effect at the end of the filtration process.

top of the filter cake is lowest for the stamp effect. This leads to an overall lower cake porosity compared to the skin effect.

3.2. Prevention of the stamp effect

After the stamp effect has been proven, a technique to avoid it in the practical process was developed. The removal of the fines by suction from the LT (Fig. 1, F, LT-trial) or by combined suction from the MT and LT (Fig. 1, G, MT/LT-trial) significantly reduced the cake compression. A higher average porosity of 0.48 (± 0.03) for the LT-trial (Fig. 4, LT) and 0.60 (± 0.02) for the MT/LT-trial (Fig. 4, MT/LT) proved the success of the technique. Because layer 1 demonstrates a similar or even higher porosity compared with layers 2–4 for both trials, it can be concluded that the stamp effect is reduced. For the MT/LT-trial, the average porosity is similar to the initial cake porosity (Fig. 4, start filtration). In addition, the porosity increases for the MT/LT-trial from the bottom to top. Because this is typical for common filtration processes, it indicates that the skin effect prevails and that the stamp effect is no longer present.

Two effects are responsible for the lower compression of the cake for both techniques. First, based on a lower amount of fines on top of the filter cake, the stamp effect was significantly reduced. Second, the filtrate was recovered directly from the removed suspension via centrifugation. Consequently, the volume that had to be filtered through the cake was reduced, which results in a decreased compression.

The impact of a reduced stamp effect using the new techniques was verified by investigating the flow rate and the blocking potential (Fig. 5). For the LT-trial, as well as the MT/LT-trial, the characteristic blocking of the cake is significantly lower, which can be observed in a high flow rate of 104 g/min (± 12) for the LT-trial and 90 g/min (± 16) for the MT/LT-trial. This serves as a proof that the stamp effect can be avoided by removing the fines in the practical filtration process. No significant difference was observed between the flow rate of the LT- and MT/LT-trial, which means that suction from the top of the LT is already sufficient to avoid cake blocking.

3.3. Verification in pilot scale

The technique was verified on a pilot-scale plant to investigate the effects on the process time, yield and product quality.

Compared with the SF-trial, the time is reduced by 45% for the LT-trial and by 46% for the MT/LT-trial (Table 1). The reduction is mainly based on the lack of the first wort filtration time, which constitutes 40% of the total process time. Considering the occupation time of the LT only, the time saving for suction from MT/LT is even 55% compared with the SF-trial, because removal of a part of the suspension was already conducted in the MT. Consequently, a part of the sparging water was already added in the MT, which reduced the required time for the first sparging in the LT. Based on a higher cake porosity, the flow rate during sparging was increased, which further reduced the time. As a side

Table 1

Overview of the process time for the pilot-scale trials of the standard filtration (SF) test compared with the suction from the lauter tun (LT) and combined suction from mash and lauter tun (MT/LT) (n = 3).

	SF	LT	MT/LT
Sedimentation rest MT (min)	–	–	5
Suction MT (min)	–	–	3
Sedimentation rest LT (min)	5	5	5
Suction LT (min)	–	5	5
Cloudy filtrate recirculation (min)	5	5	5
First wort (min)	36 (± 3)	–	–
First sparging (min)	26.3 (± 0.5)	17 (± 2)	9.0 (± 0.8)
Second sparging (min)	16.3 (± 0.5)	17 (± 1)	15.7 (± 0.5)
Overall process duration (min)	88.6	49	47.7
Overall time saving (%)	–	45	46
Time saving in LT (%)	–	45	55

effect, deep cuts during raking could be avoided in the suction trials. In addition, there was no need to recirculate the cloudy filtrate back to the filter for both suction trials. Instead, it was added to the fine-particle suspension that was centrifuged, reducing the amount of fluid that had to be filtered through the cake. The centrifugation of the fine-particle suspension was executed parallel to the LT operation and, therefore, had no effect on the total process time.

The fine particles recovered after centrifugation were not washed with water during sparging. Consequently, the remaining washable extract (dry matter) in the fine particles was significantly higher for the LT-trial (53.9% \pm 0.9%) and MT/LT-trial (52% \pm 1%) compared with the remaining extract in the entire filter cake for the SF-trial (5.0% \pm 0.4%). However, a comparison of the extract yield of the total process reveals no significant differences for the suction trials compared with the SF-trial (Table 2). This is due to the small amount of fine particles removed from the suspension. Compared with the initial amount of raw material, only 0.33% (\pm 0.06%) of fine-particle dry matter was removed for the LT-trial and 0.40% (\pm 0.06%) for the MT/LT-trial. Therefore, the extract loss based on the fines has no significant influence on the total extract yield in relation to the entire filter cake.

The turbidity of the first wort is significantly reduced for the LT-trial and in an even higher degree for the MT/LT-trial compared with the SF-trial (Table 2). This is due to the more efficient separation of the particles based on the centrifugation. For the total filtrate, no significant difference was observed for the LT-trial compared with the SF-trial, which can be a side effect of the higher cake porosity. Because the amount of centrifuged suspension is the highest in the MT/LT-trial, the turbidity is the lowest for first wort and total filtrate.

No significant difference for the photometric iodine value was observed for the total wort of the LT-trial compared with the SF-trial (Table 2). For the MT/LT-trial, a significant lower iodine value was obtained.

Because the critical filtrate characteristics (turbidity and iodine value) of the product are either constant or even lower for the suction trials compared with the SF-trial, no negative effects on the subsequent process steps or product quality are to be expected for the new filtration techniques.

4. Conclusions

A new method for cake fixation and porosity determination was developed to prove the stamp effect in the LT operation. The method was successfully implemented. Freezing of the cake structure enabled sampling at different time of filtration and from individual cake layers. This approach enabled the consideration of the special requirements of the inhomogeneous filter cake in the LT. In combination with the optical porosity determination via a measurement of the surface roughness, an investigation of the stamp effect was successful.

Fine particles on the top of the filter cake were found to be responsible for the stamp effect in the LT, which resulted in the compression of the bottom layer and, thus, reduction of the overall flow rate. The stamp effect turned out to be the predominant factor influencing the filtration behaviour. Contrary to that observed in other types of cake filtration, the skin effect next to the filter medium has only a minor impact in the LT. However, factors such as the raw material or the influence of oxidation in the practical process determine the strength of the stamp effect.

Up to now, there are no approaches to avoid the stamp effect in the practical LT operation. Therefore, an alternative filtration technique was developed based on the new findings. The fines were removed from the filter prior to the filtration process, which resulted in a lower cake compression and higher flow rate. A transfer to the pilot scale revealed that a significant reduction in the process time is possible without negative effects on the yield or filtrate quality. The verification of the filtration technique serves as a proof that the prevention of the stamp effect improves the process.

The present work serves as a suggestion for an industrial scale-up of

Table 2

Overview of extract yield, turbidity and iodine value for the pilot-scale trials of the standard filtration (SF) test compared with the suction from the lauter tun (LT) and combined suction from mash and lauter tun (MT/LT) ($n = 3$).

	SF	LT	MT/LT
Extract yield (%)	68.6 (\pm 0.9)	67.6 (\pm 0.5)	68.0 (\pm 0.6)
First wort turbidity 25° (EBC)	253 (\pm 21)	145 (\pm 14)	104 (\pm 6)
Total filtrate turbidity 25° (EBC)	155 (\pm 15)	186 (\pm 19)	114.7 (\pm 0.9)
Iodine value (–)	0.31 (\pm 0.04)	0.22 (\pm 0.03)	0.18 (\pm 0.01)

the technique. A possible implementation in the brewery could involve the suction of the suspension after the mash transfer using an opening on the side of the LT above the bottom layer of the filter cake. After transferring the suspension to a storage tank, a disc stack centrifuge could be used to clarify the wort. The filtrate could then be transferred directly to the wort kettle for the subsequent production step.

However, one has to consider that the new technique includes an additional process because the filtrate has to be recovered from the fine-particle suspension. In an industrial scale-up, it must be checked if higher acquisition and operating costs are weighed up by a reduced process time.

Funding

This IGF Project of the FEI was supported via AiF (19359 N) within the programme for promoting the Industrial Collective Research (IGF) of the German Ministry of Economic Affairs and Energy (BMWi) based on a resolution of the German Parliament.

Declaration of competing interest

The authors declare that they have no known competing financial interests or personal relationships that could have appeared to influence the work reported in this paper.

Acknowledgement

We are grateful to Ahmed Fahmy (Technical University Munich) for his skilful help in the development of the pressure measuring device.

References

- Alles, C.M., Anlauf, H., 2003. Filtration mit kompressiblen Kuchen: Effiziente Konzepte für eine anspruchsvolle Trennaufgabe. *Chem. Ing. Tech.* 75 (9), 1221–1230. <https://doi.org/10.1002/cite.200303268>.
- Barrett, J., Clapperton, J.F., Divers, D.M., Rennie, H., 1973. Factors affecting wort separation. *J. Inst. Brew.* 79 (5), 407–413. <https://doi.org/10.1002/j.2050-0416.1973.tb03558.x>.
- Bühler, T.M., McKechnie, M.T., Wakeman, R.J., 1996. A model describing the lautering process. *Monatsschrift für Brauwissenschaft* 7/8, 226–233.
- Bühler, T.M., McKechnie, M.T., Wakeman, R.J., 1996. Temperature induced particle aggregation in mashing and its effect on filtration performance. *Food Bioprod. Process.* 74 (4), 207–211. <https://doi.org/10.1205/096030896531208>.
- Engstle, J., Briesen, H., Först, P., 2017. Mash separation in the lauter tun - a particle size dependent separation process. *Brew. Sci.* 70, 26–30.
- Engstle, J., Reichhardt, N., Först, P., 2015. Filter cake resistance of horizontal filter layers of lautering filter cakes. *MBAA Tech Q* 52 (2), 29–35. <https://doi.org/10.1094/tq-52-2-0405-01>.
- Engstle, J., Ueffing, H., Först, P., 2015. Bildanalytische Überwachung des Läutervorganges. *Brauwelt* 36, 1040–1042.
- Hennemann, M., Gastl, M., Becker, T., 2019. Inhomogeneity in the lauter tun: a chromatographic view. *Eur. Food Res. Technol.* 245, 521–533. <https://doi.org/10.1007/s00217-018-03226-4>.
- La Heij, E.J., Kerkhof, P.J.A.M., Kopinga, K., Pel, L., 1996. Determining porosity profiles during filtration and expression of sewage sludge by NMR imaging. *AIChE J.* 42 (4), 953–959. <https://doi.org/10.1002/aic.690420408>.
- Martin, W.D., Putman, B.J., Kaye, N.B., 2013. Using image analysis to measure the porosity distribution of a porous pavement. *Construct. Build. Mater.* 48, 210–217. <https://doi.org/10.1016/j.conbuildmat.2013.06.093>.
- Mathamann, K., Kuhn, M., Briesen, H., 2014. Application of micro-computed tomography in food and beverage technology using the examples of textured vegetable protein and filtration steps in the brewing process. *Wels, Österreich*.

3 Results

M. Hennemann et al.

Journal of Food Engineering 293 (2021) 110405

Miedaner, H., 2002. Brautechnische Analysemethoden. Methodensammlung der Mitteleuropäischen Brautechnischen Analysekommision 2 (Freising-Weißenstephan).

Rebollo, M.A., Hogert, E.N., Albano, J., Raffo, C.A., Gaggioli, N.G., 1996. Correlation between roughness and porosity in rocks. *Optic Laser Technol.* 28 (1), 21–23. [https://doi.org/10.1016/0030-3992\(95\)00051-8](https://doi.org/10.1016/0030-3992(95)00051-8).

Sakai, T., Nakamura, A.M., 2005. Quantification of porosity and surface roughness in laboratory measurements of the bidirectional reflectance of asteroid surface analogues. *Earth Planets Space* 57, 71–76. <https://doi.org/10.1186/BF03351807>.

Tiller, F.M., Green, T.C., 1973. Role of porosity in filtration IX Skin effect with highly compressible materials. *AIChE J.* 19 (6), 1266–1269. <https://doi.org/10.1002/aic.690190633>.

Tippmann, J., Voigt, J., Sommer, K., 2011. Measuring particle size distribution of mash with laser diffraction to evaluate the process success. *Brew. Sci.* 64, 13–21.

3.2.4 Compression Mechanism in Multilayered Filter Cakes

Martin Hennemann
Ehsan Fattahi
Martina Gastl*
Thomas Becker

Compression Mechanism in Multilayered Filter Cakes

Sedimentation combined with a broad particle size distribution in the suspension results in multilayered filter cakes, where a fine particle layer forms on top of a compressible bottom layer. Owing to their high resistance, the fine particles act as a stiff layer and compress the bottom layer during filtration. This was investigated using a model cake composed of a compressible bottom layer and an artificial fine layer. Compression was determined via a volumetric porosity measurement. A reduction in porosity due to compression increased the filter cake resistance significantly. The use of different types of fine particles demonstrated that if the top layer resistance is higher than that of the bottom, a differential pressure results that pulls the top layer down and compresses the bottom layer.

Keywords: Cake filtration, Compression, Fine particles, Multilayered filter cakes, Porosity

Received: June 01, 2021; *revised:* August 21, 2021; *accepted:* August 24, 2021

DOI: 10.1002/ceat.202100258

 This is an open access article under the terms of the Creative Commons Attribution-NonCommercial-NoDerivs License, which permits use and distribution in any medium, provided the original work is properly cited, the use is non-commercial and no modifications or adaptations are made.

1 Introduction

Cake filtration is a critical operation in various production processes, e.g., in food or biotechnology. It is applied to separate the liquid phase of a suspension from the solids, which form a porous filter cake after being deposited on a filter medium. This porous filter cake exerts a resistance to flow, resulting in a pressure drop (Δp)¹ that is expressed by Darcy's law as follows:

$$\Delta p = \frac{\dot{V}}{A} \eta m \alpha_h \quad (1)$$

with volumetric flow rate (\dot{V}) per filter area (A), cake height (h), and viscosity (η) [1]. The height-related specific filter cake resistance (α_h) can be approximated by the Carman-Kozeny equation as:

$$\alpha_h = 180 \frac{(1 - \epsilon)^2}{\epsilon^3 d_s^2} \quad (2)$$

which depends on the Sauter diameter (d_s) of the particles and the cake's porosity (ϵ). The porosity is the relation between the solids volume (V_{solid}) and the total volume (V_{total}) according to the following relation:

$$\epsilon = 1 - \frac{V_{\text{solid}}}{V_{\text{total}}} \quad (3)$$

For practical reasons, it is convenient to determine the mass-related filter cake resistance (α_m) instead of α_h [1]. Both descriptors of the resistance are related as:

$$\alpha_h = \frac{\alpha_m m}{A h} \quad (4)$$

which depends on the cake mass (m). When combining Eqs. (1) and (4), a modified form of Darcy's law results:

$$\Delta p = \frac{\dot{V}}{A^2} m \eta \alpha_m \quad (5)$$

Darcy's law, in combination with the Carman-Kozeny equation, indicates that the pressure drop for a constant flow rate depends on α_m , which is a function of the porosity. Because most cakes are compressible [2], their porosity can decrease during filtration, leading to higher α_m and thus a higher pressure drop. Usually, compression is only based on the frictional drag force of the liquid that causes a compressive stress on the porous cake structure [1]. However, this is only true for cakes with a homogeneous structure and not for inhomogeneous multilayered cakes.

A multilayered cake is caused by a nonuniform distribution of particle sizes in the suspension in combination with sedimentation effects [3]. After sedimentation, the structure of the cake consists of different layers parallel to the filter medium. This is based on differences in the particle sedimentation velocities (w_f), which depend on particle (ρ_s) and fluid densities (ρ_f), the gravitational field strength (g), and the particle size (d) according to:

$$w_f = \frac{\rho_s - \rho_f}{18 \eta} g d^2 \quad (6)$$

Martin Hennemann, Dr. Ehsan Fattahi, Dr. Martina Gastl, Prof. Dr. Thomas Becker
martina.gastl@tum.de
Technical University Munich, Chair of Brewing and Beverage Technology, Weißenstephaner Steig 20, 85354 Freising, Germany.

1) List of symbols at the end of the paper.

Consequently, larger and denser particles settle first and form a bottom layer, whereas smaller and less dense fine particles settle afterward and create a top layer. The resulting differences in particle size distributions of multilayered cakes were demonstrated, e.g., by simulation [3] and filtration experiments [4, 5].

Another prominent example of a multilayered cake occurs in the lautering process in beer production, which is the separation of the solids (brewer's spent grains, BSG) from the liquid of interest [6, 7]. For this example, it was shown that the top part of the multilayered cake affects cake porosity by compressing the bottom layer during filtration [8]. The compression from the top is caused by a significantly higher α_m of the fine layer than that of the bottom layer [9]. Due to smaller particle size and consequently, smaller void size, it creates high flow resistance and acts as a stiff layer, which leads to the highest pressure drop at this location, in contrast to a high pressure drop next to the filter medium in homogeneous cakes [10].

The investigation of bottom layer compression in multilayered cakes was the aim of this paper. Compression was induced using a model filtration experiment, i.e., compressible glass fiber filter cake. Bottom layer compression was examined on the basis of changes in cake height and porosity, for which a volumetric method of porosity determination was established. In addition, the resulting pressure drop during filtration was analyzed and α_m was calculated. The results were compared with a homogeneous cake without a top layer. Different types of fine particles (SiLibeads, silica gel, BSG fines, and CaCO_3) were used as a top layer to investigate the influence of their α_m on the compression of the bottom layer.

2 Materials and Methods

2.1 Filtration with Multilayered Cakes

Multilayered cakes are assumed to consist of a fine layer on the top and a compressible bottom layer (Fig. 1). The hypothesis is that if the liquid flow is hindered mainly by the high resistance of the top layer compared with the bottom layer ($\alpha_1 > \alpha_2$, with

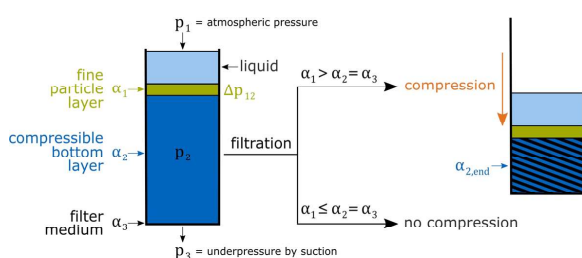


Figure 1. Schematic illustration of filtration with a multilayered filter cake showing the compression of the bottom layer if a high resistance of the fine particle layer is present at the top. The driving force of filtration is suction, which generates a low pressure under the filter medium ($p_1 > p_3$). Both pressures (p_1 and p_3) are kept constant. A constant liquid level is assumed, and its hydrostatic pressure is neglected. The resistances of the filter medium and the bottom layer are assumed to be significantly smaller than that of the fine layer ($\Delta p_{12} > \Delta p_{23}$).

α either α_h or α_m), then compression of the bottom layer occurs. This compression is based on the differential pressure (Δp_{12}), which leads to a pull and, hence, a downward movement of the top layer boundary. On the basis of the compression, the resulting reduction in the porosity of the bottom layer increases its resistance ($\alpha_{2, \text{end}}$). In contrast, if the resistance of the top layer is not higher than that of the bottom layer ($\alpha_1 \leq \alpha_2$), then no compression occurs. It is assumed that there is no migration of fine particles from the top into the bottom layer, according to Engstle et al. [11], and the differential pressure is entirely based on the top layer ($\Delta p_{\text{total}} \approx \Delta p_{12}$) due to the high flow resistance at this location [8].

2.2 Cake Composition and Particle Characteristics

Model cakes were used to reveal the differences in filtration with homogeneous and multilayered cakes. Homogeneous cakes were composed only of the compressible bottom layer, whereas multilayered cakes additionally consisted of an artificial fine layer on the top (Fig. 2d). The bottom layer for both types of cakes was composed of monodisperse glass fibers (Fig. 2c, DD Composite GmbH, Bad Liebenwerda, Germany) with a length of 6.3 mm (± 1 mm) and a diameter of 17 μm (± 4 μm). The particle Sauter diameter was calculated using the fiber specific surface area (S_V) based on:

$$d_s = \frac{6}{S_V} \quad (7)$$

The model cakes were assembled by covering the filter medium with 3000 g distilled water followed by the addition of 1100 g glass fibers. The fibers were loosely filled to ensure random packing, similar to what was described by Rahli et al. [12]. Owing to the particle structure, the compressibility of the glass fiber filter cake is based on rearrangement effects [2]. On top of the cake, 1200 g distilled water were overlaid, and the water level was kept constant during filtration.

For the multilayered cake reference trials, a sealed piston (Fig. 2a) constructed from TPU 95A (Ultimaker B.V., Utrecht, The Netherlands) was placed on the glass fiber cake as an artificial fine layer. This piston had a height of 26 mm and five flexible laminar extensions on its side. These extensions formed a seal between the piston and the filter wall to prevent liquid from passing. This sealed piston was used as a reference to artificially induce compression based on its high resistance because the liquid is prevented from passing the piston. Friction between piston and filter wall was neglected.

A different version of the piston referred to as a modified piston (Fig. 2b) was used to modify the filtration trials with actual fine particles as the top layer. This version serves as a supporting mesh for the fines and has 61 equally distributed holes (diameter: 4 mm) through it. The holes were covered by four layers of MN 514 $\frac{1}{4}$ filter paper (Macherey-Nagel GmbH & Co. KG, Düren, Germany) to ensure that no fine particles pass the

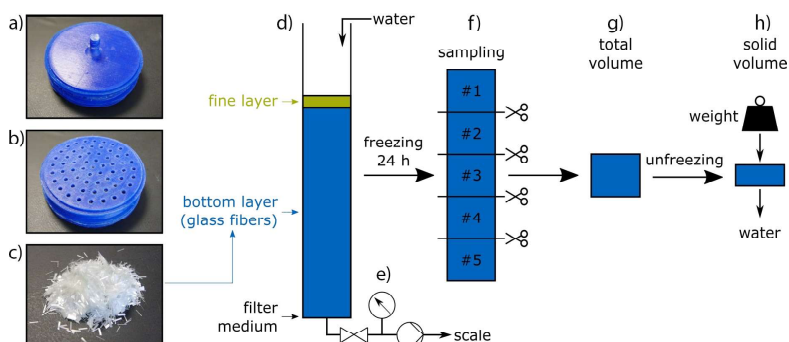


Figure 2. Experimental setup showing the sealed piston (a) and the modified piston (b) of the artificial fine layer and the glass fibers (c) forming the compressible bottom layer of the multilayered cake. The filter (d, diameter 10 cm, height 62 cm) is equipped with a pressure sensor (e) and filtrate mass per time was recorded using a scale. After the filtration test, the cake was frozen and cut into five layers parallel to the filter medium (f, #1–5) to determine the total volume of each layer (g). After unfreezing, a weight placed on a plunger aided in achieving dense packing to remove the liquid and determine the solids volume (h).

piston. This setup guaranteed that only the resistance of the particles (not the resistance of the piston) moved the piston downwards. Pretrials revealed that the modified piston had no influence on the pressure drop in contrast to the sealed piston.

Different types of fine particles were used as top layer for the modified trials, which differ in their chemical composition and particle size (Tab. 1). The particle size was measured using a Mastersizer 3000 (Malvern Panalytical GmbH, Kassel, Germany). $D[4,3]$ refers to the volumetric mean particle size. Instead of distilled water as used for the reference trials, a 10 % suspension of these particles was overlaid on the modified piston, and the filtration test was started after 5 min to ensure particle sedimentation.

Table 1. Different types of fine particles used in the modified filtration trials showing their mean particle size ($n = 30$).

Particle type	Manufacturer	$D[4,3]$ [μm]
SiLibeads (glass beads)	Sigmund Lindner GmbH, Warmensteinach, Germany	59.5 ± 0.4
Silica gel	Stabifix Brauerei-Technik GmbH & Co. KG, Gräfenfing, Germany	34 ± 2
BSG fines < 500 μm	Produced according to Hennemann et al. [9]	84 ± 9
CaCO_3	Carl Roth GmbH + Co. KG, Karlsruhe, Germany	4.1 ± 0.8

2.3 Filtration Tests

After the artificial cakes had been prepared, filtration was conducted using an iPump1Q peristaltic pump (Baoding Signal Fluid Technology Co., Ltd., Baoding, China). A constant flow

rate of 147 g min^{-1} was applied to ensure a constant low pressure ($\sim 89 \text{ kPa}$) under the filter medium. Water was added from the top during filtration to maintain a constant liquid level and to prevent the cake from drying out. The direction of flow was from top to bottom. Compared with the underpressure of the pump, the liquid hydrostatic pressure ($\sim 1.5 \text{ kPa}$) was neglected. The differential pressure (Δp_{13}) was recorded (Fig. 2e) using a DRTR-AL-10V/20mA relative pressure transmitter (B+B Thermo-Technik GmbH, Donaueschingen, Germany). Pretrials revealed that no differential pressure was detected between the bottom layer and the filter medium ($\Delta p_{\text{total}} = \Delta p_{12}$). For the filtration test with the sealed piston, a folding rule was used to measure the change in the height of the cake (average of two sides) at intervals of 5 min. The flow rate was measured by determining the filtrate mass per time using a scale.

The resistance of the fine particles was assessed using a small-scale filter according to the Verein Deutscher Ingenieure [13]. One hundred grams of a 10 % suspension was overlaid on a filter medium covered with filter paper, and the measurement was performed using a 40-kPa differential pressure.

2.4 Sampling and Porosity Measurement

The cake structure was fixed by freezing overnight to enable sampling at different time points (5, 10, 20, and 40 min) during filtration and from different horizontal layers, similar as described by Hennemann et al. [8]. The cake was cut into five equally distributed layers parallel to the filter medium (Fig. 2f) using an ice saw. Each layer was placed in a container with the same diameter as the filter, which enabled a determination of the total volume of the layer by measuring the height with a slide gauge (Fig. 2g). After unfreezing overnight, the layer was compressed by a plunger to remove the liquid phase, which corresponds to the cavity volume of the cake (Fig. 2h). A weight

placed on the plunger aided in achieving dense packing, as described by Sohn and Moreland [14]. Compression enabled the determination of the solid volume to calculate the average layer porosity according to Eq. (3).

Using the layer's average porosity, the resistance of the bottom layer was calculated according to Eq. (2). However, the Carman-Kozeny factor (180) only applies to spherical particles. Therefore, it was adapted for the fibers by making a linear correlation, with the resistance determined according to Eq. (1). A specific factor for the glass fibers (16) was calculated using values from the experiments with homogeneous and multilayered cakes ($R^2 = 0.96$, $p < 0.001$, $n = 6$). Finally, α_m was calculated using this factor and Eq. (4) to compare it with the resistance of the fine particles.

The volumetric porosity measurement was verified using a gravimetric reference method [8, 15]. Five layers from three different states of compression (low, medium, and high) were used, which resulted in a linear correlation ($R^2 = 0.97$, $p < 0.001$, $n = 15$) between the volumetric and gravimetric methods.

2.5 Investigation of the Compression Mechanism

To obtain detailed insights into the compression mechanism caused by the top layer, a second setup was employed where the glass fiber cake was prepared in a graduated glass cylinder (1000 mL). The filling of the particles in the cylinder was divided into five parts. Each part consisted of a single cake of 66 g particles and 180 g distilled water, which represented the five horizontal layers. These filter cake parts were separated by a porous ring (height: 1.5 mm, same diameter as the cylinder) that enabled a visual differentiation of the height of each individual part. By lowering a plunger (similar to a sealed piston) in five defined steps (each 100 mL), the initial volume of the cake (1000 mL) was reduced. A measurement of the height of each cake part enabled determination of the individual compression of each layer.

2.6 Statistics

All experiments were conducted in triplicate ($n = 3$) unless stated otherwise, and the means and standard deviations were calculated. OriginPro 2019b (OriginLab Corporation, Northampton, USA) was used for statistical evaluation. Significant differences between means were determined using analysis of variance and t -tests ($p < 0.05$).

3 Results and Discussion

3.1 Investigation of Compression in Multilayered Cakes

As a first step in characterizing the compression in multilayered cakes, the change in the cake height (Fig. 3) during filtration was determined when applying the artificial fine layer. In contrast to the homogeneous cake, there was a significant

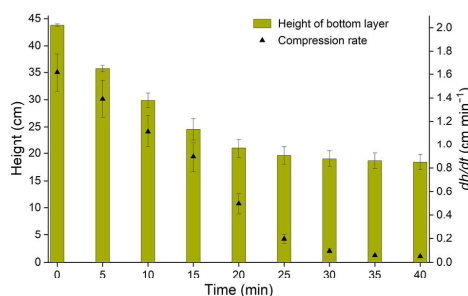


Figure 3. Height of the bottom layer (bars) and compression rate (triangles, first derivative) per filtration time for the multilayered filter cake ($n = 3$).

decrease in the height of the bottom layer of the multilayered cake, which resulted from the compression caused by the top layer.

The compression rate, expressed as the first derivative, dh/dt , was higher at the beginning of filtration than at the end. The turning point, analyzed from the second derivative, d^2h/dt^2 , occurred at 20 min, after which the compression rate decreased and the cake height declined at a lower rate. A similar effect was observed for the expression mechanism in filter cakes [16], which means that compression in multilayered cakes can be compared with a mechanical expression. The fine particles at the top act as a stiff layer similar to a piston that compresses the bottom layer.

The reduction in a multilayered cake height is directly related ($R^2 = 0.93$, $p < 0.01$, $n = 5$) to the decrease of porosity during filtration (Fig. 4a). Compared with porosity at the initial state (0.58 ± 0.01 , average of all five bottom layers), there was a large decrease (74%) for filtration with multilayered cakes (0.15 ± 0.02) at the end of filtration. Up to 20 min, the porosity declined steadily, but after 20 min, there was only a small reduction. This trend is in agreement with the cake height (Fig. 3, turning point at 20 min). With a reduction in porosity, the pore size decreases and thus the flow resistance increases. Consequently, the overall α_m of the bottom layer rose during filtration (Fig. 4b), leading to a higher value of $9 \times 10^9 \text{ m kg}^{-1}$ ($\pm 5 \times 10^9$) compared with the initial state ($7.2 \times 10^7 \pm 8 \times 10^6 \text{ m kg}^{-1}$).

In contrast, there was a small but significant decrease in the average porosity of the homogeneous cake at 5 min (0.53 ± 0.01) but no further compression for longer filtration times. The average porosity at the end of filtration (0.54 ± 0.02) was reduced by only 7% compared with that at the initial state. No significant change in α_m was observed after 5 min ($1.2 \times 10^8 \pm 1 \times 10^7 \text{ m kg}^{-1}$) until the end of filtration. This indicates that compression by the liquids' drag force can be neglected in a multilayered cake.

For filtration with multilayered cakes, the porosity of the individual layers was, in general, lower at the top than at the bottom at 10 and 20 min (Fig. 4a). The effect was reversed at the end of filtration (40 min), where the porosity was lowest at the bottom. This was a hint that compression based on the top layer starts from the top. To investigate this compression

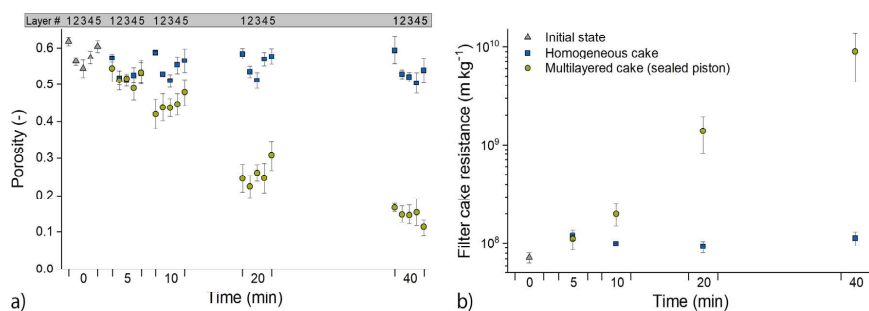


Figure 4. Changes in porosity for the individual cake layers (a, #1 = uppermost, #5 = bottom) and overall cake resistance (b, logarithmic scale) of the bottom layer during filtration. The initial state (triangles) is compared with filtration of homogeneous (squares) and multilayered (circles) filter cakes ($n = 3$).

mechanism in detail, a second setup was used to measure the individual compression of each layer (Fig. 5).

At the initial state (0), the lower layers (#2–5) had heights lower than those of the uppermost layer (#1) (Fig. 5a), which resulted from their compression due to the solids pressure of the layers above. When compression started (states 0–1), the height of the first layer decreased at a higher rate compared with the underlying layers (Fig. 5b, quantified as first derivative, dh/dx). From state 1, layer #2 started to decrease to a higher degree, and from state 2, the following layers (#3–5) started to be compressed. The compression rate of the first layer decreased as the compression of the lower layers increased.

This experiment revealed that compression by the fine layer starts from the top, where the porosity was higher at the beginning. When a certain compressive force was reached at the top (state 1), compression was transferred via the uppermost layers to the lower layers (#2–5). In the lower layers, the compression was then equally distributed. A similar effect was demonstrated for multilayered cakes in the lautering process, where compression resulting from the top layer compressed the uppermost layer to a degree higher than that of the lower layers [8].

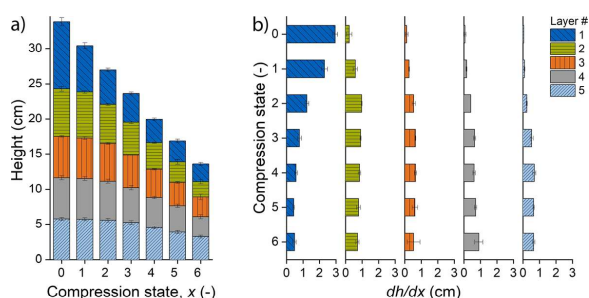


Figure 5. (a) Change in heights of the individual cake layers for different states of compression (x) using a sealed piston. (b) First derivative of the function of compression of the individual layers, to indicate compression rate (0 = initial state, 6 = maximum compression, $n = 3$).

3.2 Differential Pressure during Filtration

According to the differences in cake height, porosity, and therefore α_m , the filtrate pipe pressure differed between filtration with homogeneous and multilayered cakes. First, the top layer's effect on the compression of the bottom layer and the resultant pressure drop is displayed (Fig. 6a). Although there was no difference in the pressure detected for the homogeneous cake, the pressure started to drop for filtration of the multilayered cake, which resulted in increased differential pressure (Δp_{13}).

Up to 5 min, the top layer was pulled down owing to the pressure difference on the two sides of the stiff layer, which was a result of negative pressure from the pump. In the beginning, there was no significant resistance from the compressible bottom layer. However, the height was already reduced at this point (Fig. 3). The first indication of counterforce from the compressible bottom layer was seen at around 5 min, which resulted in differential pressure. Simultaneously, the hydrostatic pressure from the water on the top was increasing on the sealing piston. This aided in raising the compression, and therefore, the pressure drop became higher.

After about 15 more minutes, the pressure drop increased until it reached the equilibrium point between the counterforce owing to the bottom layer's compression and the force on the top layer. After this point at around 20 min, the time rate for differential pressure declined. When the forces were in equilibrium, the bottom layer was compressed very slowly, and the pressure drop did not increase significantly further. Because the piston was made of plastic, which was not fully sealed, there was a narrow gap through which water could flow. This prevented the pressure from dropping further.

After determining the differences between filtration with homogeneous and multilayered cakes using the sealed piston, the influence of different fine particles (Tab. 1) on filtration characteristics was investigated using the modified piston (Fig. 7). Unlike the sealed piston experiment, here, the top layer was permeable. According to Eq. (6), the

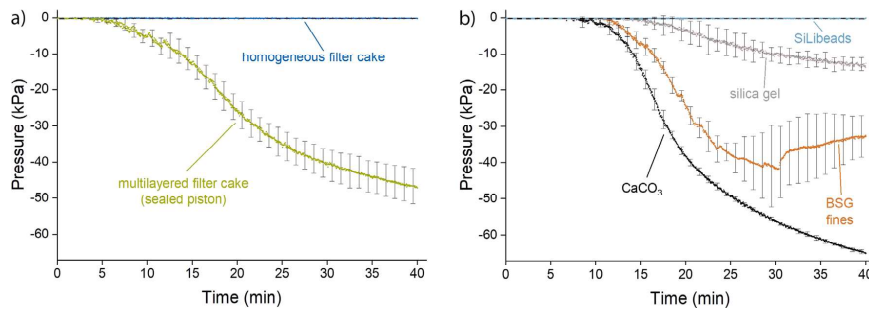


Figure 6. Pressure under the filter medium (p_2) during filtration with (a) homogeneous and multilayered filter cakes (sealed piston) and (b) different fine particles as the top layer using the modified piston ($n = 3$).

particles settled on the top layer, which resulted in an increased α_m that led to a pressure drop (Eq. (5)). The α_m of the fine particles displayed in Fig. 7a is the point at which the particles are settled on the top layer.

When using SiLi beads as fine particles, the α_m of this top layer ($5 \times 10^7 \pm 1 \times 10^7 \text{ m kg}^{-1}$, Fig. 7a) was lower than that of the bottom layer ($1.1 \times 10^8 \pm 2 \times 10^7 \text{ m kg}^{-1}$, indicated as a horizontal line in Fig. 7). This means that the pressure drop of the top layer was not higher than that of the bottom layer, which resulted in no difference in the pressure (Fig. 6b). Therefore, there was no significant difference in α_m of the bottom layer when using SiLi beads compared with the homogeneous cake without a top layer (Fig. 7b) because there was no compression.

Silica gel, as the top layer, had a higher α_m ($3.1 \times 10^9 \pm 2 \times 10^8 \text{ m kg}^{-1}$) than had the bottom layer. This created an increased pressure drop during filtration (Fig. 6b) in comparison to the homogeneous layer. The pressure difference resulted in a force that compressed the bottom layer's particles. By compressing the bottom layer, the porosity decreased, which increased the α_m of the bottom layer ($3 \times 10^9 \pm 2 \times 10^9 \text{ m kg}^{-1}$).

BSG fines showed the highest α_m ($3.0 \times 10^{13} \pm 3 \times 10^{12} \text{ m kg}^{-1}$) of all top layer particles (Fig. 7a). This resulted in higher force acting on the bottom layer and, therefore, higher compression and higher α_m ($5 \times 10^9 \pm 2 \times 10^9 \text{ m kg}^{-1}$) of the bottom layer (Fig. 7b). Although the α_m of the BSG fines was significantly higher than that of the silica gel fine particles, in the end, there was no significant difference between the resistances of the bottom layers for both trials. This was due to a break in the structure of the top cake layer as seen in an increase in the pressure at around 30 min after the pressure dropped (Fig. 6b). Consequently, the compression of the bottom layer was lower, although the α_m of the fine layer was the highest in this trial.

CaCO₃ as the top layer had a high α_m ($1.5 \times 10^{12} \pm 3 \times 10^{11} \text{ m kg}^{-1}$), which resulted in a high pressure drop and compression. Because these particles are small in size, they completely sealed the top layer in contrast to the sealed piston. Therefore, the maximum compression occurred in this case, and the α_m of the bottom layer increased to the maximum ($1.1 \times 10^{10} \pm 5 \times 10^9 \text{ m kg}^{-1}$).

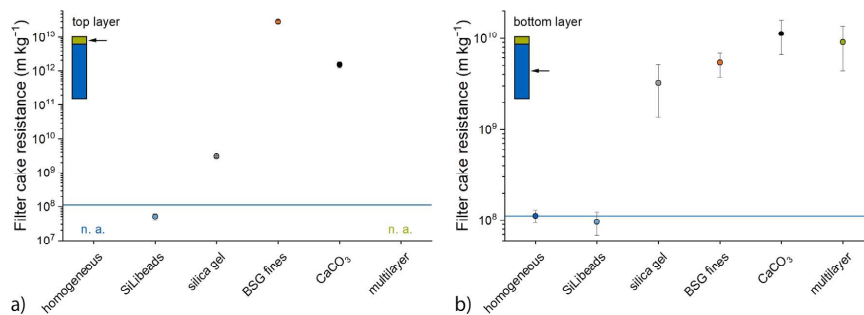


Figure 7. Filter cake resistance of the (a) top (no values measurable for the multilayered and the homogeneous cake without a top layer) and (b) bottom layer when using homogeneous and multilayered cakes (sealed piston) in comparison with different types of fine particles (SiLi beads, silica gel, BSG fines, CaCO₃) when using the modified piston. The horizontal line indicates the filter cake resistance of the homogeneous cake without the influence of the top layer (logarithmic scale, $n = 3$).

The trials with top layers with higher α_m (silica gel, BSG fines, and CaCO_3) than the homogeneous cake resulted in compressions similar to the experiment with the piston. In contrast, when using fine particles with lower α_m (SiLibeads) than the bottom layer, no compression of the bottom layer developed, and there was no difference in the α_m compared with the homogeneous cake. This showed that when a higher α_m is present in the top layer compared with that at the bottom layer, a pressure drop and a compression of the bottom layer follows.

The beginning of the pressure drop differed for the different types of fine particles (Fig. 6b). For example, the pressure started to drop for CaCO_3 at around 8 min, whereas it was delayed for silica gel around 14 min. This was due to the different settling velocities, which affected the formation of the fine layer and thus the point of pressure drop. These findings agree with the sealed piston experiment (Fig. 6a), where there was no need for particle sedimentation. Therefore, the pressure started to drop in this trial at around 4 min.

4 Conclusions

Multilayered filter cakes consist of a compressible bottom layer and a fine particle top layer. During the filtration process, the bottom layer is compressed by the fine layer from the top, which results in an increased α_m of the bottom layer. However, only when the α_m of the fine particle layer is higher than that of the bottom layer, a differential pressure results that pulls the top layer down and compresses the bottom layer. This compression leads to an overall higher α_m of the multilayered cake, which hinders the liquid flow.

On the basis of Darcy's law, an increase in the differential pressure is expected to raise the flow rate when α_m is constant. However, this may only be correct for homogeneously layered cakes. In multilayered cakes, an increasing differential pressure leads to a greater force on the bottom layer. This enlarges the compression of the bottom layer, which results in an increased α_m .

Acknowledgment

This IGF Project of the FEI was supported via AiF (19359N) within the program for promoting the Industrial Collective Research (IGF) of the German Ministry of Economic Affairs and Energy (BMWi) based on a resolution of the German Parliament. Open access funding enabled and organized by Projekt DEAL.

The authors have declared no conflict of interest.

Symbols used

A	[m ²]	filter area
$D[4,3]$	[m]	volumetric mean particle size
d	[m]	particle size
d_s	[m]	Sauter diameter
g	[m s ⁻²]	gravitational field strength

h	[m]	cake height
m	[kg]	mass
Δp	[Pa]	differential pressure
S_V	[m ⁻¹]	specific surface area
t	[s]	time
\dot{V}	[m ³ s ⁻¹]	volumetric flow rate
V_{solid}	[m ³]	volume of solids
V_{total}	[m ³]	total volume
w_f	[m s ⁻¹]	settling velocity
x	[-]	state of compression

Greek letters

α_h	[m ⁻²]	height-related filter cake resistance
α_m	[m kg ⁻¹]	mass-related filter cake resistance
ε	[-]	porosity
η	[Pa s]	viscosity
ρ_f	[kg m ⁻³]	fluid density
ρ_s	[kg m ⁻³]	particle density

Subscripts

1	on top or within fine particle layer
2	within compressible bottom layer
3	below or within filter medium

Abbreviation

BSG	brewer's spent grains
-----	-----------------------

References

- [1] *Filtration, 1. Fundamentals* (Eds.: S. Ripperger, W. Gösele, C. Alt), Ullmann's Encyclopedia of Industrial Chemistry, Wiley-VCH, Weinheim **2012**.
- [2] C. M. Alles, H. Anlauf, *Chem. Ing. Tech.* **2003**, *75* (9), 1221–1230. DOI: <https://doi.org/10.1002/cite.200303268>
- [3] W.-M. Lu, K.-L. Tung, C.-H. Pan, K.-J. Hwang, *Sep. Sci. Technol.* **1998**, *33* (12), 1723–1746. DOI: <https://doi.org/10.1080/01496399808545902>
- [4] E. Löwer, T. H. Pham, T. Leifßner, U. A. Peuker, *Powder Technol.* **2020**, *363*, 286–299. DOI: <https://doi.org/10.1016/j.powtec.2019.12.054>
- [5] R. Yao, G. Jiang, W. Li, T. Deng, H. Zhang, *Powder Technol.* **2014**, *262*, 51–61. DOI: <https://doi.org/10.1016/j.powtec.2014.04.060>
- [6] J. Tippmann, H. Scheuren, J. Voigt, K. Sommer, *Chem. Eng. Technol.* **2010**, *33* (8), 1297–1302. DOI: <https://doi.org/10.1002/ceat.201000109>
- [7] M. Hennemann, M. Gastl, T. Becker, *Eur. Food Res. Technol.* **2019**, *245*, 521–533. DOI: <https://doi.org/10.1007/s00217-018-03226-4>
- [8] M. Hennemann, M. Gastl, T. Becker, *J. Food Eng.* **2021**, *293*, 110405. DOI: <https://doi.org/10.1016/j.jfoodeng.2020.110405>
- [9] M. Hennemann, M. Gastl, T. Becker, *Sep. Purif. Technol.* **2021**, *272*, 118966. DOI: <https://doi.org/10.1016/j.seppur.2021.118966>

3 Results

- [10] F. M. Tiller, T. C. Green, *AIChE J.* **1973**, *19* (6), 1266–1269. DOI: <https://doi.org/10.1002/aic.690190633>
- [11] J. Engstle, H. Briesen, P. Först, *Brew. Sci.* **2017**, *70*, 26–30.
- [12] O. Rahli, L. Tadrist, M. Miscevic, R. Santini, *J. Fluids Eng.* **1997**, *119* (1), 188–192. DOI: <https://doi.org/10.1115/1.2819107>
- [13] VDI, *VDI 2762 Part 2. Mechanical solid-liquid separation by cake filtration. Determination of filter cake resistance*, Beuth Verlag, Berlin **2010**.
- [14] H. Y. Sohn, C. Moreland, *Can. J. Chem. Eng.* **1968**, *46* (3), 162–167.
- [15] W. D. Martin, B. J. Putman, N. B. Kaye, *Constr. Build. Mater.* **2013**, *48*, 210–217. DOI: <https://doi.org/10.1016/j.conbuildmat.2013.06.093>
- [16] M. Shirato, T. Murase, M. Negawa, T. Senda, *J. Chem. Eng. Jpn.* **1970**, *3* (1), 105–112. DOI: <https://doi.org/10.1252/jcej.3.105>

3.2.5 Influence of Particle Size Uniformity on the Filter Cake Resistance of Physically and Chemically Modified Fine Particles

Separation and Purification Technology 272 (2021) 118966



Contents lists available at ScienceDirect

Separation and Purification Technology

journal homepage: www.elsevier.com/locate/seppur



Influence of particle size uniformity on the filter cake resistance of physically and chemically modified fine particles

Martin Hennemann, Martina Gastl^{*}, Thomas Becker

Technical University Munich, Chair of Brewing and Beverage Technology, Weihenstephaner Steig 20, Freising 85354, Germany

ARTICLE INFO

Keywords:
Cake filtration
Filter cake resistance
Fine particles
Lautering
Uniformity

ABSTRACT

The filter cake resistance determines the flow rate in cake filtration. The resistance depends not only on the mean size of the particles but also on their overall distribution. An example of where we have insufficient understanding of the effect of particle size is lautering—a separation process used in beer production. In this type of filtration, a layer of biological fine particles (<500 μm) with a high filter cake resistance forms on top of the cake and is responsible for a reduction in flow rate. Herein, differences in the resistance of fine particles based on alteration of their size distribution were investigated. An experimental setup was developed to isolate the fine particles from the filter cake, and their chemical and structural compositions were determined. To alter the particle size distribution, physical (heating, agitation) and chemical (prevention of oxidation, polyphenol addition, pH adjustment, ion concentration alteration) modifications were applied. The modifications affected the interparticle interactions, which influenced the size distribution and thus the resistance. The lowest resistance was achieved by heating (−88%) and the highest by agitation (+69%). Contrary to earlier findings, the results of this study show that not only the mean particle size determined resistance; low resistance also depended on high uniformity of the particle size distribution ($R^2 = 0.856$). Compared with a uniform size distribution, a wide size distribution resulted in lower porosity, which was responsible for higher filter cake resistance. The universal validity of the results from the biological suspension was determined using glass beads as an inert model system.

1. Introduction

Cake filtration is applied in many industries (e.g., in biotechnology or the food sector) to separate the solids of a suspension from the liquid phase. In this process, biological fine particles often form a layer with high resistance which hinders the flow of liquid and extends the process time. A better understanding of how the flow rate through a fine particle filter cake is affected by physical and chemical modifications will help to optimize the filtration process.

The general principle of the process is the formation of a filter cake via the deposition of particles on a filter medium. After particle deposition, the cake serves as a primary filter medium.

A critical characteristic of the effectiveness of cake filtration is the flow rate of the liquid through the cake, which is expressed as filtrate volume (V) per filtration time (t) according to

$$\frac{V}{t} = \frac{A \cdot \Delta p}{\alpha_M \cdot h \cdot \eta} \quad (1)$$

The flow rate depends on filter area (A), pressure drop (Δp), cake height (h), and viscosity (η). Filter cake resistance (FCR)—either expressed relative to cake height (α_M) or dry cake mass (α_M)—is an important characteristic that influences flow rate [1]. FCR can be approximated for incompressible cakes according to the Kozeny–Carman equation (developed for a porous medium consisting of uniform solid particles):

$$\alpha_M = \frac{180}{d^2} \frac{(1 - \epsilon)^2}{\epsilon^3} \quad (2)$$

which indicates that a low FCR depends on a large particle size (d). In addition, FCR is related to porosity (ϵ), which depends not on the size of the particles but on the particle size distribution (PSD) of the system.

Abbreviations: CLSM, confocal laser scanning microscopy; FCR, filter cake resistance; FTIR, Fourier transform infrared spectroscopy; MPS, mean particle size; PSD, particle size distribution.

^{*} Corresponding author.

E-mail address: martina.gastl@tum.de (M. Gastl).

<https://doi.org/10.1016/j.seppur.2021.118966>

Received 9 December 2020; Received in revised form 11 May 2021; Accepted 11 May 2021

Available online 18 May 2021

1383-5866/© 2021 Elsevier B.V. All rights reserved.

3 Results

This is known from the work of Sohn and Moreland [2] and Hwang et al. [3] who expressed this relation based on packing density. A wide PSD (poly-disperse) decreases porosity because smaller particles of the distribution occupy the voids between larger particles. On the other hand, a narrower PSD leads to a higher porosity owing to the presence of larger voids between the particles. The porosity of different poly-disperse PSDs is constant regardless of the particle size if their standard deviation remains constant [2]. This impact of PSD on porosity means that not only the median or mean particle size (MPS) but also the entire distribution affects FCR. Therefore, MPS is not the only important descriptor when evaluating the influence of particles on FCR. Characteristics such as the standard deviation [2] or the width [4] of the PSD are necessary to correctly describe the influence of particle size.

Despite the importance of PSD characteristics in terms of FCR, there is insufficient understanding of this relation in certain cake filtration processes, e.g., the lautering process in beer production. Lautering is the separation of the liquid phase from the biological suspension (mash) that is produced in the previous mashing step from the raw material (malt) [5]. It is a discontinuous process, meaning that sedimentation of the particles takes place prior to filtration, resulting in the formation of a multi-layered filter cake [6]. The multiple layers are caused by the range of different particle sizes in the suspension, which range from nano- to milli-meter sizes [7,8]. This is a particularly wide range when compared with other types of filtration, as summarized by Droppo [9]. Since the particles vary in size and density, different settling velocities are evident prior to filtration. Based on these sedimentation variations of the different particles, a structurally and chemically inhomogeneous filter cake forms [10]. This cake can be divided into two horizontal layers: coarse particles (e.g., husks) settle first and form a compressible bottom layer that serves as a primary filter medium for fine particles (fines), which are deposited during filtration (Fig. 1).

Owing to the small particle size of the fines (<500 μm), the top layer has a higher resistance compared with the bottom layer according to Eq. (2). This has been demonstrated in the literature [11]. Due to the high FCR of the top layer, the compressible bottom layer is compacted during filtration [12]. This compaction decreases the porosity and thus increases the FCR of the bottom layer. As a result, the flow rate through the entire cake is reduced (Eq. (1)). It is therefore expected that a decrease in

the FCR of the top layer improves the filtration process. Contrary to other forms of cake filtration, a skin layer next to the filter medium plays only a minor role in the flow rate when compared with the marked impact of the top layer [12]. Considering the importance of the fine layer on the compression of the bottom layer, the top layer influences the entire filtration process. To examine this critical layer, the current work aimed to understand the impact of particle characteristics of the fine layer on its FCR. Therefore, discussions of the MPS and PSD hereinafter refer only to the fine particles in the top layer (rather than the wide range of particles in the mash, which are responsible for the formation of the multi-layered filter cake).

To date, the only particle characteristic related to fine particles considered in the literature when examining the filtration process in a lauter tun has been the MPS. A large MPS was shown to decrease the FCR of the fines whereas a low MPS increases the FCR [13,14]. However, an evaluation regarding only the MPS does not take into account the complexity of the particle effect based on the influence of the PSD on the porosity and thus FCR (Eq. (2)). Therefore, the influence of PSD on FCR was assessed in the present work. To obtain different PSDs, the agglomeration behavior of the porous organic particles was modified, e.g., by influencing the suspension stability. These modifications were differentiated into physical and chemical types.

Physical modifications such as heating and agitation have already been shown to influence the flow rate of fines. According to the literature [13,15], heating decreases FCR because of an increase in MPS, owing to aggregation of the protein fraction of the fines. On the contrary, agitation results in a mechanical attrition of the agglomerates that reduces MPS and increases FCR [14,16].

Chemical modifications are also known to affect the filtration behavior of fines, e.g., due to an influence on the suspension stability, as a result of which the particle aggregation can change. For example, although it is known that oxidation impairs the flow rate during filtration [17], reasons for this effect based on its influence on the particles have not yet been precisely clarified. Fines consist of proteins at high concentrations [18], which are connected via disulfide bridges [19]; therefore, it is expected that oxidation favors the formation of inter-particle disulfide bridges, which affects the PSD. In addition, poly-phenols can interact with proteins and have previously been shown to influence flow rate during filtration [20]; their reducing potential is also expected to affect PSD. The fine particles are further expected to be exposed to repulsive and attractive forces based on their surface charges, which determines the stability of the suspension. If attractive forces prevail, the suspension is unstable and the particles agglomerate whereas the suspension is stable when repulsive forces prevail and particles do not agglomerate [1,21]. Changes in surface charges are known to influence the cake structure and thus the flow rate [21–23], as previously shown for fines in a lauter tun by altering the pH value [15]; a similar effect is expected for changes in ion concentration. The current work assessed the influence of chemical and physical modifications on the PSD and hence FCR of fines.

The high FCR of the fines (as compared to the coarse particles of the bottom layer) was revealed to highlight the marked impact of the top layer on flow rate. Since the coarse particles of a suspension can affect the analysis, an experimental setup was developed to isolate the fines and maintain constant conditions during the tests. The isolated fines were first analyzed in terms of their chemical composition, which allowed a subsequent structural analysis. Afterward, physical (heating, agitation) and chemical (prevention of oxidation, addition of poly-phenols, pH adjustment, ion concentration alteration) modifications were applied to obtain a wide range of PSDs. Changes in the particle structures were evaluated using Fourier transform infrared (FTIR) spectroscopy, e.g., by revealing changes in the secondary structures of the protein fraction. Since different types of raw material are used in the actual lautering process, the influence of these modifications can differ for each malt [24]. Therefore, the modifications yielding the largest impacts were applied to different malt types to verify the universal

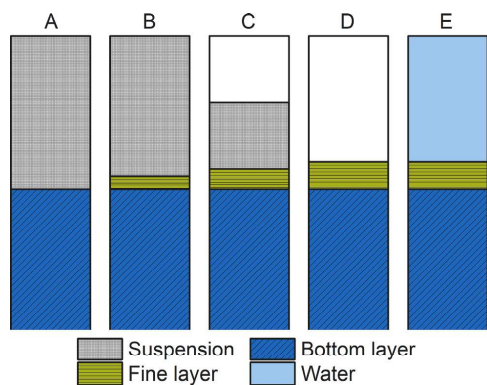


Fig. 1. Scheme of the build-up of the filter cake during filtration. Coarse particles settle immediately on the filter medium after transfer of the suspension to the filter (A). Fine particles (high filter cake resistance) settle later on the coarse particles (low filter cake resistance), which serve as a primary filter medium (B). During filtration (C, D), more fine particles are deposited, leading to a blocking layer atop the compressible bottom layer. After run-off of the first filtrate, the cake is washed with water (E), which has to be filtered through the fine layer. For simplification, the compression of the bottom layer during filtration is neglected in the figure.

validity of the effects. After identifying the particle effects that impacted the flow rate in the natural system (biological suspension), the influences of PSD on porosity and thus FCR were verified using glass beads as an inert model system.

This work shows how the PSD of the fine particles on top of the multi-layered filter cake affects their FCR. The knowledge gained will help to develop modifications to the suspension to reduce the FCR in the practical process, thereby reducing the compression of the bottom layer and thus increasing the flow rate for more economical filtration.

2. Materials and methods

2.1. Isolation of fines

An isolation procedure was developed to (i) obtain pure fine particles and (ii) eliminate the influence of the liquid phase or coarser particles on the analysis. Three different types of malt (A–C) were used as raw materials. The malts differed in terms of barley variety and cytolytic degree of modification (evaluated in terms of friability [25]), thus inducing various filtration behaviors. For the standard tests, malt A was used based on its intermediate degree of modification compared with malt B (high friability) and malt C (low friability), which were both later used for verification. The raw material was milled in a DLFU disk mill (Bühler AG, Uzwil, Switzerland) at a grinding gap of 0.65 mm. After mixing 100 g grist with 350 g distilled water (60 °C), the suspension was stirred using a laboratory mashing bath (Dinkelberg Analytics, Gablingen, Germany). After pauses in heating at 62 °C (30 min) and 72 °C (30 min) for enzymatic conversion, the temperature was increased to 78 °C (according to the actual mashing process). The suspension was then immediately filtered through a MN 514 ¼ filter paper (Macherey-Nagel GmbH & Co. KG, Düren, Germany).

According to Engstle et al. [26], fines were defined as all suspension particles smaller than 500 µm. To separate the fines from the coarse particles, the solids were wet sieved twice using a 500 µm sieve. Samples were stored in a refrigerator because pre-trials revealed that freezing of the fines has an influence on their PSD. During storage, the samples were preserved by adding 0.05 g L⁻¹ potassium metabisulfite (Merck KGaA, Darmstadt, Germany) to the suspension in order to avoid the growth of malt's own microorganisms due to the release of SO₂, unless stated otherwise.

During wet sieving, the particles were washed using a phosphate-citrate buffer to maintain a constant pH value. In order to obtain buffers with different pH values, 0.2 mol L⁻¹ Na₂HPO₄ and 0.1 mol L⁻¹ citric acid (both VWR International GmbH, Darmstadt, Germany) were mixed in appropriate volumes. Unless stated otherwise, the pH was set to 5.35, which was in accordance with the original pH of the suspension. The suspension was centrifuged (4000 rpm, 5 min) in a Heraeus Multifuge 4KR (Thermo Fisher Scientific Inc., Waltham, USA) and the supernatant was discarded to obtain pure particles.

The viscosities of the buffers at 76 °C (filtration temperature) were determined using an AR-G2 rheometer (TA Instruments Ltd., New Castle, USA) at a constant shear rate of 30 s⁻¹. The densities were measured using a DMA 4500 density meter (Anton Paar GmbH, Graz, Austria).

2.2. Chemical and structural analyses

The chemical composition and structure of the particles were determined to obtain detailed insights into the fines. To avoid interferences in the analyses, the particles were washed with distilled water instead of buffer during the isolation procedure. Fines were freeze dried for the chemical analysis and the water content was determined by drying at 130 °C until constant weight was reached. A Rapid MAX N Exceed protein analyzer (Elementar Analysensysteme GmbH, Langenselbold, Germany) was used to determine the protein concentration. The starch content (including resistant starch) was analyzed using the total

starch assay (K-TSTA-100A) and β-glucan was determined using the mixed-linkage β-glucan assay (K-BGLU, both assays from Megazyme Ltd., Bray, Ireland). According to Barrett et al. [18], the sum of ether soluble compounds was gravimetrically determined after Soxhlet extraction for 4 h using petroleum ether (Carl Roth GmbH + Co. KG, Karlsruhe, Germany). Subsequently, the sum of ethanol soluble compounds was extracted from the same sample using ethanol (VWR International GmbH, Darmstadt, Germany) for 2 h. Arabinoxylan was determined by staining with phloroglucinol (Thermo Fisher GmbH, Kandel, Germany) after acid hydrolysis according to the modified Douglas method [27]. The total ash content was measured according to a modified method (Niemi et al. [28]) by combustion in a muffle furnace for 3 h at 900 °C.

Structural analysis was performed using confocal laser scanning microscopy (CLSM). An eclipse Ti – U inverted microscope with an e – C1 plus confocal system (Nikon GmbH, Düsseldorf, Germany) and a 10× objective was used. Fines were stained with rhodamine B and safranin O (both Merck KGaA, Darmstadt, Germany) to visualize proteins and starch at excitation wavelengths of 543 nm and 488 nm, respectively [29].

It was assumed that the porosity of the individual fine particles (in contrast to the porosity of the entire cake) is independent of the modifications used.

2.3. Filtration experiments

The FCR was determined according to the standards of the Verein Deutscher Ingenieure [30]. The filter medium was covered with a MN 514 ¼ filter paper before 3 mL of buffer was added. Fines (6.7 g) were suspended in buffer (20 mL) to obtain a total solid-liquid ratio of 1:3.5. The suspension was stirred (350 rpm) at a filtration temperature of 76 °C for 11 min and then transferred into the filter cell, which was heated to 76 °C. Immediately after the transfer, filtration was performed using a 40-kPa differential pressure. Filtrate mass per time was recorded using a scale and the conversion into volume was performed based on the buffer densities. According to the integrated form of Eq. (1),

$$\frac{t}{V} = \frac{k_M \eta \alpha_M}{2 \cdot A^2 \cdot \Delta p} V + \frac{R_M \eta}{A \cdot \Delta p} \quad (3)$$

the FCR, expressed as α_M , was calculated from a linearized form of the t/V vs. V plot. The filter medium and therefore its resistance (R_M) were constant for all trials, and the latter was assumed to be 0. The concentration constant (k_M) was obtained from the filter cake mass (M) and filtrate volume at the end of filtration (V_e) according to

$$k_M = \frac{M}{V_e} \quad (4)$$

Sedimentation effects were neglected owing to the high concentration of the suspension. An incompressible cake could be assumed since only a low pressure difference was applied.

In order to demonstrate the high FCR of the fines, the FCR was additionally determined for the coarse particles. To account for the approximately six-times higher amount of coarse particles (compared with the fines) in the natural filter cake, the mass of particles for the filtration test was increased to 40.0 g using the same buffer ratio.

2.4. Modification of fine particles

Different modifications were tested to change the PSD of the fines, as follows.

Heating: After suspending the fines at 76 °C for 7 min, the suspension was boiled (5, 15, 25, 35, 45, 55, 65, 75, 115 s) in an Ambiano microwave oven (EIE Import GmbH, Sattledt, Austria) at 700 W, which ensured rapid and homogeneous heating. The filtration test was started after cooling to 76 °C for 4 min under stirring. The maximum heating

time tested was 115 s, which showed that the FCR did not change any further.

Agitation: The suspension was exposed to ultrasound in an ultrasonic bath at 76 °C for 1, 2, 4, 6, 9, 15, and 20 min. 20 min was the maximum ultrasound exposure at which no further change in FCR occurred.

Prevention of oxidation: Pre-trials revealed that the production of the suspension resulted in oxidation of the particles. Further oxidation using an oxidizing agent showed no influence on the particles. Therefore, the effect of oxidation was assessed by the addition of potassium metabisulfite (Merck KGaA, Darmstadt, Germany) as a reducing agent (0, 0.05, 0.1, 0.15, 0.2, 0.4, 0.6, 1.0 g L⁻¹) at the beginning of mashing. 1.0 g L⁻¹ was the maximum concentration at which no further change in FCR occurred.

Polyphenols: Similar to that described by Karabín et al. [20], polyphenols (20, 40, 80, 120, 160 mg L⁻¹) were added at the beginning of mashing in the form of a freshly prepared tannic acid solution (Merck KGaA, Darmstadt, Germany).

pH: The pH was varied in the range 4.55–6.95 (step size: 0.2) using different buffers. Lower pH values than the standard of 5.35 were tested as they occur in the actual mashing process during acidification of the suspension. The filter cake is washed with hot water during lautering, which increases the pH of the suspension; for this reason, pH values up to 6.95 were tested.

Ion concentration: The Ca²⁺ concentration (20, 40, 80, 160 mg L⁻¹) in the suspension buffer was adjusted by the addition of CaSO₄ (VWR International GmbH, Darmstadt, Germany). The maximum Ca²⁺ concentration was within a normal range for water used in brewing [31].

2.5. Particle size distribution

The PSD of the fines was measured to detect changes resulting from the introduced modifications. The measurement was conducted by laser diffraction using a Mastersizer 3000 (Malvern Panalytical GmbH, Kassel, Germany) equipped with a Hydro EV dispersing unit. The size classes were determined by the Mastersizer software (version 3.62) with which the volume density was calculated. Different characteristics were quantified to evaluate the particles in terms of their PSD. D_x refer to the diameter of the particles, which is equal to or greater than x percent of the volume of particles present. D_{50} is the median, $D[3,2]$ the Sauter diameter, and $D[4,3]$ the volumetric MPS. The span describes the width of the PSD [4,32]:

$$\text{span} = \frac{D_{90} - D_{10}}{D_{50}} \quad (5)$$

The geometric standard deviation (σ_g) can be calculated according to

$$\sigma_g = \sqrt{\frac{D_{84.13}}{D_{15.87}}} \quad (6)$$

to describe the uniformity of a bimodal distribution [33]. Another common descriptor for the uniformity is the coefficient of uniformity (C_u) [34,35]:

$$C_u = \frac{D_{60}}{D_{10}} \quad (7)$$

A low C_u value indicates high uniformity.

2.6. Fourier transform infrared spectroscopy

FTIR spectra of the fines were evaluated to study changes in the secondary structures and disulfide bridges of the protein fraction. A Frontier FT – IR spectrometer (PerkinElmer Inc., Waltham, USA) was used to record spectra in the frequency range 4000–650 cm⁻¹ with attenuated total reflection. After normalization, second-derivative spectra were calculated using a five-point, two-degree polynomial function [36]. Noise was reduced by smoothing using an 11-point, two-

degree polynomial Savitsky–Golay function [37]. Changes in protein secondary structures were determined by analyzing the amide III region (1350–1200 cm⁻¹) [38]. Additionally, changes in thiol groups (2577 and 2601 cm⁻¹) were investigated.

2.7. Model system

An inert model system was used to verify the influence of PSD on FCR. The model allowed an investigation of any effects in the absence of chemical influences and interparticle interactions. In addition, porosity was determined experimentally and permeability was calculated to explain differences in FCR for various PSDs. Permeability was used for a correlation with FCR to compare the experimental and theoretical results.

SiLibeads glass beads (Sigmund Lindner GmbH, Warmensteinach, Germany) in various particle size fractions up to 600 μm (see results section for classification) were used to simulate the fines. The glass beads had a lower FCR compared to the fines owing to their ideal round shape. In addition, it must be noted that due to the porous structure of the fine particles, the filtration behavior can differ from that of the non-porous glass particles. Therefore, the model system could only be compared in relative terms to the natural fines. A five-times higher amount of solids (33.5 g) was used to highlight differences in FCR. In addition to the individual size fractions, an artificial PSD with a high C_u (referred to as *wide*) was generated in pre-trials by combining different quantities of these size fractions.

According to the method of Sohn and Moreland [2], porosity was determined by measuring the total volume (V_{total}) of the particle system after pouring it into a graduated cylinder. Tapping the cylinder until the volume was not reduced further enabled dense packing. A piston on the top ensured a horizontal surface of the particles and aided dense packing. The volume of the particles ($V_{particle}$) was determined by converting the mass into volume using the particle density (2500 kg m⁻³), which enabled the calculation of porosity according to

$$\varepsilon = \frac{V_{total} - V_{particle}}{V_{total}} \quad (8)$$

Permeability (K) was calculated based on α_H (using $D[3,2]$ as diameter) according to [1]

$$K = \frac{1}{\alpha_H} \quad (9)$$

2.8. Statistics

Filtration tests and chemical analyses were conducted in triplicate ($n = 3$). PSD analyses are presented as the average of 30 measurements ($n = 30$). Means and standard deviations were determined. Statistical evaluation was performed using OriginPro 2019b (OriginLab Corporation, Northampton, USA) and significant differences between means were determined using a t -test ($p < 0.05$).

3. Results and discussion

3.1. Filter cake resistance of different particles in the cake

The large impact of the top layer on the filtration process can be highlighted by comparing the FCR of the fines to that of the coarse particles. Fines exhibited a FCR of $3.4 \cdot 10^{13}$ m kg⁻¹ ($\pm 2 \cdot 10^{12}$, $n = 3$), as determined in the standard filtration test without modifications. Compared with the coarse particles ($2.4 \cdot 10^{11} \pm 1 \cdot 10^{10}$ m kg⁻¹, $n = 3$), the FCR of the fines is about 100 times higher. This result is in agreement with the negative influence of the top layer on the compression of the bottom layer of the filter cake [12]. It is further supported by the work of Engstle et al. [11] who showed that the top layer exhibited a much lower permeability compared with the bottom layers. Owing to the high

importance of the fines in the filtration process, these particles were investigated in more detail, as described in the following.

3.2. Chemical composition of fines and structural analysis

Chemical analysis revealed that fines mainly consist of protein (Table 1). This corresponds to the literature review of Hennemann et al. [10], in which the high protein content in the top part of the inhomogeneous filter cake was described. Although the degradation of starch is the main purpose of the mashing process, it is still present in the second largest proportion in the fines. High protein and starch contents were also reported by Barrett et al. [18], showing concurrence with our results. Ether soluble substances (e.g., lipids [39]), arabinoxylan, and ethanol soluble substances (e.g., polyphenols [40]) represent about one-third of the composition. Ash and β -glucan are present only in minor concentrations. Impurities based on the coarser particles consist mainly of cellulose or lignin [41] and make up the remaining content (~3%, not determined).

After determining the chemical composition, the structure of the fines was analyzed using CLSM imaging. The main constituents (protein and starch) were visualized to reveal the structural features of the particles (Fig. 2).

Large starch granules (10–30 μm) appeared as ordered structures (Fig. 2, #1), suggesting that they were crystalline in nature. These were not broken up during milling or enzymatically solved during mashing and were surrounded by a protein layer. Further particles were present in a high proportion and showed similar intensities for starch and protein (Fig. 2, #2). This suggests that these particles were precipitated proteins incorporating small starch granules (<6 μm).

3.3. Modification of fines

The main components of fines (starch and protein) were expected to be influenced by physical (heating, agitation) and chemical (prevention of oxidation, addition of polyphenols, pH adjustment, ion concentration alteration) modifications. These modifications are thought to change the structure or agglomeration behavior of the fines, which then has an impact on the PSD and thus influences the FCR.

The first modification considered is heating, which decreased the FCR of the particles. A minimum was reached at 55 s of heating (Fig. 3a), at which point a decrease of 88% was observed.

To explain the decrease in FCR, changes in the PSDs were evaluated. The shifts in the maximum of the size classes, changes in volume density, MPS (D_{50} , $D[3,2]$, $D[4,3]$), and uniformity (span, σ_g , C_u) were compared with the standard test. For each modification, the parameter with the largest effect was described in detail as the most pertinent example (Fig. 4, Table 2) and changes within a modification were visualized using heat maps.

The change in PSD during heating explains the decrease in FCR (Fig. 3b, size classes of interest between 1 and 300 μm are shown, logarithmic scale). Continuous heating shifted the maximum up to a larger size class compared with the standard. In addition to the shift, there was an increase in the volume density near the maximum, which was accompanied by a decrease in the density of both small and large particles. This resulted from the agglomeration of small particles and de-

agglomeration of large particles, leading to the formation of a narrower PSD (see example in Fig. 4a). These findings indicate that there was not only an increase in the MPS during heating, as previously reported by Bühler et al. [13].

The uniformity was calculated to evaluate changes in the PSD. A high uniformity of particles is represented by a low C_u value. Compared with the standard, the uniformity increased during heating (Table 2). A similar effect has been reported in the literature for other types of protein–polysaccharide complexes, for which more homogeneous complexes can form during heating [42]. Consequently, not only the descriptor of the MPS ($D[3,2]$) but also those of the particle uniformity show a significant correlation with the FCR for heating (Table 3).

The increase in particle uniformity can be explained by the structure of the fines. Thermal energy broke up the starch agglomerates (Fig. 2, #1), which resulted in a reduction of their size. The resulting maximum in the volume density at 42.8 μm is in accordance with the presence of a large amount of free large starch granules. Heating also led to the denaturation of proteins, which resulted in further agglomeration of the starch–protein agglomerates (Fig. 2, #2) and reduced the density in small size classes. After 65 s, a trend of the maximum size class towards lower sizes can be seen, which can be attributed to a stronger breakdown of larger particles compared with agglomeration due to denaturation.

FTIR spectra were evaluated to verify the effect of heating on the particle structure. A change in protein secondary structure elements at the beginning of heating was mainly assigned to random coils. The appearance of these random coils explains the thermal denaturation. In the course of heating, further changes in α -helices, β -turns, and β -sheets were observed, which serves as evidence of ongoing denaturation based on the altered protein structure [38,43].

In contrast to heating, agitation by ultrasound increased the FCR up to 69%, reaching a maximum at 15 min (Fig. 5a). No significant difference in the FCR was observed between 15 and 20 min, which means that the effect of agitation was at its maximum at this point.

Agitation results in particle de-agglomeration through mechanical breakage of particle–particle interactions. The maximum PSD shifted to a smaller size class during ultrasound exposure (Fig. 5b). The difference in PSD reveals that the density decreased for large particles and increased for small particles (see example in Fig. 4a). Consequently, agitation broadened the PSD and decreased its uniformity, as seen by a higher C_u compared with the standard (Table 2). A significant correlation of FCR to MPS (D_{50} and $D[3,2]$) and uniformity descriptors (span and σ_g) was found (Table 3), which confirms that not only a lower MPS can increase FCR. Although a general higher C_u was found for agitation, no significant correlation with FCR was found for this descriptor. This shows that not every descriptor can be applied in the same way to the various modifications to describe the uniformity.

Tse et al. [16] used a different setup to investigate the effect of agitation on mash particles by differing the impeller tip speed during stirring. They reported an increase in the amount of fines formed but no decrease in their size. In contrast, our model experiment using ultrasound revealed that there was a shift in volume density from larger to smaller particles, which means that the size of the particles decreased owing to ultrasonic attrition.

The effect of oxidation on the fines was investigated by the prevention of oxidation using an increasing concentration of reducing agent. With up to 0.10 g L⁻¹ potassium metabisulfite, no significant difference in FCR was observed (Fig. 6a). From 0.15 g L⁻¹, the FCR decreased, reaching a minimum at 0.60 g L⁻¹ (~50%). No significant differences were observed at higher concentrations. This indicates that the effect of oxidation caused by the mashing process is maximal at up to 0.10 g L⁻¹ and minimal at 0.60 g L⁻¹ potassium metabisulfite.

With an increasing concentration of reducing agent, the maximum volume density shifted to a smaller size class, while the PSD decreased in large size classes and increased in small size classes (Fig. 6b and example in Fig. 4b). In contrast to agitation, the shift to smaller size classes increased the uniformity (C_u) of the PSD (Table 2). Consequently, the

Table 1
Chemical composition of fines (dry weight, n = 3).

Substance	Concentration (%)
Protein	53.9 ± 0.2
Starch	12.3 ± 0.1
Ether soluble fraction	11.0 ± 0.3
Arabinoxylan	9.3 ± 0.2
Ethanol soluble fraction	8.4 ± 0.3
Ash	1.36 ± 0.04
β -glucan	0.277 ± 0.004

3 Results

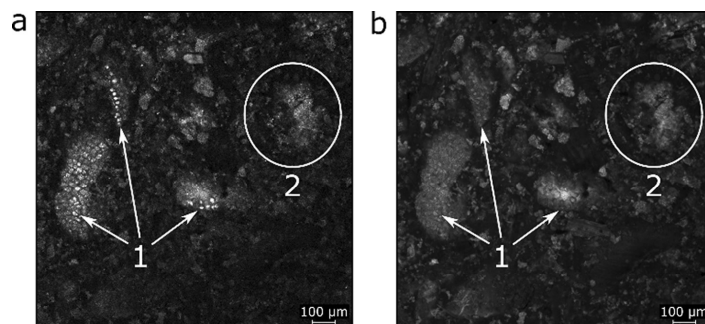


Fig. 2. CLSM images of fines stained with safranin O and rhodamine B to visualize (a) starch and (b) protein. Stained substances are displayed in white. Indicated are ordered structures of large starch granules (1) and protein-starch precipitates (2).

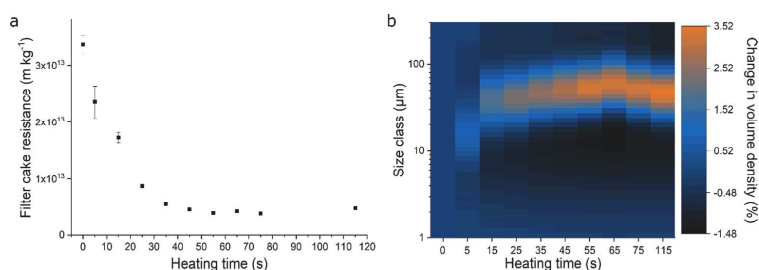


Fig. 3. (a) Filter cake resistance of the fines in relation to heating time ($n = 3$). (b) Change in volume density of the particle size distribution ($n = 30$) compared with the standard (0 s heating).

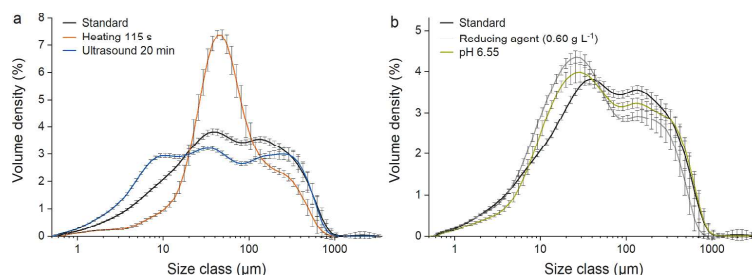


Fig. 4. Comparison of the particle size distributions of the standard test with (a) heating and ultrasound as well as (b) reducing agent and pH, which showed the largest influence among the modifications examined ($n = 30$, logarithmic scale).

FCR decreased even though the particles had a smaller MPS. A significant correlation of FCR to the descriptors of MPS as well as uniformity (C_u and span) was found (Table 3), which emphasizes the importance of the particle uniformity in the explanation of FCR.

FTIR analysis revealed that the addition of a reducing agent resulted in the alteration of protein secondary structure elements, which was responsible for alterations in the PSD. In addition, changes in the band region for thiol groups were observed. Although the intensities of thiols are generally weak in FTIR spectra, the changes can be assigned to the disulfide bridges of proteins. This is in agreement with the work of Moonen et al. [19] who reported an extended disulfide bonded network in the top layer. The results indicate that the reducing agent led to a reduction in the protein disulfide bridges in the particles. Consequently,

interparticle connections were broken down, which explains the deagglomeration and the PSD shift to smaller size classes.

The addition of polyphenols had only a minor influence on FCR (data not shown). At a concentration of 80 mg L^{-1} , FCR decreased by 13%. An increase in the concentration showed no further improvement. This corresponds to the results of Karabın et al. [20] who found a reduction in filtration time within a similar range by the addition of polyphenols. Only a small change in PSD was observed when uniformity increased slightly (Table 2) and thus no significant correlation with the descriptors of PSD was found (Table 3). According to Karabın et al. [20], polyphenols can act as a reducing agent. However, compared with the trials using potassium metabisulfite, the addition of polyphenols had only a weak influence on the PSD and thus on the FCR.

3 Results

Table 2
Overview of changes to descriptors based on exemplary modifications that showed the greatest influence on FCR (n = 30).

Modification	D_{50} (μm)	$D[3,2]$ (μm)	$D[4,3]$ (μm)	span (-)	σ_g (-)	C_u (-)
Standard	55 ± 4	16.5 ± 0.7	118 ± 12	5.9 ± 0.4	4.7 ± 0.2	12.3 ± 0.6
Heating (115 s)	52 ± 4	26 ± 2	93 ± 7	4.3 ± 0.5	2.7 ± 0.1	4.0 ± 0.1
Ultrasound (20 min)	40 ± 2	12.0 ± 0.3	109 ± 10	8.3 ± 0.5	6.0 ± 0.2	14.1 ± 0.8
Reducing agent (0.60 g L ⁻¹)	37 ± 2	14.8 ± 0.5	92 ± 7	7.1 ± 0.4	4.5 ± 0.2	8.3 ± 0.5
Polyphenols (80 mg L ⁻¹)	51 ± 3	16.1 ± 0.5	111 ± 10	6.0 ± 0.4	4.6 ± 0.2	11.3 ± 0.7
pH 6.55	50 ± 2	19 ± 1	120 ± 12	6.8 ± 0.4	4.6 ± 0.2	9.2 ± 0.8
Ca ²⁺ (160 mg L ⁻¹)	54 ± 4	16.0 ± 0.5	118 ± 13	6.0 ± 0.3	4.8 ± 0.1	12.7 ± 0.6

A change in the pH of the suspension influences electrostatic forces, which can affect FCR (Fig. 7a). Within a practical mash pH range of 5.35–5.75, only small differences in FCR were observed that were also influenced by the experimental error (e.g., when adjusting the pH using different buffers). At a higher pH of 5.95, there was a small increase in the FCR whereas for a pH lower than 5.35 a decrease in FCR was found. This trend indicates that mash acidification can decrease FCR. This result is supported by the work of Engstle et al. [15] who found the greatest filterability of fines at pH 4. However, extremely low pH values are not viable in the mashing process since enzymatic conversion would be hindered. Compared with the standard pH of 5.35, a significantly lower FCR was found at pH 6.55 (–56%) and to a smaller extent at pH 6.75.

Alteration of pH resulted in only small changes in PSD of the fines. Small deviations between pH 4.55 and 6.15 may be due to the experimental error. Large differences from the standard (pH = 5.35) were observed only for pH values between 6.35 and 6.75 (Fig. 7b). At these higher pH values, positively charged amine groups of the proteins are deprotonated, which leads to an increase in the negative charge of the particles, similar to that described by Ruiz et al [44]. Among the pH

Table 3
Statistical evaluation of fine particle modifications showing the correlation (R²) of FCR to descriptors of PSD (a: p < 0.001, b: p < 0.05, c: p > 0.05).

Descriptor	Heating	Agitation	Prevention of oxidation	Addition of polyphenols	pH adjustment	Ion concentration alteration
D_{50}	0.294 ^c	0.708 ^b	0.781 ^b	0.309 ^c	0.121 ^c	0.108 ^c
$D[3,2]$	0.864 ^a	0.552 ^b	0.515 ^b	0.078 ^c	0.182 ^c	0.399 ^c
$D[4,3]$	0.010 ^c	<0.001 ^c	0.736 ^b	0.465 ^c	0.027 ^c	0.217 ^c
span	0.726 ^b	0.877 ^a	0.695 ^b	0.006 ^c	0.203 ^c	0.110 ^c
σ_g	0.946 ^a	0.792 ^b	0.488 ^c	0.376 ^c	0.131 ^c	0.336 ^c
C_u	0.941 ^a	0.116 ^c	0.853 ^b	0.581 ^c	0.344 ^b	0.449 ^c

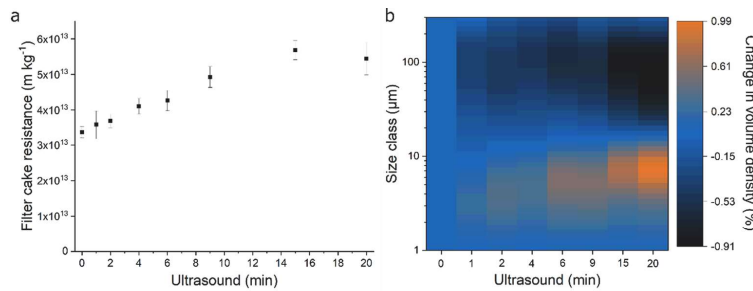


Fig. 5. (a) Filter cake resistance of the fines in relation to ultrasound time (n = 3). (b) Change in volume density of the particle size distribution (n = 30) compared with the standard (0 min ultrasound).

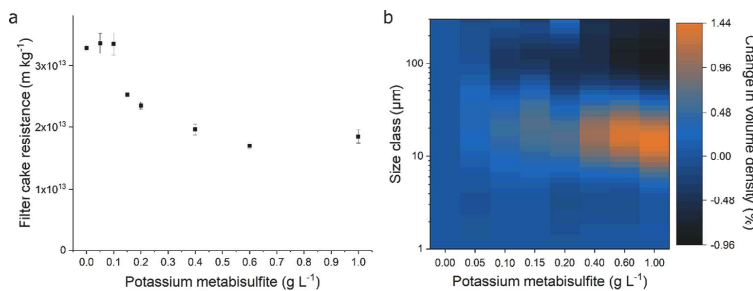


Fig. 6. (a) Filter cake resistance of the fines in relation to potassium metabisulfite concentration (n = 3). (b) Change in volume density of the particle size distribution (n = 30) compared with particles without potassium metabisulfite addition.

3 Results

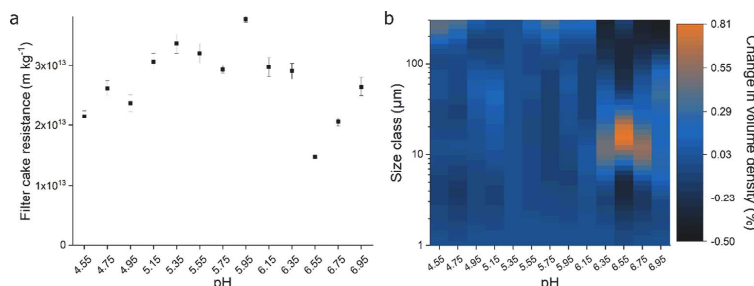


Fig. 7. (a) Filter cake resistance of the fines in relation to pH ($n = 3$). (b) Change in volume density of the particle size distribution ($n = 30$) compared with the standard (pH = 5.35).

values examined, this indicates that the isoelectric point is reached at pH 6.55, where the suspension is unstable and smaller particles agglomerate. The agglomeration can be attributed to particle sizes up to 30 μm . This is in agreement with the work of Tiller et al. [45] who reported that interparticle forces prevail for particles under 10–20 μm .

At high pH values (>6.35), an additional decrease in the particle size of larger size classes (>40 μm) was observed. This may be due to the incipient degradation of crystalline starch under alkaline conditions, similar to that reported in the literature for starch nanocrystals [46,47].

Consequently, the volume density is shifted to an intermediate size class at pH 6.55 (see example in Fig. 4b) based on an agglomeration of small proteins and a degradation of larger starch particles. This decreased the C_u and thus increased uniformity (Table 2) and is responsible for the low FCR.

Since only minor changes in PSD were observed for the pH values under investigation, only a low but significant correlation with FCR was found for uniformity (Table 3).

Accordingly, particle size differences for specific pH values were found, which contrasts with results available in the literature [15].

Only small changes in random coils were observed by FTIR analysis. This means that a change in secondary structural elements based on the pH alteration did not result in protein denaturation. It is the change in pH that affects electrostatic charges on the surface of the particles, which can influence their agglomeration behavior.

Since not only pH is known to have an influence on the surface forces of particles, the effect of an increased Ca^{2+} concentration was tested. However, the FCR was influenced only slightly (+12%) at the maximum concentration of 160 mg L^{-1} and no significant difference from the standard was observed for lower concentrations (data not shown). Only small changes in PSD were observed (Table 2) and thus no correlation with the descriptors of PSD was found (Table 3). These findings indicate that the effect of ions on the surface charge of the fines was rather weak when compared with a change in pH. A strong influence of ionic strength, as seen for other types of protein–polysaccharide complexes [48], was not observed. This may have been a result of the composition of the suspension. Since ions are already present at high concentrations in mash [10], a further increase in the concentration had only a minor influence.

3.4. Validity for different raw materials

The modifications discussed above were tested for malt A. However, different types of malt can be used for different batches in the brewing process. Therefore, the impacts of the modifications when applied to different types of raw material (malts B and C) were also quantified. The strongest influences on the FCR (heating, pH adjustment, prevention of oxidation) were tested.

In the absence of modifications, the FCR was lower for malts B

(–42%) and C (–60%) compared with malt A, which corresponds to the greater uniformity of the PSDs ($C_u = 8.3 \pm 0.2$ and 8.6 ± 0.2 , respectively). Heating decreased the FCR for all malt types in a similar manner when compared with the respective standard trial (A: –88%, B: –89%, C: –85%). The prevention of oxidation had a similar effect (A: –50%, B: –69%, C: –47%). Therefore, both modifications showed similar results independent of malt type. However, pH dependence did not generally apply for all malt types. For malt A, a decrease of 56% was observed when changing the pH from 5.35 to 6.55. A smaller decrease in FCR resulted when applying the same pH change for malts B (–10%) and C (–4%). This may have been due to differences in the chemical composition of the fines, which resulted in different surface charges.

3.5. Summary of the effects of the modifications

The investigated modifications were found to potentially alter the PSD of the fines. The break-up of particle agglomerates can be a result of thermal energy, attrition, or the chemical reduction of disulphide bridges. On the other hand, particles can agglomerate because of protein denaturation or attractive electrostatic forces. Therefore, physical and chemical influences have an effect on the particles, which determines the PSD and thus the FCR.

Among the modifications, increased heating time resulted in the greatest reduction of FCR, followed by changes in pH and prevention of oxidation. In contrast, increased exposure to agitation increased FCR. The addition of polyphenols and a change in the ion concentration led to only small changes in FCR.

The results indicate that a reduction of the filtration time can be achieved by heating the mash, e.g., by applying a decoction mashing process. Furthermore, oxidation and shear forces have to be prevented to avoid an increased filtration time resulting from a high FCR of the fines. Depending on pH, the FCR can be either high or low; however, the necessary pH value to decrease the FCR would need to be determined for each malt type, which is not viable for the actual process.

3.6. Correlation between PSD and FCR

Particle size related characteristics were evaluated to explain the influence of MPS and PSD on FCR. Different descriptors were calculated (Table 4), wherein all investigated modifications and malt types ($n = 53$) were considered.

The descriptors of MPS show only a low dependence ($D[3,2]$) on FCR and are therefore not the only reason for a low FCR. This is contrary to the results of Bühler et al. [13,14] who reported that a high MPS is responsible for the high filterability of particles up to 106 μm . The differences to our results can be explained by the additional modifications under investigation and the use of particles sizes up to 500 μm in our work.

Table 4

Correlations between particle size descriptors and filter cake resistance of physically and chemically modified fine particles and different malt types ($n = 53$, a: $p < 0.001$, b: $p < 0.05$, c: $p > 0.05$).

Descriptor	R ²
D_{50}	0.064 ^c
$D[3.2]$	0.610 ^a
$D[4.3]$	0.086 ^b
span	0.540 ^a
σ_g	0.845 ^a
C_u	0.856 ^a

Kinnarinen et al. [32] reported that the width of the PSD can affect filter cake porosity and thereby its resistance to flow. The PSD span showed a significant correlation with FCR, although the correlation coefficient was low. This may have been a result of the large D_{90} values (compared with the low D_{10} values) that were used for the calculation of the span, which overemphasizes the dependence on large particles [32].

A higher correlation was found for σ_g and C_u (Fig. 8), which are both descriptors of the uniformity. It can be concluded that a more uniform PSD correlates with a lower FCR; this applies even if the MPS is low. A similar effect has been observed previously, e.g., in the filtration of mineral slurries [4,32], where a uniform particle size improves filtration characteristics in spite of the reduction in MPS. Our results confirm that this effect applies not only to suspensions made from minerals but also to complex biological suspensions like the fine particles in lautering.

3.7. Verification using a model system

To verify the effect of particle uniformity on FCR, a model system with particles of a similar size range to the fines was tested. Glass beads were used to avoid interparticle interactions and chemical influences.

The model revealed that a low FCR depended on a high MPS for individual particle size fractions (Fig. 9a and b). In particular, particles up to 50 μm yielded a high FCR owing to their small MPS. A minimum in FCR was found for the 200–300 μm fraction and no further decrease was found for larger particle sizes. Although it was expected that the FCR continues to decrease with increasing MPS (Eq. (2)), a very rapidly filtering cake (according to Ripperger et al. [11]) was formed already at 200–300 μm . Therefore, a further increase in the MPS did not result in a further decrease in the FCR in this model system (not detectable by the experimental setup). In addition, an increasing MPS correlated with a decreasing FCR only when using size fractions with a low C_u (Fig. 9c). For wide particles (with a wide, artificially-produced poly-disperse PSD), a volumetric MPS (159 \pm 6 μm) similar to the 100–200 μm fraction (151

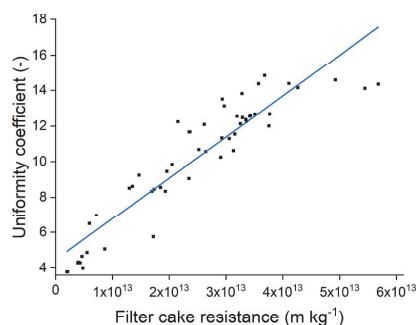


Fig. 8. Filter cake resistance of physically and chemically modified fine particles and different malt types as a function of the uniformity coefficient.

\pm 5 μm) was found, although the FCR was about three times higher. The high FCR depended on the low uniformity, as seen from the approximately three-times higher C_u value (5.5 ± 0.1) compared with the 100–200 μm fraction (1.63 ± 0.02). This provides evidence for the influence of particle uniformity on the FCR of the fines. Accordingly, uniformity rather than MPS determined the FCR of non-homogeneous PSDs within a similar average size range.

The reason for the increase in FCR for the wide particle size fraction is that small particles occupied the voids between large particles. The resulting low porosity of the wide particles (0.255 ± 0.008) compared with that of the 100–200 μm fraction (0.365 ± 0.005) is responsible for a lower permeability (wide: $1.7 \cdot 10^{-13} \pm 2 \cdot 10^{-14} \text{ m}^2$, 100–200 μm fraction: $1.01 \cdot 10^{-11} \pm 4 \cdot 10^{-13} \text{ m}^2$) and thus a higher FCR (Fig. 9d). This influence of low uniformity on the occupation of voids by particles is supported in the literature [2,35] and confirmed in the present study for biological particles.

The small changes in the porosity of the uniform size fractions are in agreement with the work of Sohn and Moreland [2] who showed that the packing density and therefore porosity is independent of particle size. For the case of similar uniformity, only changes in MPS affected FCR.

The experimentally determined FCR shows no correlation ($R^2 = 0.147$, $p > 0.05$) to the calculated permeability. This shows that the MPS is not the most important factor in evaluating the FCR. It is also necessary to take into account the PSD, which affects the porosity and therefore permeability as well as FCR.

A scheme of the influence of PSD on the porosity of a filter cake is shown in Fig. 10. For the ideal case of only one particle size in the distribution, PSD is narrow and hence uniform. The resulting cake structure is then loosely packed and the porosity is high. If there is a wide distribution of particles with different sizes, the voids between the large particles are filled by small particles. Although the average particle size is similar to that of the uniform distribution, the resulting porosity of the cake is lower for the wide distribution.

4. Conclusions

The top layer of the filter cake in a lauter tun has a marked impact on the filtration process. This is because of the high FCR of the fine particles in this layer. Physical and chemical modifications of these porous organic aggregates influence the suspension stability or agglomeration behavior, which affects the macromolecular morphology or the number of molecules per agglomerate. The resulting change in PSD influences then the FCR.

Contrary to earlier results regarding the particle characteristics of fines, it was shown that not only a high MPS is responsible for a low FCR; rather, high particle uniformity is necessary to decrease the FCR and improve the filtration process. The low FCR can be explained by the high porosity of the filter cake of the biological particles.

The best condition to increase particle uniformity and thus improve the filtration process would be to heat (100 °C) for about 60 s before filtration. During mashing, this physical influence on the PSD can only be achieved with a decoction process. In practice, however, this boiling step cannot be applied to every product. It is also essential to avoid shear forces and oxidation during preparation of the particles in order to maintain a low FCR. In general, a low FCR can be achieved by finding an optimal pH of the particles that shows the lowest FCR. However, this may not be feasible in the practical process. The choice of raw material has also a great impact on FCR of fines. However, the cytolytic characteristic (friability) investigated has not been shown to be the main influence on FCR. Rather, the protein fraction of the malt is responsible for the filtration behavior of the fines and requires further investigations.

Similar results with regard to fine particle filtration can be expected for applications in which particles with a high protein content are filtered (e.g. protein concentration using microfiltration, filtration of whey proteins).

3 Results

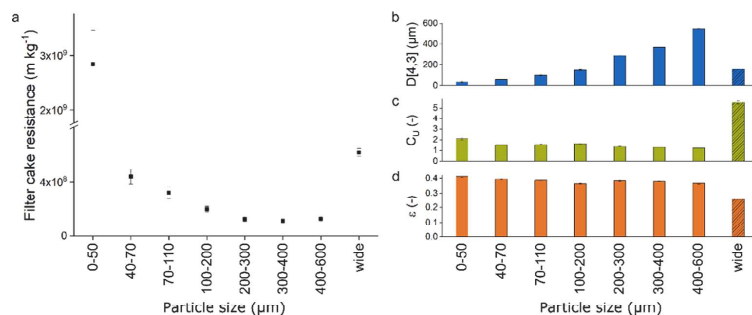


Fig. 9. (a) Filter cake resistance, (b) volume-based mean particle size, (c) coefficient of uniformity, and (d) porosity for different particle classes of the glass beads model system. Wide refers to an artificially-produced wide particle size distribution ($n = 3$).

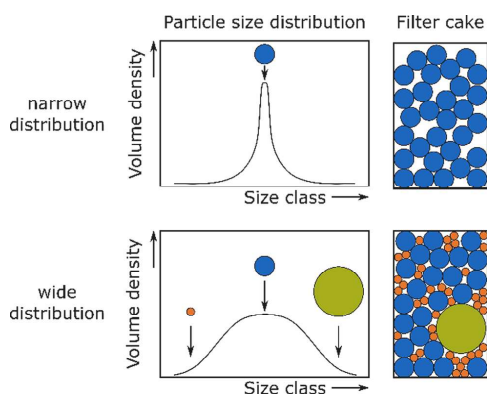


Fig. 10. Scheme of the influence of narrow and wide particle size distributions on porosity of the filter cake.

Funding

This IGF Project of the FEI was supported via AiF (19359N) within the programme for promoting the Industrial Collective Research (IGF) of the German Ministry of Economic Affairs and Energy (BMWi), based on a resolution of the German Parliament.

CRediT authorship contribution statement

Martin Hennemann: Conceptualization, Data curation, Formal analysis, Investigation, Methodology, Software, Validation, Visualization, Writing - original draft, Writing - review & editing. **Martina Gastl:** Conceptualization, Methodology, Investigation, Validation, Visualization, Resources, Funding acquisition, Project administration, Supervision, Writing - original draft, Writing - review & editing. **Thomas Becker:** Resources, Funding acquisition, Project administration, Supervision. : Writing - original draft.

Declaration of Competing Interest

The authors declare that they have no known competing financial interests or personal relationships that could have appeared to influence the work reported in this paper.

Acknowledgments

We are grateful to Monika Wehrli (Chair of Brewing and Beverage Technology, Technical University Munich) and Tim Kratky (Catalysis Research Center, Technical University Munich) for their skillful help with the FTIR experiments.

References

- [1] S. Ripperger, W. Gösele, C. Alt, *Filtration, 1. Fundamentals*, Wiley-VCH, Weinheim, 2012.
- [2] H.Y. Sohn, C. Moreland, The effect of particle size distribution on packing density, *Can. J. Chem. Eng.* 46 (3) (1968) 162–167.
- [3] K.-J. Hwang, Y.-S. Wu, W.-M. Lu, Effect of the size distribution of spheroidal particles on the surface structure of a filter cake, *Powder Technol.* 91 (1997) 105–113.
- [4] T. Kinnarinen, R. Tuunila, A. Häkkinen, Reduction of the width of particle size distribution to improve pressure filtration properties of slurries, *Miner. Eng.* 102 (2017) 68–74.
- [5] J. Tippmann, T. Becker, Das Zusammenspiel von Verfahrenstechnik und Technologie in der Brauerei, *Chemie Ingenieur Technik* 88 (12) (2016) 1857–1868.
- [6] W.-M. Lu, K.-L. Tung, C.-H. Pan, K.-J. Hwang, The effect of particle sedimentation on gravity filtration, *Sep. Sci. Technol.* 33 (12) (1998) 1723–1746.
- [7] F. Kühbeck, W. Back, M. Krottenhauer, T. Kurz, Particle size distribution in wort during large scale brewhouse operations, *AIChE J.* 53 (5) (2007) 1373–1388.
- [8] J. Tippmann, J. Voigt, K. Sommer, Measuring particle size distribution of mash with laser diffraction to evaluate the process success, *Brew Sci.* 64 (2011) 13–21.
- [9] I.G. Droppo, *Filtration in particle size analysis*, Encyclopedia of Analytical Chemistry, 2006.
- [10] M. Hennemann, M. Gastl, T. Becker, Inhomogeneity in the lauter tun: a chromatographic view, *Eur. Food Res. Technol.* 245 (2019) 521–533.
- [11] J. Engstle, N. Reichhardt, P. Först, Filter cake resistance of horizontal filter layers of lautering filter cakes, *MBAA Tech Q* 52 (2) (2015) 29–35.
- [12] M. Hennemann, M. Gastl, T. Becker, Optical method for porosity determination to prove the stamp effect in filter cakes, *J. Food Eng.* 293 (2021), 110405.
- [13] T.M. Bühler, M.T. McKechnie, R.J. Wakeman, Temperature induced particle aggregation in mashing and its effect on filtration performance, *Food Bioprocess Process.* 74 (4) (1996) 207–211.
- [14] T.M. Bühler, G. Matzner, M.T. McKechnie, *Agitation in mashing*, 1995.
- [15] J. Engstle, P. Först, Surface forces and their effect on lautering, 2015.
- [16] K.L. Tse, C.D. Boswell, A.W. Nienow, P.J. Fryer, Assessment of the effects of agitation on mashing for beer production in a small scale vessel, *Food Bioprocess Process.* 81 (1) (2003) 3–12.
- [17] G.C.J. Muts, L. Pesman, The influence of raw materials and brewing process on lautertun filtration, *Maffliers* (1986).
- [18] J. Barrett, G.N. Bathgate, J.F. Clapperton, The composition of fine particles which affect mash filtration, *J. Instit. Brewing* 81 (1) (1975) 31–36.
- [19] J.H.E. Moonen, A. Graveland, G.C.J. Muts, The molecular structure of gelprotein from barley, its behaviour in wort-filtration and analysis, *J. Instit. Brewing* 93 (1987) 125–130.
- [20] M. Karabin, V. Hanko, J. Nešpor, L. Jelinek, P. Dostálek, Hop tannin extract: a promising tool for acceleration of lautering, *J. Instit. Brewing* (2018).
- [21] J.-E. Roth, Grenzflächeneffekte bei der Fest/Flüssig-Trennung, *Chemie Ingenieur Technik* 63 (2) (1991) 104–115.
- [22] M. Hieke, J. Ruland, H. Anlauf, H. Nirschl, Analysis of the porosity of filter cakes obtained by filtration of colloidal suspensions, *Chem. Eng. Technol.* 32 (7) (2009) 1095–1101.
- [23] R. Hofmann, C. Posten, Improvement of dead-end filtration of biopolymers with pressure electrofiltration, *Chem. Eng. Sci.* 58 (17) (2003) 3847–3858.

3 Results

M. Hennemann et al.

Separation and Purification Technology 272 (2021) 118966

- [24] M. Gastl, M. Kupetz, T. Becker, Determination of cytolytic malt modification – Part II: impact on Wort separation, *J. Am. Soc. Brewing Chem.* (2020) 1–9.
- [25] M. Gastl, M. Kupetz, T. Becker, Determination of Cytolytic Malt Modification – Part I: Influence of Variety Characteristics, *J. Am. Soc. Brewing Chem.* (2020) 1–13.
- [26] J. Engstle, H. Briesen, P. Först, Mash separation in the lauter tun - a particle size dependent separation process, *Brew. Sci.* 70 (2017) 26–30.
- [27] A.M. Kiszonas, C.M. Courtin, C.F. Morris, A critical assessment of the quantification of wheat grain arabinoxylans using a phloroglucinol colorimetric assay, *Cereal Chem.* 89 (3) (2012) 143–150.
- [28] P. Niemi, T. Tamminen, A. Smeds, K. Viljanen, T. Ohra-aho, U. Holopainen-Mantila, C. B. Faulds, K. Poutanen, J. Buchert, Characterization of lipids and lignans in brewer's spent grain and its enzymatically extracted fraction, *J. Agric. Food Chem.* 60(39), pp. 9910–9917, Oct 3, 2012.
- [29] M. Jekle, T. Becker, Wheat dough microstructure: the relation between visual structure and mechanical behavior, *Crit. Rev. Food Sci. Nutr.* 55 (3) (2015) 369–382.
- [30] VDI, 2762 Part 2. Mechanical solid-liquid separation by cake filtration. Determination of filter cake resistance, Beuth Verlag, Berlin, 2010.
- [31] L. Narziß, W. Back, *Die Bierbrauerei: Band 2: Die Technologie der Würzbereitung*, Wiley-VCH, Weinheim, 2009.
- [32] T. Kinnarinen, R. Tuunila, M. Huhtanen, A. Häkkinen, P. Kejik, T. Sverak, Wet grinding of CaCO₃ with a stirred media mill: Influence of obtained particle size distributions on pressure filtration properties, *Powder Technol.* 273 (2015) 54–61.
- [33] C. Papastefanou, Chapter 11 - Radioactive Aerosol Analysis, in: M.F. L'Annunziata (Ed.), *Handbook of Radioactivity Analysis*, third ed. Academic Press, Amsterdam, 2012, pp. 727–767.
- [34] R.D. Holtz, W.D. Kovacs, *An introduction to geotechnical engineering*, Prentice-Hall Inc, New Jersey, 1981.
- [35] H.F. Taylor, C. O'Sullivan, T. Shire, W.W. Moinet, Influence of the coefficient of uniformity on the size and frequency of constrictions in sand filters, *Géotechnique* 69 (3) (2019) 274–282.
- [36] H. Susi, D.M. Byler, Protein structure by Fourier transform infrared spectroscopy: second derivative spectra, *Biochem. Biophys. Res. Commun.* 115 (1) (1983) 391–397.
- [37] A. Savitzky, M.J.E. Golay, Smoothing and differentiation of data by simplified least squares procedures, *Anal. Chem.* 36 (8) (1964) 1627–1639.
- [38] S. Cai, B.R. Singh, Identification of β -turn and random coil amide III infrared bands for secondary structure estimation of proteins, *Biophys. Chem.* 80 (1) (1999) 7–20.
- [39] I. Parekh, A. Khanvilkar, A. Naik, Barley-wheat brewers' spent grain: A potential source of antioxidant rich lipids, *J. Food Process. Pres.* 41 (6) (2017) 1–8.
- [40] A. Oreopoulou, D. Tsimogiannis, V. Oreopoulou, Chapter 15 - Extraction of Polyphenols From Aromatic and Medicinal Plants: An Overview of the Methods and the Effect of Extraction Parameters, in: *Polyphenols in Plants*, second ed., Academic Press, 2019, pp. 243–259.
- [41] J. Steiner, S. Procopio, T. Becker, Brewer's spent grain: source of value-added polysaccharides for the food industry in reference to the health claims, *Eur. Food Res. Technol.* 241 (3) (2015) 303–315.
- [42] Q. Li, Z. Zhao, Characterization of the Structural and Colloidal Properties of alpha-Lactalbumin/Chitosan Complexes as a Function of Heating, *J. Agric. Food Chem.* 66(4) (2018), pp. 972–978.
- [43] V. Sathya Devi, D.R. Coleman, J. Truntzer, Thermal unfolding curves of high concentration bovine IgG measured by FTIR spectroscopy, *Protein J.* 30(6) (2011) pp. 395–403.
- [44] G.A. Ruiz, W. Xiao, M. van Boekel, M. Minor, M. Stieger, Effect of extraction pH on heat-induced aggregation, gelation and microstructure of protein isolate from quinoa (*Chenopodium quinoa* Willd), *Food Chem.* 209 (2016) 203–210.
- [45] F.M. Tiller, C.S. Yeh, W.F. Leu, Compressibility of particulate structures in relation to thickening, filtration, and expression — A review, *Sep. Sci. Technol.* 22 (2–3) (1987) 1037–1063.
- [46] A. Romdhane, M. Arousseau, A. Guillet, E. Mauret, Effect of pH and ionic strength on the electrical charge and particle size distribution of starch nanocrystal suspensions, *Starch - Stärke* 67 (3–4) (2015) 319–327.
- [47] B. Wei, X. Hu, H. Li, C. Wu, X. Xu, Z. Jin, Y. Tian, Effect of pHs on dispersity of maize starch nanocrystals in aqueous medium, *Food Hydrocolloids* 36 (2014) 369–373.
- [48] F. Weinbreck, H. Nieuwenhuijse, G.W. Robijn, C.G. De Kruif, Complexation of whey proteins with carrageenan, *J. Agric. Food Chem.* 52(11) (2004) pp. 3550–3555.

4 Discussion

It was hypothesized that the different characteristics of the layers affect the filtration process in multilayered cakes: high-resistance fine particles at the top act as a stiff layer that compresses the underlying coarse particle bottom layer during filtration. The effect was investigated using the example of the lautering process and verified using model systems. The following results were identified based on the outline of the thesis (Section 1.7):

1. Formation and characteristics of the multiple cake layers
 - Differences in the settling velocities of the particles depend mainly on their size. Large particles settle earlier and form the bottom layer, smaller fine particles settle later on top.
 - A high temperature favors the formation of the different layers in the lauter tun. The settling velocity of coarse particles increases with temperature, while the settling of fine particles is hindered at high temperatures due to a buoyancy effect.
 - The horizontal cake layers differ not only in their particle size but also in their chemical composition, which affects the filtration process.
2. Compression effects in multilayered cakes
 - An optical method for porosity determination was established, which is based on a measurement of the surface roughness of the cake layers after fixation by freezing. This enabled the examination of the compression due to changes in the cake porosity during filtration.
 - The lauter tun filter cake compresses during filtration based on the high resistance to flow of the top layer. A model filter cake confirmed that a differential pressure pulls the top layer down. The resulting compression of the bottom layer increases the resistance to flow throughout the cake. Cake compression starts from the top and is then transferred to the bottom layers.

- The use of different types of fine particles showed that the resistance of the stiff top layer determines the degree of compression of the bottom layer.
3. Prevention of compression in multilayered cakes
- Structural and chemical analysis showed that fine particles consist of protein and starch in high concentrations. These substances form modifiable complexes, which make up the largest proportion of particles.
 - The application of physical and chemical modifications changed the particle size distribution of the fine particle layer via particle agglomeration and deagglomeration. A high uniformity of the particle size distribution was found to reduce the resistance, which was verified using a model suspension.
 - High temperatures in the lauter tun prevent fine particles at the top of the cake from settling due to a buoyancy effect, which decreases the resistance of the top layer.
 - A filtration technique that involves the removal of the fine particles from the top prior to the filtration proved to reduce the cake compression and increased the flow rate.

4.1 Formation and Characteristics of the Multiple Cake Layers

The filter cake in the lauter tun serves as prominent example for describing the formation and characteristics of multilayered cakes, which was summarized in a literature review (Section 3.2.1, [Hennemann et al., 2019]). The formation of the layers depends on differences in the particle settling during the sedimentation rest prior to the filtration. Coarse particles of the wide particle size distribution of the mash, e.g., husks of the grain, have a higher settling velocity compared with fine particles, which can be explained by Stokes' Law (Equation 1.19). The high settling velocity depends mainly on the large size of the coarse compared with the fine particles. Coarse particles settle therefore first; fine particles settle later due to their small size. Consequently, a multilayered filter cake results: fine particles are mainly on the top layer, coarse particles in the bottom layer (Figure 1.3 or page 28, Figure 3). In addition to the particle size, factors like the particle density, shape, and the concentration of the suspension affect the particle settling.

The differences in the settling rates of the various particles of the suspension, which lead to the formation of the multilayered cake, were investigated (Section 3.2.2, [Hennemann et al., 2021d]). For this calculation, the concentration of the suspension as well as

4 Discussion

shape factors for the different particle types were considered, as described in Section 1.4. The calculation showed that the settling velocity increases with an increasing particle size and density (Page 42, Figure 5a). This estimation confirms that the formation of the multiple layers depends on differences in the characteristics of the particles, with the particle size being the main factor.

In addition to the particle-related factors that determine the settling velocity, the influence of temperature was taken into account in the calculation (Page 42, Figure 5). With an increasing temperature, the calculated settling velocity increased for all particle sizes. This was based on a reduction in the fluids density and viscosity (Page 40, Figure 3), which increased the settling velocity according to Equation 1.19. The temperature influence was confirmed for larger particles of the bottom layer using a sedimentation test, where the settling was finished with increasing temperature in a shorter time (Page 42, Figure 6a). For fine particles of the top layer, however, this effect could not be confirmed. Instead of faster settling, the particles remained in suspension as the temperature increased to $>60\text{ }^{\circ}\text{C}$ (Page 42, Figure 6b). This was verified using a small-scale sedimentation test where the settling of only the fine particles was investigated. With an increasing temperature, the particle size in the supernatant on top of the sediment was increasing (Page 43, Figure 8), which showed that settling of fine particles was hindered at higher temperatures.

The hindered settling can be explained by a buoyancy effect due to thermal convection, which depends on temperature differences in the supernatant. There is an insulation at the sides of the filter but not in the center, which means the temperature decreases at the center and thus the density increases at this location (Page 44, Figure 10). As a result of the density differences, a circulating motion results, as described in the literature [Gotoh et al., 2004]. This movement prevents the fine particles from settling. Brownian motion as an explanation of the particle motion can be ruled out due to the large size of the fine particles [Newburgh et al., 2006]. Coarse particles of the bottom layer were not affected by the convection, as the particle size was even higher and the resulting higher settling velocity at high temperatures was the dominant factor (Page 42, Figure 6a).

The temperature dependence of the particle settling influences the cake structure. High temperatures in the lauter tun favor the formation of the multiple layers of the filter cake. On the one hand, fine particles are hindered from settling due to the buoyancy effect and are therefore located in a larger concentration on the top of the filter cake. On the other hand, coarse particles that form the bottom layer settle faster with increasing temperature. The coarse particles are not influenced by the convection, which makes the layering even more pronounced.

4 Discussion

When suspending the particles in water instead of wort, there was no buoyancy effect (Page 43, Figure 8). Due to the low density and viscosity of water, the settling velocity was already high at low temperatures and increased even more with increasing temperature. Therefore, particle buoyancy at high temperature was less pronounced compared with the high settling velocity. This shows that the high temperature in combination with the special characteristics of the wort (high density and viscosity compared with water) are responsible for the buoyancy effect.

In the case of the lauter tun filter cake, the horizontal layers differ not only in the sizes and shapes of the particles but also in their chemical composition (Section 3.2.1, [Henne-mann et al., 2019]). The literature review revealed that fine particles at the top consist in a high concentration of proteins and lipids, while the lower parts of the cake consist of non-starch polysaccharides (β -glucan and arabinoxylan) in a high concentration (Page 33, Figure 5). This is due to the presence of a wide range of different compounds in the malt and thus in the mash, which means that the chemical composition of the particles that make up the top and bottom layer differs. Fine particles have a high protein concentration, which means that also the top layer of the cake consists mainly of protein. In contrast, coarse particles in the lower layers (e.g., husks) consist in a high concentration of cell wall material of the aleurone cells and the endosperm of the malt. Non-starch polysaccharides are frequently found in these particles [Gastl et al., 2020a], which explains the high concentration of these substances in the lower areas of the cake.

The differences in the chemical composition of the cake, particularly the high protein concentration at the top, can affect the cake structure and thus the filtration process. For example, a decrease in the flow rate due to the influence of oxygen (Section 1.5) affects especially the fine particle layer on the top based on the high amount of proteins. Furthermore, proteins in these particles can be charged. This means that in particular attractive and repulsive forces affect the fine particles, which influences the size of the particles and thus the structure of the filter cake (Section 1.3). Agglomeration due to increasing temperatures is another factor that affects especially the proteinaceous particles in the top layer. Therefore, not only the small size of the particles at the top determines the flow rate. It is also the chemical composition of the top layer that has an influence on the resistance to flow.

The filter cake in the lauter tun is not only inhomogeneous with regard to the chemical composition of its horizontal layers. The composition also changes during the filtration process, as components of the cake are extracted to different degrees when the cake is washed (Page 32, Figure 4). For example, the main component of the raw material malt is starch, which is almost entirely transferred to the liquid phase during mashing

and mash separation. This component, among others, is responsible for the density and viscosity of the liquid. In contrast, there are substances such as cellulose, which remain entirely in the solid phase of the filter cake. Proteins as important substance that influence the flow rate remain to about 65% in the filter cake. Therefore, the composition of the filtration critical top layer, which consists of proteins in the highest concentration, changes only slightly in its composition during filtration.

In summary, the lauter tun is a special case of filtration with a multilayered filter cake. Not only the wide particle size distribution of the suspension, but also the high temperature during filtration in combination with the high density and viscosity of the liquid phase favors the formation of the multiple layers. In these horizontal layers, not only differences in the particle size but also in the chemical composition affect the filtration process.

4.2 Compression Effects in Multilayered Cakes

It was hypothesized that if a high resistance to flow is located at the top of the cake, the resulting differential pressure at this location pulls the top layer downwards. A compression of the bottom layer results, which increases the resistance to flow of the entire filter cake. The compression of the cake in the lauter tun was investigated using different types of filtration tests (Section 3.2.3, [Hennemann et al., 2021e]). A mid-scale filtration test revealed the relationship between cake compression, pressure drop, and decrease in the flow rate (Page 50, Figure 3). At the beginning of filtration, the resistance to flow was low. There was a constant flow rate and no differential pressure. When the fine particles of the suspension settled at the top of the cake in higher amounts during filtration, there was a blocking at this location and the resistance increased. Due to the constant driving force of the pump under the filter medium, a differential pressure resulted. This pressure difference pulled the fine particle layer downwards and thereby compressing the lower layer. A change in the cake height served as first indicator of the compression. At the beginning, there was only a small compression. When the blocking started, the cake height reduced in a higher rate. After the main reduction in the cake height, the flow rate decreased and the height reduced only to a minor degree until the end of filtration. Compared with the starting point of the pressure drop, the decrease in the flow rate was delayed in time. This was based on the compression of the cake from the top. Liquid within the voids of the porous bottom layer could initially flow out of the cake unhindered at the beginning of the compression, so that the flow rate at this point was not impaired even when the pressure already dropped. As the compression of the

4 Discussion

bottom layer increased, less fluid was able to flow out of the voids without resistance and the flow rate decreased. After this point, the flow rate depended on the high resistance of the fine particle layer and the compressed cake.

To investigate the compression in the lauter tun filter cake, a new method of cake fixation and an optical porosity determination was developed (Section 3.2.3, [Hennemann et al., 2021e]). First, the cake was frozen at different time points during filtration to fix the structure. One has to consider that slow freezing could result in the formation of ice crystals, which can influence the particle structure. However, no ice crystals were observed on a macroscopic scale in these experiments, which means that an influence on the porosity values could be neglected. The fixation also made it possible to take samples from different horizontal cake layers, which is an advantage over existing methods that often only allow a determination of the average cake porosity. Sampling by cutting the frozen cake must be possible without affecting the structure (e.g., particle abrasion) to avoid an influence on the optical porosity measurement. This was possible for the cake consisting of mash particles that could be cut without abrasion.

After the samples of the cake were thawed, the porosity of the slices could be determined by an optical method using a microscope (Section 3.2.3). The surface roughness of the samples was determined, which correlates with their internal porosity according to the literature [Rebollo et al., 1996, Sakai and Nakamura, 2005]. The optical method was calibrated with a gravimetric reference method using samples with different degrees of compression that were taken at different time points during filtration (Page 49, Figure 2). A linear correlation between surface roughness and porosity was found. After the calibration, a rapid and reproducible method for porosity measurement was established.

The optical method proved to be applicable to the bottom layers of the cake based on the large particle sizes, which resulted in a detectable surface roughness. The roughness of the top layer, however, could not be determined using the microscope based on the small particle size. Nevertheless, a measurement of only the bottom layers was sufficient for the investigation of the compression in the lauter tun and the porosity of the fine particle layer could be neglected in these tests. For an evaluation of the top layers influence on the filtration process, a gravimetric method (e.g., as described in Section 3.2.2) or an estimation according to Equations 1.1 and 1.6 is necessary to evaluate the filter cake resistance. Hence, a detailed examination of the fine particles influence on the filtration process is described in Section 4.3.

The compression in the lauter tun was investigated using the optical porosity measurement (Section 3.2.3, [Hennemann et al., 2021e]). The average cake porosity at the

beginning of the filtration corresponded to the literature values [Bühler et al., 1996a] and decreased during filtration based on the compression of the bottom layer (Page 50, Figure 4). The resulting porosity values of the individual cake layers showed an unusual effect. Instead of a minimum porosity next to the filter medium based on the skin effect (Section 1.2), the lowest porosity was found in the uppermost bottom layer. This indicated that the filter cake was compressed from above by the fine particle layer (stamp-effect hypothesis). Hence, a different porosity curve compared with homogeneous cakes results in multilayered cakes (Page 51, Figure 6). With an increasing distance from the filter medium, there is a decrease in the porosity instead of an increase as observed for homogeneous cakes. Consequently, the compression from above leads to a reduction in porosity in all layers of the cake, in contrast to the skin effect, which only reduces the porosity next to the filter medium. This suggests that the resistance to flow across the cake can be higher for multilayered than for homogeneous cakes.

A modification of the filtration test revealed that the degree of compression depends on the resistance of the fine layer. When using an oxidized form of the mash, the resulting porosity of all layers was lower compared with the standard test (Page 50, Figure 4). This was based on the negative effect of oxygen on the filter cake resistance of the fine particles (described in detail in Section 4.3), which increased the compression from the top. In contrast, a higher porosity was found when the amount of fine particles in the mash was reduced by wet sieving prior to the filtration. The lower resistance at the top of the cake resulted in decreased compression of the bottom layers. These modifications confirmed that it is the fine particle layer at the top and its high resistance that is responsible for the compression of the bottom layer.

The degree of compression of the bottom layer also depended on the quality of the raw material. Malt quality was evaluated in terms of the degree of cytolytic modification. When using a high quality malt, there was a lower cake compression, which resulted in a higher flow rate after blocking (Page 51, Figure 5). In contrast, a higher compression and thus reduced flow rate was observed when using a low quality malt. This indicates that malt quality affects the resistance to flow of the fine particles and thus the compression. The reasons for differences in the filtration behavior of different malt types is described in Section 4.3.

After revealing the cake compression in the lauter tun, a model filter cake was used to verify the universal validity of the compression in multilayered cakes and to investigate the compression mechanism in detail (Section 3.2.4, [Hennemann et al., 2021f]). The filter cake consisted of glass fibers, which formed a compressible bottom layer, and an artificial fine particle layer at the top (Page 56, Figure 2). The use of these inert particles

4 Discussion

made it possible to study the compression without the influence of chemical interactions of the particles or differences in the properties of the liquid, as would be the case with the use of mash.

The reduction in the cake height during filtration was examined as first indication of the compression. In contrast to a homogeneously layered cake, the height of the multilayered cake reduced significantly during filtration (Page 57, Figure 3). The compression rate was first high and reduced when a turning point was reached. This is similar to compression effects in filter cakes [Shirato et al., 1970] and indicates that the top layer acts as a stiff piston, as with mechanical compression. The decrease in the cake height was directly related to a decrease in porosity (Page 58, Figure 4a). The reduced porosity resulted in an increase in the filter cake resistance during the filtration (Page 58, Figure 4b) according to Equation 1.6. A reference experiment using a homogeneously layered cake showed that only a small reduction in porosity resulted, which means that a compression due to the drag force of the liquid can be neglected. As a result, the compression in the multilayered cake mainly depended on the top layer.

A measurement of the height of the individual bottom layers showed that the compression in multilayered cakes starts from the top (Page 58, Figure 5). At the beginning of compression, the height of the uppermost layer decreased in a higher rate than the layers below. With continuing compression, the compressive force at the top increased and was transferred to the lower layers. At a certain point, the compression was equally distributed among the layers.

The compression from the top depended on the fine particle layer, which resulted in a pressure drop based on the high resistance at this location. High pressure (atmospheric pressure) was present at the top of the layer; low pressure was present under this layer due to suction by the pump (Page 55, Figure 1). The resulting pressure difference increased during filtration (Page 59, Figure 6a). The differential pressure on the two sides of the stiff top layer created a tensile force that moved the layer downwards, compressing the bottom layer. First, the bottom layer exerted no significant resistance to compression although the height was already reduced at this point. As the filtration continued, the bottom layer counteracted the compression, which increased the pressure difference. Consequently, the differential pressure increased in a high rate. When the point was reached at which the forces on the top layer and the opposing force of the compressed bottom layer were in equilibrium, the pressure dropped in a lower degree. The minimum pressure of the pump was reached after this point, which was in agreement with a lower compression rate (Page 57, Figure 3).

4 Discussion

A modified form of the artificial top layer that served as supporting mesh to retain particles (Page 56, Figure 2) was used to investigate the influence of different types of fine particles on the compression of the bottom layer. Particles with a filter cake resistance lower and higher than the bottom layer were tested (Page 59, Figure 7a). When using low resistance particles (glass beads), no differential pressure resulted (Page 59, Figure 6b). As a result, there was no compression of the bottom layer and thus no increase in resistance, similar to that of homogeneous filter cakes (Page 59, Figure 7b). In contrast, fine particles at the top with a higher resistance than the bottom layer (silica gel, fine particles from spent grains, calcium carbonate) resulted in a compression, which increased the filter cake resistance of the bottom layer. In general, the higher the resistance of the fine particles, the higher was the compression. For the spent grains fine particles, however, there was a break in the structure. In this case, the differential pressure and thus the compression was reduced although these particles showed the highest resistance at the top layer.

Based on the compression of the bottom layer by the fine particle layer, the hypothesis of the compression effect in multilayered cakes (Figure 1.5b) was confirmed. However, a skin effect as it occurs in homogeneous filter cakes (Figure 1.5a) was not observed in the model filter cake. This was based on the low resistance of the homogeneous cake, which did not result in a significant compression (Page 58, Figure 4) and thus no skin effect. A lower porosity next to the filter medium that indicated a skin effect was only found for the lauter tun filter cake when an increasing amount of fine particles was removed from the top of the cake (Page 50, Figure 4). The particle removal resulted in a more homogeneous cake and thus compression effects were similar to these types of cakes. However, one has to consider that the porosity in these trials was already low next to the filter medium at the beginning of filtration due to the compressive pressure of the upper layers.

The results also show that an increase in the differential pressure during filtration of the multilayered cake does not result in a higher flow rate, contrary to what Equation 1.1 suggests. As the differential pressure increases, there would be a greater pull on the top layer, compressing the lower layer and increasing its resistance in a higher degree.

It can be concluded that the compression of the multilayered filter cake depends on the degree of resistance to flow of the top layer. This was confirmed for the lauter tun filter cake and verified using an inert model system. For the example of lautering, modifications of the mash showed that the degree of compression can be influenced. Therefore, a deeper understanding is required that reveals how the resistance of the fine

particles at the top layer can be influenced to prevent the compression in multilayered cakes.

4.3 Prevention of Compression in Multilayered Cakes

A low resistance of the top layer resulted in a reduced pressure drop and thus decreased the compression in multilayered cakes. Therefore, different approaches to influence the top layer were tested using the example of the lautering process. First, physical and chemical modifications that alter the particle size distribution and thus the resistance of the fine particles were applied. Then, the influence of high temperatures on the particle settling, which was expected to affect the fine particles in particular, was investigated. Finally, a lautering technique is presented, which is based on a removal of the fine particles at the top prior to the filtration, to reduce the compression.

Structural and chemical analysis of the fine particles were conducted prior to the application of the modifications (Section 3.2.5, [Hennemann et al., 2021a]). The analysis showed that fine particles consist in a high concentration of proteins (Page 66, Table 1), which is in agreement with the literature review (Section 3.2.1). In addition to proteins, starch is present in a high concentration. Both substances could be specifically stained and made visible using confocal laser scanning microscopy, which revealed the structural composition of the particles (Page 67, Figure 2). The top layer consists mainly of two types of particles. Precipitated proteins that have small starch granules incorporated form the largest amount of particles. Large starch granules form larger particles with ordered and crystalline structures, which are surrounded by a protein layer.

The structural analysis revealed that the top layer consists of single particles. In contrast to other systems that have a high protein and starch content (e.g., wheat dough in bread making [Bernklau et al., 2016]), the particles are not connected via a protein network that spans the entire layer. A description as a gel-like layer at the top, as is often used in the literature [Muts and Pesman, 1986, Moonen et al., 1987], is therefore misleading. Rather, the top of the cake can be described as a suspension of individual particles that form a structured cake after sedimentation.

Particle agglomeration or de-agglomeration can be induced by modifications to alter their sizes. For example, cross-links of the proteins in the mash result in larger particle complexes, as described by Bühler [Bühler, 1996]. To examine this in terms of the fine particles, different physical (heating and agitation) and chemical (prevention of oxidation, addition of polyphenols, pH adjustment, and ion concentration alteration) modifications were tested to alter the particle sizes. The influence of these particle

4 Discussion

size changes on the filter cake resistance was investigated. Heating of the suspension resulted in a shift of the particle sizes (Page 67, Figure 3b). Smaller particles agglomerated to larger sizes based on denaturation of proteins. The denaturation was verified using Fourier transform infrared spectroscopy that showed changes in protein secondary structure elements with increasing heating time, which were responsible for the agglomeration. In addition to agglomeration, larger starch agglomerates were broken up due to the thermal energy, which reduced the sizes of larger particles. Consequently, not only a larger mean particle size was found when heating the particles, in contrast to what is described in the literature [Bühler, 1996, Bühler et al., 1996b]. The uniformity of the particle sizes also increased with increasing heating time, which means that the particle size distribution became more narrow (Page 68, Table 2). In contrast to heating, an influence of agitation due to attrition reduced the mean particle size and also the uniformity (Page 68, Figure 5b). This change in the particle size distribution was based on a mechanical breakage of the particle-particle interactions, which reduced the size of larger particles. A reduction in the sizes of larger particles was also found when oxidation was prevented using reducing agent (Page 68, Figure 6b). In contrast to agitation, however, the reduction in the mean particle size did increase the uniformity of the size distribution. Fourier transform infrared spectroscopy analysis showed changes in the band region for thiol groups of the proteins, which indicates that disulfide bridges were reduced by the reducing agent. This resulted in a breakdown of larger particles, which was responsible for the shift in the size distribution. An alteration of the pH changed the particle sizes only to a small degree (Page 69, Figure 7b). Large deviations from the standard (pH 5.35) were only observed at a pH between 6.35 and 6.75. At pH 6.55, a large change in the particle size distribution indicates the isoelectric point. Due to the reduction in the electrical charge at the surface of the particles at this pH, the suspension became unstable and smaller particles agglomerated (Section 1.3). In addition, larger starch particles decreased in their size based on degradation under alkaline conditions. Consequently, a more uniform particle size distribution was found. The influence of polyphenols and an increase in the ion concentration were also tested but did not show a large influence on the particle size distribution (Page 68, Table 2).

The changes in the particle sizes due to the modifications affected the filter cake resistance. For example, an increase in the mean particle size and uniformity when heating the particles decreased the filter cake resistance significantly (Page 67, Figure 3a). In contrast, a reduction in the mean particle size and uniformity increased the resistance (Page 68, Figure 5a). In addition to the modifications, fine particles from different malt types were tested. The malts differed in their cytolytic degree of modification, which

showed no correlation with the filter cake resistance. It was also the uniformity of the particle size distribution that determined the resistance to flow when using the different malt types. This indicates that particle size related characteristics of the suspension are more important in evaluating the filtration process in the lauter tun compared with cytolytic characteristics of the malt.

Not only descriptors of the mean particle size (as described by Bühler et al. [Bühler et al., 1995, Bühler et al., 1996b]) are important to evaluate the resistance to flow. An evaluation of all modifications as well as the use of different malt types (Page 70, Table 4) showed that the highest correlation between filter cake resistance and descriptors of the particle sizes were found for the uniformity (Page 70, Figure 8) and only to a minor degree for the mean particle size. Therefore, the particle size uniformity must be taken into account when evaluating the filter cake resistance of the fine particles in the lauter tun. A similar effect was previously shown for inorganic particles. Kinnarinen et al. [Kinnarinen et al., 2015, Kinnarinen et al., 2017] showed that an increase in the particle size uniformity improves the filtration process of mineral slurries in spite of a reduction in the mean particle size. The modification tests using the example of lautering confirmed this and revealed that the particle size effect can be applied not only to inorganic but also to biological particles.

The influence of the particle size uniformity on the filter cake resistance was verified using an inert glass beads model system (Page 71, Figure 9). A filtration test showed that a low resistance depends on a high mean particle size. However, this was only true when the uniformity of the particle sizes was high. In contrast, using a wide size distribution showed a higher filter cake resistance compared to a uniformity distribution, although the mean particle sizes were similar. This can be explained with the cavern effect (Section 1.3). Small particles fill the voids between larger particles in the wide distribution (Page 71, Figure 10), which is responsible for a lower porosity and thus higher resistance to flow.

The modifications showed that temperature can influence the size and thus the resistance of the particles. In addition, temperature can affect the filtration process in other ways. For example, a reduction of the liquids viscosity due to high temperatures increases the flow rate (Equation 1.1) and is a reason why lautering is carried out at high temperatures of up to 78 °C (Section 1.5). However, the impact of the viscosity on the filtration in the lauter tun is controversially discussed in the literature [Barrett et al., 1973, Greffin and Krauß, 1978, Bühler et al., 1996b, Bühler, 1996]. It was therefore expected that temperature affects the filtration in an additional way with regard to the

4 Discussion

fine particles. The influence of varying temperatures was tested, in which the particle agglomeration was kept constant (Section 3.2.2, [Hennemann et al., 2021d]).

Temperature-dependent changes in the flow rate differed between the start of filtration and after fine particle dependent blocking (Page 42, Figure 4b). This indicates that the flow rate after blocking is influenced by temperature in a high degree. In addition, the flow rate had only a low correlation to the viscosity. This confirms that the temperature-dependent viscosity (Page 40, Figure 3) has only a minor influence on the filtration process.

The temperature affects not only the particle sizes and viscosity but also the particle settling, as described in Section 4.1. A buoyancy effect due to thermal convection hindered fine particles of the top layer from sedimentation at increasing temperature (Page 43, Figure 8). This not only affected the formation of the multiple layers but also increased the porosity of the top layer due to a loose packing of the particles. The fine particles tended to stay in suspension rather than settle on the lower layer (Page 44, Figure 10). Hence, the filter cake resistance at the beginning of filtration was lower at high compared with low temperatures (Page 43, Figure 7). The buoyancy indicator had a high correlation to the temperature as well as to the flow rate and filter cake resistance. This shows that the temperature-dependent buoyancy of the filtration critical fine particles determines the flow rate during lautering. The reduction in the resistance of the top layer at high temperature resulted in a reduced compression of the bottom layer compared with low temperature. This confirms that a low resistance at the top layer prevents the compression in the multilayered cake.

Modifications of the fine particles as well as high temperatures during the filtration proved to reduce the resistance of the top layer and thus the compression in multilayered filter cakes. However, these factors may not be effective in reducing the resistance in any filtration process. For example, a change in the pH did not reduce the resistance in the same way when using different types of malt. This can be due to differences in the protein layer around the particles, which lead to different electrostatic charges. In addition, increasing the temperature to induce particle agglomeration may not be possible for various types of products (e.g., beer types). Therefore, to obtain an universal solution to the fine particle problem, a procedural approach was developed.

A lautering technique was developed, which involved a removal of the top layer fine particles prior to the filtration (Section 3.2.3, [Hennemann et al., 2021e]). The fine particle suspension was removed either from the lauter tun or combined from the mash and lauter tun (Page 47, Figure 1) to reduce the amount of particles in the top layer. This decreased the compression in the multilayered filter cake significantly. Compared

4 Discussion

with the reference trial, a higher cake porosity after filtration was found when removing the particles from the lauter tun (Page 50, Figure 4). The additional removal of particles from the mash tun reduced the compression even more. Compared with the reference, the characteristic blocking of the filter cake was reduced in the suction trials (Page 51, Figure 5). Hence, the flow rate was significantly improved.

In addition to a higher flow rate due to a reduced cake compression, this lautering technique has further advantages. The removal of the suspension by suction in combination with a clarification by centrifugation enabled a fast collection of filtrate. Furthermore, the trub wort, which normally has to be re-circulated at the beginning of filtration (Section 1.5), could be clarified directly by centrifugation. Based on a lower degree of compression, a reduced use of the raking knives during filtration was required. These advantages resulted in a shorter process time, as demonstrated in pilot scale experiments (Page 51, Table 1).

Although the removed particles were not washed during filtration as in the normal lautering process, no significant decrease in extract yield was found (Page 52, Table 2). This was based on the only low amount of particles that were removed, which did not contain large amounts of extract. Other critical filtrate characteristics (iodine value and turbidity) were either constant or lower than the reference based on the efficient particle separation by centrifugation. Only a small increase in the amount of fatty acids in the filtrate was found [Hennemann et al., 2021c]. This was due to the removal of the particles from the top, which contain these substances in large quantities (Section 3.2.1). The fatty acids are in this case not retained within the filter cake by depth filtration, as described for the standard lautering process [Engstle et al., 2017]. Hence, the concentration of this compound was increased in the removed suspension. The resulting influence on the entire production process (e.g., fermentation) and the final product beer (e.g., sensory) must be checked. In addition, the practicality of the removal of fine particles by suction and the particle separation using a centrifuge has to be verified in a further up-scale to the industrial scale.

In summary, different factors, such as physical-chemical modifications and high temperatures, can influence the resistance at the top and thus the compression of the multilayered cake. A technique, in which the particles are either removed before transfer to the filter or from the top of the cake after the transfer, improved the filtration process.

5 Conclusions

The findings in this thesis shed new light on the filtration with multilayered filter cakes, which was investigated using the example of the lauterling process. New insights into the formation of the multiple layers and their characteristics enabled a subsequent investigation of the compression mechanism. It was found that the resistance of the fine particles at the top layer determines the compression of the bottom layer.

The compression in the multilayered cake can be avoided by reducing the resistance of the top layer. Modifications showed that a change to more uniform particle sizes decreased the resistance. In addition, the presence of a buoyancy effect indicates that the resistance of the top layer can be reduced when applying high temperatures. Knowledge about these effects not only improve filtration with multilayered cakes but also other filtration processes with biological fine particle suspensions that have a high resistance to flow. However, the factors to reduce the resistance of the fine particle layer may not be viable in other areas of filtration, where a temperature increase or a modification of the particles is not possible to maintain the product quality. Therefore, a removal of the fine particles prior to the filtration can reduce their negative effects on the filtration process without influencing the filtrate quality. This was demonstrated for the lauterling process, but can be applied generally for different types of filtration with multilayered cakes. A separation of the removed fine particle suspension (e.g., by centrifugation) has to be checked when applying this new technique in the industrial scale.

The compression in multilayered cakes differs from that of homogeneous cakes. Due to the predominant compression effect from the top, a skin effect at the filter medium plays no relevant role in multilayered cakes. Both effects (skin effect and compression from top) can reduce the flow rate during the filtration process and have to be avoided. In contrast to the skin effect, however, the compression from the top can be avoided, as shown in this thesis.

References

- [Alles and Anlauf, 2003] Alles, C. and Anlauf, H. (2003). Filtration mit kompressiblen Kuchen: Effiziente Konzepte für eine anspruchsvolle Trennaufgabe. *Chem Ing Tech*, 75(9):1221–1230.
- [Bandelt Riess et al., 2018] Bandelt Riess, P. M., Kuhn, M., Briesen, H., and Först, P. (2018). Increasing wort flow by flocculation of fine particle fractions. *Brew Sci*, 71:68–72.
- [Barrett et al., 1973] Barrett, J., Clapperton, J. F., Divers, D. M., and Rennie, H. (1973). Factors affecting wort separation. *J Inst Brew*, 79(5):407–413.
- [Barrett et al., 1975] Barrett, J., Bathgate, G. N., and Clapperton, J. F. (1975). The composition of fine particles which affect mash filtration. *J Inst Brew*, 81(1):31–36.
- [Bayindirli et al., 1989] Bayindirli, L., Özilgen, M., and Ungan, S. (1989). Modeling of apple juice filtrations. *J Food Sci*, 54(4):1003–1006.
- [Bernklau et al., 2016] Bernklau, I., Lucas, L., Jekle, M., and Becker, T. (2016). Protein network analysis - a new approach for quantifying wheat dough microstructure. *Food Res Int*, 89(Pt 1):812–819.
- [Bühler, 1996] Bühler, T. M. (1996). *Effects of physical parameters in mashing on lautering performance*. Thesis.
- [Bühler et al., 1995] Bühler, T. M., Matzner, G., and McKechnie, M. T. (1995). Agitation in mashing. In *Proceedings of the 25th European Brewing Convention*.
- [Bühler et al., 1996a] Bühler, T. M., McKechnie, M. T., and Wakeman, R. J. (1996a). A model describing the lautering process. *Monatsschrift für Brauwissenschaft*, 7/8:226–233.
- [Bühler et al., 1996b] Bühler, T. M., McKechnie, M. T., and Wakeman, R. J. (1996b). Temperature induced particle aggregation in mashing and its effect on filtration performance. *Food Bioprod Process*, 74(4):207–211.

REFERENCES

- [Bockstal et al., 1985] Bockstal, F., Fouarge, L., Hermia, J., and Rahier, G. (1985). Constant pressure cake filtration with simultaneous sedimentation. *Filtr Sep*, 22:255–257.
- [Bourcier et al., 2016] Bourcier, D., Féraud, J. P., Colson, D., Mandrick, K., Ode, D., Brackx, E., and Puel, F. (2016). Influence of particle size and shape properties on cake resistance and compressibility during pressure filtration. *Chem Eng Sci*, 144:176–187.
- [Carman, 1937] Carman, P. C. (1937). Fluid flow through granular beds. *Transactions Inst Chem Eng*, 15:150–166.
- [Carta and Jungbauer, 2020] Carta, G. and Jungbauer, A. (2020). *Protein Chromatography: Process Development and Scale-Up*. Wiley-VCH, Weinheim.
- [Darcy, 1856] Darcy, H. (1856). *Les fontaines publiques de la ville de Dijon: Exposition et application des principes a suivre et des formules a employer dans les questions de distribution d'eau*. Dalmont, Paris.
- [Derjaguin and Landau, 1941] Derjaguin, B. and Landau, L. D. (1941). Theory of the stability of strongly charged lyophobic sols and of the adhesion of strongly charged particles in solutions of electrolytes. *Acta Physicochimica U.R.S.S.*, 14:633–662.
- [Draxler and Siebenhofer, 2014] Draxler, J. and Siebenhofer, M. (2014). *Verfahrenstechnik in Beispielen*. Springer Vieweg, Wiesbaden.
- [Droppo, 2006] Droppo, I. G. (2006). *Filtration in Particle Size Analysis*.
- [Engstle and Först, 2015] Engstle, J. and Först, P. (2015). Surface forces and their effect on lautering. In *MBAA Annual Conference*.
- [Engstle et al., 2014] Engstle, J., Först, P., and Kuhn, M. (2014). Characterization of horizontal layers of the lautering filter cake. In *2014 MBAA Annual Conference*.
- [Engstle et al., 2015] Engstle, J., Reichhardt, N., and Först, P. (2015). Filter cake resistance of horizontal filter layers of lautering filter cakes. *MBAA Tech Q*, 52(2):29–35.
- [Engstle et al., 2017] Engstle, J., Briesen, H., and Först, P. (2017). Mash separation in the lauter tun – a particle size dependent separation process. *Brew Sci*, 70:26–30.
- [Gastl et al., 2020a] Gastl, M., Kupetz, M., and Becker, T. (2020a). Determination of cytolytic malt modification – Part I: Influence of variety characteristics. *J Am Soc Brew Chem*, 79(1):53-65.

REFERENCES

- [Gastl et al., 2020b] Gastl, M., Kupetz, M., and Becker, T. (2020b). Determination of cytolytic malt modification – Part II: Impact on wort separation. *J Am Soc Brew Chem*, 79(1):66-74.
- [Gotoh et al., 2004] Gotoh, K., Yamada, S., and Nishimura, T. (2004). Influence of thermal convection on particle behavior in solid-liquid suspensions. *Adv Powder Technology*, 15(5):499–514.
- [Greffin and Krauß, 1978] Greffin, W. and Krauß, G. (1978). Schrotten und Läutern. II. Arbeit mit konventioneller Trockenschrotmühle und Läuterbottich - eine Literaturübersicht. *Monatsschrift für Brauwissenschaft*, 31(6):192–212.
- [Gözke and Posten, 2010] Gözke, G. and Posten, C. (2010). Electrofiltration of biopolymers. *Food Eng Rev*, 2(2):131–146.
- [Hennemann et al., 2019] Hennemann, M., Gastl, M., and Becker, T. (2019). Inhomogeneity in the lauter tun: a chromatographic view. *Eur Food Res Technol*, 245:521–533.
- [Hennemann et al., 2021a] Hennemann, M., Gastl, M., and Becker, T. (2021a). Influence of particle size uniformity on the filter cake resistance of physically and chemically modified fine particles. *Sep Purif Technol*, 272:118966.
- [Hennemann et al., 2021b] Hennemann, M., Gastl, M., and Becker, T. (2021b). Influence of temperature on the permeability of the lauter tun filter cake. In *2021 Virtual ASBC Meeting*.
- [Hennemann et al., 2021c] Hennemann, M., Gastl, M., and Becker, T. (2021c). Optische Methode der Porositätsbestimmung zum Nachweis des Stempleffekts in Filterkuchen. In *Jahrestreffen der ProcessNet-Fachgruppen Lebensmittelverfahrenstechnik, Mischvorgänge, Grenzflächenbestimmte Systeme und Prozesse*.
- [Hennemann et al., 2021d] Hennemann, M., Gastl, M., and Becker, T. (2021d). Influence of temperature on the filter cake resistance in a lauter tun. *Brew Sci*, 74:100–106.
- [Hennemann et al., 2021e] Hennemann, M., Gastl, M., and Becker, T. (2021e). Optical method for porosity determination to prove the stamp effect in filter cakes. *J Food Eng*, 293:110405.
- [Hennemann et al., 2021f] Hennemann, M., Fattahi, E., Gastl, M., and Becker, T. (2021f). Compression mechanism in multilayered filter cakes. *Chem Eng Technol*, 44(10):1900–1907.

REFERENCES

- [Hieke et al., 2009] Hieke, M., Ruland, J., Anlauf, H., and Nirschl, H. (2009). Analysis of the porosity of filter cakes obtained by filtration of colloidal suspensions. *Chem Eng Technol*, 32(7):1095–1101.
- [Hofmann and Posten, 2003] Hofmann, R. and Posten, C. (2003). Improvement of dead-end filtration of biopolymers with pressure electrofiltration. *Chem Eng Sci*, 58(17):3847–3858.
- [Holtz and Kovacs, 1981] Holtz, R. D. and Kovacs, W. D. (1981). *An introduction to geotechnical engineering*. Prentice-Hall, Inc., New Jersey.
- [Hwang et al., 1997] Hwang, K.-J., Wu, Y.-S., and Lu, W.-M. (1997). Effect of the size distribution of spheroidal particles on the surface structure of a filter cake. *Powder Technol*, 91:105–113.
- [ISO, 2014] ISO (2014). *ISO 9276-2: Representation of results of particle size analysis — Part 2: Calculation of average particle sizes/diameters and moments from particle size distributions*. International Organization for Standardization, Switzerland, 2nd edition.
- [Jiao et al., 2017] Jiao, R., Fabris, R., Chow, C. W. K., Drikas, M., van Leeuwen, J., Wang, D., and Xu, Z. (2017). Influence of coagulation mechanisms and floc formation on filterability. *J Environ Sci (China)*, 57:338–345.
- [Kinnarinen et al., 2015] Kinnarinen, T., Tuunila, R., Huhtanen, M., Häkkinen, A., Kejjik, P., and Sverak, T. (2015). Wet grinding of CaCO_3 with a stirred media mill: Influence of obtained particle size distributions on pressure filtration properties. *Powder Technol*, 273:54–61.
- [Kinnarinen et al., 2017] Kinnarinen, T., Tuunila, R., and Häkkinen, A. (2017). Reduction of the width of particle size distribution to improve pressure filtration properties of slurries. *Minerals Eng*, 102:68–74.
- [Kiszonas et al., 2012] Kiszonas, A. M., Courtin, C. M., and Morris, C. F. (2012). A critical assessment of the quantification of wheat grain arabinoxylans using a phloroglucinol colorimetric assay. *Cereal Chem*, 89(3):143–150.
- [Kozeny, 1927] Kozeny, J. (1927). Über kapillare Leitung des Wassers im Boden. *Sitzungsber. Akad. Wiss. Wien*, 136:271–306.
- [Kunze, 2004] Kunze, W. (2004). *Technology brewing and malting*. VLB, Berlin.

REFERENCES

- [Lewis and Oh, 1985] Lewis, M. J. and Oh, S. S. (1985). Influence of precipitation of malt proteins in lautering. *MBAA Tech Q*, 22(3):108–111.
- [Li and Ma, 2011] Li, L. and Ma, W. (2011). Experimental study on the effective particle diameter of a packed bed with non-spherical particles. *Transport in Porous Media*, 89(1):35–48.
- [Lu et al., 1998] Lu, W.-M., Tung, K.-L., Pan, C.-H., and Hwang, K.-J. (1998). The effect of particle sedimentation on gravity filtration. *Sep Sci Technol*, 33(12):1723–1746.
- [Luckert, 2004] Luckert, K. (2004). *Handbuch der mechanischen Fest-Flüssig-Trennung*. Vulkan-Verlag, Essen.
- [Löwer et al., 2020] Löwer, E., Pham, T. H., Leißner, T., and Peuker, U. A. (2020). Study on the influence of solids volume fraction on filter cake structures using micro tomography. *Powder Technol*, 363:286–299.
- [Martin, 1980] Martin, H. (1980). Wärme- und Stoffübertragung in der Wirbelschicht. *Chemie Ingenieur Technik*, 52(3):199–209.
- [Mattsson et al., 2012] Mattsson, T., Sedin, M., and Theliander, H. (2012). Filtration properties and skin formation of micro-crystalline cellulose. *Sep Purif Technol*, 96:139–146.
- [Miedaner, 2002] Miedaner, H. (2002). *Brautechnische Analysenmethoden (Band II). Methodensammlung der Mitteleuropäischen Brautechnischen Analysekommision*, volume 4. Freising-Weihenstephan.
- [Moonen et al., 1987] Moonen, J. H. E., Graveland, A., and Muts, G. C. J. (1987). The molecular structure of gelprotein from barley, its behaviour in wort-filtration and analysis. *J Inst Brew*, 93:125–130.
- [Muts and Pesman, 1986] Muts, G. C. J. and Pesman, L. (1986). *The influence of raw materials and brewing process on lautertun filtration*. EBC Monograph XI, Symposium on Wort Production. Maffliers.
- [Narziß and Back, 2009] Narziß, L. and Back, W. (2009). *Die Bierbrauerei: Band 2: Die Technologie der Würzebereitung*, volume 8. Wiley-VCH, Weinheim.
- [Newburgh et al., 2006] Newburgh, R., Peidle, J., and Rueckner, W. (2006). Einstein, perrin, and the reality of atoms: 1905 revisited. *Am J Phys*, 74(6):478–481.

REFERENCES

- [Papastefanou, 2012] Papastefanou, C. (2012). *Chapter 11 - Radioactive Aerosol Analysis*, pages 727–767. Academic Press, Amsterdam.
- [Rebollo et al., 1996] Rebollo, M. A., Hogert, E. N., Albano, J., Raffo, C. A., and Gaggioli, N. G. (1996). Correlation between roughness and porosity in rocks. *Opt Laser Tech*, 28(1):21–23.
- [Rhea et al., 2017] Rhea, N., Groppo, J., and Crofcheck, C. (2017). Evaluation of flocculation, sedimentation, and filtration for dewatering of scenedesmus algae. *Transactions ASABE*, 60(4):1359–1367.
- [Richardson and Zaki, 1954] Richardson, J. F. and Zaki, W. N. (1954). The sedimentation of a suspension of uniform spheres under conditions of viscous flow. *Chem Eng Sci*, 3(2):65–73.
- [Ripperger et al., 2012] Ripperger, S., Gösele, W., and Alt, C. (2012). *Filtration, 1. Fundamentals*. Ullmann’s Encyclopedia of Industrial Chemistry. Wiley-VCH, Weinheim.
- [Roth, 1991] Roth, J.-E. (1991). Grenzflächeneffekte bei der fest/flüssig-Trennung. *Chem Ing Tech*, 63(2):104–115.
- [Sakai and Nakamura, 2005] Sakai, T. and Nakamura, A. M. (2005). Quantification of porosity and surface roughness in laboratory measurements of the bidirectional reflectance of asteroid surface analogues. *Earth Planets Space*, 57:71–76.
- [Salmela and Oja, 2006] Salmela, N. and Oja, M. (2006). Monitoring and modelling of starch cake washing. *Int J Food Sci Technol*, 41(6):688–697.
- [Shi et al., 2020] Shi, Q., Lu, Y., Guo, W., Wang, T., Zhu, Q., Zhang, Y., Wang, H., Li, F., Xu, T., and Li, C. (2020). Application of a cellulose filter aid in municipal sewage sludge dewatering and drying: Jar, pilot, and factory scale. *Water Env Res*, 92(4):495–503.
- [Shirato et al., 1970] Shirato, M., Murase, T., Negawa, M., and Senda, T. (1970). Fundamental studies of expression under variable pressure. *J Chem Eng Japan*, 3(1):105–112.
- [Sievers et al., 2015] Sievers, D. A., Lischeske, J. J., Bidy, M. J., and Stickel, J. J. (2015). A low-cost solid-liquid separation process for enzymatically hydrolyzed corn stover slurries. *Bioresour Technol*, 187:37–42.

REFERENCES

- [Sohn and Moreland, 1968] Sohn, H. Y. and Moreland, C. (1968). The effect of particle size distribution on packing density. *Can J Chem Eng*, 46(3):162–167.
- [Stieß, 1995a] Stieß, M. (1995a). *Mechanische Verfahrenstechnik 1*. Springer, Berlin-Heidelberg.
- [Stieß, 1995b] Stieß, M. (1995b). *Mechanische Verfahrenstechnik 2*. Springer, Berlin-Heidelberg.
- [Taylor et al., 2019] Taylor, H. F., O’Sullivan, C., Shire, T., and Moinet, W. W. (2019). Influence of the coefficient of uniformity on the size and frequency of constrictions in sand filters. *Géotechnique*, 69(3):274–282.
- [Tiller and Green, 1973] Tiller, F. M. and Green, T. C. (1973). Role of porosity in filtration IX Skin effect with highly compressible materials. *AIChE J*, 19(6):1266–1269.
- [Tiller et al., 1972] Tiller, F. M., Haynes Jr., S., and Lu, W.-M. (1972). The role of porosity in filtration VII Effect of side-wall friction in compression-permeability cells. *AIChE J*, 18(1):13–20.
- [Tiller et al., 1987] Tiller, F. M., Yeh, C. S., and Leu, W. F. (1987). Compressibility of particulate structures in relation to thickening, filtration, and expression — a review. *Sep Sci and Technology*, 22(2-3):1037–1063.
- [Tiller et al., 1995] Tiller, F. M., Hsyung, N. B., and Cong, D. Z. (1995). Role of porosity in filtration: XII. Filtration with sedimentation. *AIChE J*, 41(5):1153–1164.
- [Tippmann and Becker, 2016] Tippmann, J. and Becker, T. (2016). Das Zusammenspiel von Verfahrenstechnik und Technologie in der Brauerei. *Chem Ing Tech*, 88(12):1857–1868.
- [Tippmann et al., 2010] Tippmann, J., Scheuren, H., Voigt, J., and Sommer, K. (2010). Procedural investigations of the lautering process. *Chem Eng Technol*, 33(8):1297–1302.
- [Tippmann et al., 2011] Tippmann, J., Voigt, J., and Sommer, K. (2011). Measuring particle size distribution of mash with laser diffraction to evaluate the process success. *Brew Sci*, 64:13–21.

REFERENCES

- [Tse et al., 2003] Tse, K. L., Boswell, C. D., Nienow, A. W., and Fryer, P. J. (2003). Assessment of the effects of agitation on mashing for beer production in a small scale vessel. *Food Bioprod Process*, 81(1):3–12.
- [VDI, 2010] VDI (2010). *VDI 2762 Part 2. Mechanical solid-liquid separation by cake filtration. Determination of filter cake resistance*. Beuth Verlag, Berlin.
- [Verwey and Overbeek, 1948] Verwey, E. J. W. and Overbeek, J. T. G. (1948). *Theory of the Stability of Lyophobic Colloids: The Interaction of Sol Particles Having an Electric Double Layer*. Elsevier, Amsterdam.
- [Wadell, 1935] Wadell, H. (1935). Volume, shape, and roundness of quartz particles. *J Geol*, 43(3):250–280.
- [Yao et al., 2014] Yao, R., Jiang, G., Li, W., Deng, T., and Zhang, H. (2014). Effect of water-based drilling fluid components on filter cake structure. *Powder Technol*, 262:51–61.

A Appendix

A.1 Non-Reviewed Paper

Hennemann, M., Gastl, M., and Becker, T. (2021). Schneller Läutern: alternatives Läuterverfahren. *Brauwelt*, 5-6:115–118.

Hennemann, M., Gastl, M., and Becker, T. (2022). Jedes Grad zählt: Optimierung des Läuterns. *Brauwelt*, 5:133–136.

A.2 Oral and Poster Presentations

Hennemann, M., Gastl, M., and Becker, T. (2021). Optische Methode der Porositätsbestimmung zum Nachweis des Stempoeffekts in Filterkuchen. In *Jahrestreffen der Process-Net-Fachgruppen Lebensmittelverfahrenstechnik, Mischvorgänge, Grenzflächenbestimmte Systeme und Prozesse*.

Hennemann, M., Gastl, M., and Becker, T. (2021). Influence of temperature on the permeability of the lauter tun filter cake. In *2021 Virtual ASBC Meeting*.

Hennemann, M., Gastl, M., and Becker, T. (2022). Neue Erkenntnisse zur Verbesserung des Läuterprozesses. In *54. Technologisches Seminar Weihenstephan*.